Combined use of spectral signatures and ultrasonic sward height for the assessment of biomass and quality parameters in heterogeneous pastures

Hanieh Safari

Doctoral thesis

University of Kassel

Department of Grassland Science and Renewable Plant Resources

Witzenhausen, December 2016

This work has been accepted by the Faculty of Organic Agricultural Sciences of the University of Kassel as a thesis for acquiring the academic degree of Doktor der Agrarwissenschaften (Dr. agr.).

1. Supervisor: Prof. Dr. Michael Wachendorf (University of Kassel)
2. Supervisor: Prof. Dr. Johannes Isselstein (University of Göttingen)

Defence day: 16.05.2017

Eidesstattliche Erklärung

Hiermit versichere ich, dass ich die vorliegende Dissertation selbstständig, ohne unerlaubte Hilfe Dritter angefertigt und andere als die in der Dissertation angegebenen Hilfsmittel nicht benutzt habe. Alle Stellen, die wörtlich oder sinngemäß aus veröffentlichten oder unveröffentlichten Schriften entnommen sind, habe ich als solche kenntlich gemacht. Dritte waren an der inhaltlich-materiellen Erstellung der Dissertation nicht beteiligt; insbesondere habe ich hierfür nicht die Hilfe eines Promotionsberaters in Anspruch genommen. Kein Teil dieser Arbeit ist in einem anderen Promotions - oder Habilitationsverfahren verwendet worden.

Witzenhausen, den 08. December 2016

Hanieh Safari

Preface

This thesis is submitted to the Faculty of Organic Agricultural Sciences of the University of Kassel to fulfil the requirements for the degree Doktor der Agrarwissenschaften (Dr. agr.). This thesis is based on three papers, which are published by or submitted to international scientific peer reviewed journals. The papers are included in chapter 3, 4 and 5 which are listed on the next page. General introduction and research objectives are given in first two chapters. In chapter 6 the findings of this research are summarized and overall discussion and conclusions are drawn. This chapter also gives recommendations for future research.

Many people have supported my research in many various ways. First of all, my sincerest appreciation goes to my supervisor Prof. Dr. Michael Wachendorf for his continuous support, encouragement and valuable advices during the period of my study. I highly acknowledge his excellent advisory support during many difficult situations and many inspiring scientific discussion we shared. Further, I would like to express my gratitude to Dr. Thomas Fricke for the invaluable contribution and help I received from him. This work would not have been possible without his expertise and considerable time and support he devoted to my work. Special thanks go to my PhD colleague Björn Redderson who helped me tremendously during my fieldwork and data analysis. I also want to thank Dr. Thomas Moeckel for his contribution into my research.

I am very thankful to the technicians Andrea Gerke, Wolfgang Funke and Julia Sondermann and my PhD colleague Nodirjon Nurmatov for their help during laboratory and field experiments. Many thanks go to my friends Miriam Ehret and Lutz Bühle for their help, the hospitality and friendship.

I would like to thank the whole GNR department for their support. I appreciate the friendly atmosphere and pleasant chats during coffee breaks. I extend my gratitude to RTG 1397 group for very enjoyable and interesting times we spend together during my PhD.

I also wish to gratefully acknowledge the German Research Foundation (DFG) for financing this research.

I want to thank my son Aron who accompanied his mom during the last phase of PhD and brought so much joy and happiness into my life. I also would like to express my heartfelt thanks to my family especially my mother.

Last but not least, there is no way to thank my husband Mansour for his generous support and contributions to the entire process. I am deeply thankful for your appreciations, trust, patience, faith and most of all for your unconditional love which enabled me to complete this work successfully. Thank you for being the best friend of mine and the man of all seasons.

Witzenhausen, December 2016

Hanieh Safari

List of Papers

Chapter 3: Möckel T., Safari H., Reddersen B., Fricke T., Wachendorf M. (2016): Fusion of ultrasonic and spectral sensor data for improving the estimation of biomass in grassland with diverse sward structure. Remote Sensing journal, submitted.

Chapter 4: Safari H., Fricke T., Wachendorf M. (2016): Determination of fibre and protein content in heterogeneous pastures using field spectroscopy and ultrasonic sward height measurements. Computers and Electronics in Agriculture, 123, 256-263.

Chapter 5: Safari H., Fricke T., Reddersen B., Wachendorf M. (2016): Comparing mobile and static assessment of biomass in heterogeneous grassland with a multi-sensor system. Journal of Sensors and Sensor Systems (JSSS), 5, 1-13.

Table of contents

List of Tables

List of figures

Abbreviations

ADF acid detergent fibre

CP crude protein

CR continuum removed reflectance

CV cross validation

DGPS Differential Global Positioning System

DM dry matter

DMY dry matter yield

DMP dead material proportion

FDR first-order derivative reflectance

FM fresh matter

FMY fresh matter yield

FOV field of view

GIS geographic information system

GPS global positioning system

MPLSR modified least square regression

NDSI normalized spectral vegetation index

NDVI normalized difference vegetation index

NIR near infrared

PCA principle component analysis

PLSR partial least square regression

R^2 coefficient of determination

RE RapidEye

REIP red edge inflection point

RMSE Root mean square error

RPD residual predictive value

SAVI soil adjusted vegetation index

SE standard error

SD standard deviation

SDR second-order derivative reflectance

SLU standard livestock unit

USH ultrasonic sward height

VI vegetation index

VIS visible

WI water index

WV2 WorldView

1 General Introduction

Grasslands cover a large portion of the earth's surface and they are a very important source of livestock feed (Suttie et al., 2005). In these ecosystems, the energy available to the animal for metabolism (maintenance, growth and production) is limited by the quantity and quality of forage resource (Rattray et al., 2007). Hence, herbage biomass and its quality is a primary concern in continuous grazing systems (Silvia Cid et al., 1998). Timely assessment of these elements in grasslands is essential in grazing management and can help livestock managers in making critical decisions in terms of planning grazing time, grazing period, grazing interval and stocking rate (FAO, 2010; Suzuki et al., 2012).

Within site, herbage mass and quality are highly variable because they are affected by species composition, sward maturity, sward height and density as well as soil type, topography, geology and climatic factors (Ayantunde et al., 1999; Suzuki et al., 2012). Heterogeneity of pasture characteristics occurs within a spatial and temporal scale and is influenced by patch or selective grazing. Free-ranging grazing animals differentiate between pasture areas, plant species and plant parts in choosing their diets. They prefer vegetation patches and plants that contain relatively high nutrients and avoid previously ungrazed patches with tall mature swards (Teague and Dowhower, 2003). This selective behavior generates a mosaic in which short, heavily grazed patches having small herbage mass alternate with taller, ungrazed or lightly grazed patches having large herbage mass (Hirata 2000). In subsequent years heavily grazed patches are more likely to be heavily used while previously neglected patches will likely receive little subsequent use (Teague et al., 2004). Grazing management can affect the creation and maintenance of such patterns, since reports suggest low stocking density is better able to create relatively stable grazed and ungrazed patches over time (Van den Bos and Bakker, 1990; Dumont et al., 2012) while higher stocking rates result in reduced selectivity and patchiness (Barnes et al., 2008). Site-specific determination of biomass and nutritive values (such as crude protein and acid detergent fiber) and quantifying the spatial heterogeneity over time in the field can help in detecting grazing patch dynamics in the pastures and subsequently help in optimizing utilization of grassland resources (e.g. by stocking rate adjustments or changing grazing intervals). However, the evaluation and mapping of vegetation heterogeneity at temporal and spatial scale over large areas is a challenge, as it requires targeted and efficient means to assess such numerous data. Although direct plant sampling techniques such as clipping and weighing method for measuring yield or traditional chemical analysis and

laboratory based VIS/NIR techniques to assess forage quality (which still requires the collection and preparation of vegetation samples), are accurate, these procedures are only practical on experimental area of limited size and not applicable to obtain the distribution of vegetation characteristics on a large-scale field as they are costly, destructive, labor and time consuming (Pullanagari et al., 2012a, 2013).

Remote-sensing based techniques such as satellite and airborne imagery have been developed during the past decades for monitoring vegetation with non-destructive and rapid data acquisition over vast areas. However the application of these techniques with low spatial and spectral resolution in pastures is difficult due to complexity and continuous changes in these environments and there is a need for higher resolution and spatially continuous measurements to obtain more detailed information regarding distribution of sward characteristics (Schellberg et al., 2008). Moreover the infrequent availability of cloud-free images or the short-term operation of the monitoring system constrain their utility by a lack of temporally replicated data (Ouyang et al., 2012). In contrast proximal (ground-based) technologies provide an opportunity to monitor spatio-temporal variations of grasslands with high resolution data collections (Flynn et al., 2008; Fricke et al., 2011; Lee et al., 2011). These techniques may be combined with a global positioning system (GPS) and allow interpolation of spatial data from a moving vehicle and mapping sward characteristics on a large-scale field. In this context, several types of ground-based mobile sensing strategies by mounting different types of sensors (e.g. laser, ultrasonic and spectral) are employed for measuring and fine-scale mapping of height (Ehlert et al., 2008; Fricke et al., 2011) forage biomass (Flynn et al., 2008; Fricke and Wachendorf, 2013) and nutritional status (Lee et al., 2011) in grasslands.

Decisions upon site-specific management require maps containing field attributes that have precisely been detected (Schellberg et al., 2008). Especially in pastures with high levels of heterogeneity it is challenging to develop a real-time ground-based sensing system with sufficient measurement accuracy due to considerable variations in sward properties which limits the ability to create a robust estimation model. Multi sensor data fusion is the process of combining information from different types of sensors to improve accuracies of property estimates (Adamchuk et al., 2011). Such sensing strategies may overcome the limitations of canopy measurements by enhancing the magnitude in data collection and provide opportunity for creation of robust estimation models (Pittman et al., 2015). Hyperspectral sensors have been utilized for measuring

different structural and functional characteristics of vegetation such as biomass, plant nitrogen, leaf area index, vegetation cover or water status in grassland swards. These sensors with hundreds of narrow and continuous spectral wavebands have the potential to estimate variables which are difficult to be measured by conventional multi spectral sensors. Vegetation indices (VIs) derived from those multi-spectral sensors like the normalized difference vegetation index (NDVI) suffer from the saturation effect by increasing greenness (around a leaf area index of 2 to 2.5). Mutanga and Skidmore (2004) could overcome the saturation problem in biomass estimation using narrow band vegetation indices derived from hyperspectral data. Many studies have documented the importance of hyperspecral indices for estimating biophysical and biochemical parameters of vegetation in grassland swards (Mutanga et al., 2005; Fricke and Wachendorf, 2013; Darvishzadeh et al., 2008; Reddersen et al., 2014; Psomas et al., 2011; Fava et al., 2009; Duan et al., 2014; Starks et al., 2006). Narrowband VIs use a limited number of wavelengths from the huge range of hyperspectral data. In contrast, other approaches such as partial least square regression (PLSR) integrate spectral information of the whole hyperspectral range. Even though using such techniques have been addressed to be successful in many studies for measuring grassland properties (Biewer et al., 2009b and c; Thulin et al., 2012; Marabel and Alvarez-Taboada, 2013; Pellissier et al., 2015) they lack transferability to be used for practical implementation at the field. Moreover, hyperspectral sensors are costly and sensing strategies should be cost effective thus the limitation of wavelengths by reduction of hyper spectral range or selection of few wavelengths (e.g. using narrowband VIs) is desirable (Reddersen et al., 2014). However this may cause the loss of prediction quality (Biewer et al., 2009b). Other factors such as variations in solar angel and atmospheric conditions can also change the spectral characteristics and reduce the accuracy of spectral data (Pinter, 1993). Therefore the combination of low-cost ultrasonic sensors and spectral reflectance sensors may be beneficial for the prediction of biomass yield and pasture quality. Ultrasonic proximity sensors have been deployed for measuring canopy height by measuring the distance between the target and sensor mounted vertically, facing the canopy. The distance is calculated by measuring the time differences between the emission and the reception of the signal, after it is reflected back from the target (Vitali et al., 2013). Prediction of biomass yield with an ultrasonic distance sensor used for height measurements in pure and binary legume-grass mixtures resulted in fair to good prediction accuracies (Fricke et al., 2011). Presence of weeds or inflorescences caused an unbalanced sward density along the height gradient which limited the performance of ultrasonic sensor. The increased structural complexity existing in pastures might

reduce the performance of ultrasonic sensor even more compared to sown grasslands. Fricke and Wachendorf (2013) showed complementary effect of spectral sensor by a combined use of both sensors which prevented overestimation resulting from exclusive use of ultrasonic sward height to assess biomass of legume-grass mixtures. Pittman et al. (2015) used a mobile sensor system including laser, ultrasonic and spectral sensors for biomass estimation. Their results illustrated quantification of canopy height with ultrasonic and laser sensors could provide for biomass estimation models equivalent to and/or more effective than those which include spectral components. Sui and Thomasson (2006) combined a multi-spectral optical sensor and an ultrasonic sensor to determine of nitrogen status in cotton plants. The results showed that the spectral information and plant height measured by the sensing system had significant correlation with leaf nitrogen concentration of the cotton plants. Shiratsuchi et al. (2009) found both ultrasonic and active canopy sensors had similar abilities to distinguish nitrogen differences in canopy at several growth stages for corn. They suggested that the integrated use of both sensors improves the nitrogen estimation compared to the exclusive use of either sensor. These investigations show that canopy height may provide complementary information to reflectance sensing when estimating the nitrogen status of plants. Even though ultrasonic sensors have been used simultaneously with canopy reflectance sensors in crops and cutting systems, to our knowledge such combined sensing techniques have not yet been examined in heterogeneous pastures.

2 Research objectives

Precision management of grasslands requires accurate information on sward characteristics at a spatial and temporal scale. Multi-sensor data fusion provides data for site-specific grassland management.

The overall aim of the study is to explore the potential of data fusion of ultrasonic and hyper-spectral reflectance sensors to acquire accurate information on pasture swards in terms of quantity and quality at field scale. The specific objectives are described in the following chapters:

Chapter 3: Investigates the potential of ultrasonic and hyper-spectral sensor data fusion to predict biomass in heterogeneous pastures under different stocking densities and with high structural sward diversity in different periods of the growing season. Several spectral approaches such as narrow and broad band vegetation indices, principle component analysis (PCA) derived components and multi-spectral broadbands of RapidEye and WorldView2 satellites were tested exclusively and in combination with ultrasonic sward height (USH) to identify calibration models of high predictive capability. This chapter also explores the important wavelength for predicting pasture biomass in exclusive or combined approaches.

Chapter 4: Describes the ability of the same sensors to predict grassland quality parameters including crude protein (CP) and acid detergent fiber (ADF) of heterogeneous pastures. In this chapter, spectral variables derived from hyper-spectral reflections (narrow-band vegetation indices and WorldView2 satellite broad-bands) combined with ultrasonic sward height (USH) and compared to modified partial least square regression (MPLSR) models to improve the accuracy of predictions in different seasons of the year (spring, summer, autumn) during two year pasture measurements.

Chapter 5: Evaluates the ability of a mobile sensing system equipped with ultrasonic and spectral sensors and a high precision GPS to quantify within-field variations which

would be the primary application of such system. This was directly tested in the same study site used for calibration dataset by comparing predictions of mobile and static measurements of sensors. This chapter also explores the possible position errors associated with mobile sensor system.

3 Fusion of ultrasonic and spectral sensor data for improving the estimation of biomass in grassland with diverse sward structure

Abstract An accurate estimation of biomass is needed to understand the spatio-temporal changes of forage resources in pasture ecosystems and to support grazing management decisions. However, a timely evaluation of biomass is a challenge, as it requires targeted and efficient means like technical sensing methods to assess numerous data for the creation of continuous maps. In order to calibrate ultrasonic and spectral sensors, a field experiment with heterogeneous pastures continuously stocked by cows at three levels of grazing intensity was used providing a broad range of biomass characteristics for a sensor alignment. Exclusive ultrasonic sward height or spectral measurement could barely predict yield parameters of heterogeneous pastures, whereas sensor data fusion by combining ultrasonic sward height (USH) with narrow band normalized difference spectral index (NDSI) or WorldView2 (WV2) satellite broad bands increased the prediction accuracy significantly. These combinations can be on a par or even better than the use of the full hyperspectral information. Spectral regions related to plant water content were found to be most important (996-1225 nm). Narrow-band NDSI constructed with bands in these spectral regions may be preferred for research purposes where highest accuracy is essential, whereas WV2 provides interesting perspectives for practical implementation, as these bands are already implemented on satellite platforms. Fusion of ultrasonic and spectral sensors is a promising approach to assess biomass even in pastures with heterogeneous swards. However, the applicability of such concepts may be limited in the second half of the growing season due to an influence on biomass prediction accuracy of both, sward development along the vegetation period and the presence of senesced material.

3.1 Introduction

An accurate estimation of biomass is needed to understand the spatio-temporal changes of forage resources in pasture ecosystems and to support grazing management decisions (Cho et al., 2007). However, a timely evaluation of biomass is a challenge, as it requires targeted and efficient means to assess numerous data for the creation of continuous maps. Though the traditional ‘’clip-and-weigh’’ methods of measuring biomass are highly accurate, they are costly, destructive, labor intensive and time consuming to obtain biomass properties at high sampling density. Ground-based remote sensing techniques have been used alternatively as rapid and non-destructive methods to

obtain and map the temporal and spatial variability of vegetation characteristics with high spatial resolution in agricultural and pastoral ecosystems (Pullanagari et al., 2012a; Suzuki et al., 2012). Pastures are highly heterogeneous systems due to variations in sward structure, composition and phenology as well as continuous changes caused by different drivers such as environmental factors and grazing. Therefore, the application of sensors in complex grazing systems is difficult and there are some limitations for each specific sensor used for the prediction of sward characteristics (Schellberg et al., 2008). To overcome these constraints, the combination of complementary sensor technologies has been suggested to utilize both the strengths and compensate the weaknesses of individual technologies. Combined sensor systems can support multi-source information acquisition and may provide more accurate property estimates and eventually improved management (Adamchuk et al., 2011). Even though some studies have investigated such strategies in different farming fields (Jones et al., 2007; Mazzetto et al., 2010; Farooque et al., 2013), to date these techniques have not been tested in pastures with complex sward diversity. Thus, an evaluation of sward specific calibration is essential, before assessing data on a spatial scale.

Ultrasonic and reflectance sensors are two possible complementary technologies capable of providing comprehensive structural and functional characteristics of vegetation (Scotford and Miller, 2004; Farooque et al., 2013). Sward height measured by ultrasonic distance sensing (referred to as ultrasonic sward height (USH)) has been examined as a possible estimator of biomass in forage vegetation canopies (Hutchings et al., 1990). However, the main limitation of this technique is that signals are reflected predominantly from the upper canopy layers regardless of sward density (Fricke and Wachendorf, 2013). Moreover, sonic reflections can be affected by canopy architecture such as lamina size, orientation, angle and surface roughness of the leaves (Hutchings, 1992).

Hyperspectral sensors have also raised considerable interest as a potential tool for prediction of biomass and forage quality in pastures. However, difficulties occur at advanced developmental stages of vegetation, as the ability of the reflectance sensor to detect canopy characteristics could be limited by the presence of a high fraction of senescent material in biomass (Yang and Guo, 2014) or by soil background effects (Boschetti et al., 2007), atmospheric conditions (Jackson and Huete, 1991), grazing impact (Duan et al., 2014) and heterogeneous canopy structures due to mixed species composition and a wide range of phenological stages (Biewer et al., 2009a, b). Remarkably, most studies on remotely sensed data for the estimation of grassland and rangeland biomass were

conducted in tropical savannas, since these ecosystems account for 30% of the primary production of all terrestrial vegetation. Contrary, comparable studies on grasslands in temperate climates are rare (Kumar et al., 2015).

The limitations of ultrasonic and hyper-spectral reflectance sensors in heterogeneous pastures may be compensated by a combined use of measurement data from both sensors, as shown by Fricke and Wachendorf (2013) for less variable legume/grass-mixtures. Thus, the main objective of the present study was to analyze the potential of ultrasonic and hyper-spectral sensor data fusion in pastures with high structural sward diversity to predict biomass, which is a prerequisite for future mapping of spatially heterogeneous grassland.

3.2 Materials and methods

3.2.1 Study area and site characteristics

For data acquisition a long-term pasture experiment was chosen at the experimental farm Relliehausen of the University of Goettingen (51°46′55″N, 9°42′13″E, 180-230 m above mean sea level; soil type: pelosol-brown earth; soil PH: 6.3; mean annual precipitation: 879 mm; mean annual daily temperature: 8.2°C). The plant association was a moderately species-rich *Lolio-Cynosuretum* (Wrage et al., 2012). The pastures exhibited a pronounced heterogeneity in sward structure with short and tall patches and various sward height classes (Scimone et al., 2007, Jerrentrup et al., 2014). Three levels of grazing intensity were allocated to adjacent pasture paddocks of 1 ha size, which were continuously stocked by cows from beginning of May to mid-September. Grazing intensities were a) moderate stocking, average of 3.4 standard livestock units (SLU, i.e. 500 kg live weight) ha^{-1}, b) lenient stocking, average 1.8 SLU ha^{-1}, c) very lenient stocking, average 1.3 SLU ha^{-1}(Wrage et al., 2012). To ensure extensive sward variation for data assessment, one representative study plot of 30 x 50 m size was selected within each of the three paddocks using a grazed/ungrazed-classified aerial image to obtain comparable surface proportions.

3.2.2 Field measurements

Field measurements were conducted at four sampling dates (designated from now on as date 1 to date 4) in 2013: (date 1) 25th April to 2nd May (before grazing), (date 2) 3rd to 5th June, (date 3) 21st

to 23rd August and (date 4) 30th September to 2nd October (after final grazing) within each study plot . In each campaign 18 reference sample plots (each 0.25 m^2) were chosen within each of the 3 study plot adding up to 54 samples per date and representing the occurring range of available biomass levels and sward structures. To verify a representative biomass range a stratified random sampling was performed. In each study plot three levels of sward height (low, medium, high) were sampled randomly to compile all date specific biomass levels in the data set. A Trimble GeoXH GPS device (Trimble Navigation Ltd., Sunnyvale, California, USA) with DGPS correction from AXIO-net (Hannover, Germany, PED-RTK ±20 mm) was used to avoid repeated sampling at the same location during the growing season.

Sensor measurements took place prior to reference data assessment. Hyperspectral data was measured using a hand-held portable spectro-radiometer (Portable HandySpec Field VIS/NIR, tec5, Germany) in a spectral range of 305-1690 nm. Spectral readings were recorded in 1 nm intervals. Measurements were made from a height of about 1 m above and perpendicular to the soil surface between 10:00 a.m. and 14:00 p.m. (local time) in clear sunshine. The sensor had a field of view of 25 °. Spectral calibrations were performed at least after every six measurements using a greystandard (Zenith Polymer® Diffuse Reflectance Standard 25%). Ultrasonic sward height (USH) measurements took place subsequent to hyperspectral measurements using an ultrasonic distance sensor of type UC 2000-30GM-IUR2-V15 (Pepperl and Fuchs, Mannheim, Germany). The sensor specific sensing range was from 80 to 2000 mm within a sound cone formed by an opening angle of about 25° (Pepperl and Fuchs, 2010). Ultrasonic sward height (mm) was calculated by substracting the ultrasonic distance measurement value in mm from the sensor mount height using EQ 1.

$$USH\ (mm) = Mount\ height\ (mm) - Ultrasonic\ distance\ (mm) \quad \text{(Eq1)}$$

At each sampling plot, five measurements were recorded with the ultrasonic sensors placed at five positions on a frame at a height of about 1 m. Further details of the USH device and methodology can be found in Fricke et al. (2011).

In addition to sensor measurements, plant composition of all sampling plots was assessed according to the method of Klapp and Stählin (1936) by visually estimating the abundance and dominance of all plant species.

3.2.3 Sampling of reference data

The biomass of each sampling plot was cut at ground surface level. Total fresh matter yield was measured and representative sub-samples were either directly dried in the oven for 48 h at 105 °C for the calculation of total dry matter yield or sorted into fractions of grasses, legumes, herbs, mosses and dead material and subsequently also dried at 105 °C for 48h to determine the proportion of each functional group. This data was used as reference values (dependent variables) in regression analysis procedures.

3.2.4 Data analysis

Prior to analysis, an insignificant number of outliers, which appeared as extreme outliers in the box plot analysis (program package R, version 3.0.2), was excluded from the dataset due to incorrectly entered or measured data. Moreover, noisy parts of the hyperspectral data (305-360 nm, 1340-1500 nm and 1650-1700 nm) were eliminated, leaving 1126 spectral bands between 360 and 1650 nm. Datasets were combined using a common dataset (n = 214) comprising samples from all study plots (grazing intensities) and all dates, as well as subsets for each date representing a typical phenological status of plants during the vegetation period (n = 52-54). As a preprocessing step, first-order and second-order derivative reflectance (FDR and SDR) (Demetriades-Shah et al. 1990) and continuum removed reflectance (CR) (Clark and Roush, 1984) were calculated from the original spectrum using WinISI III package (Infrasoft International, LLC. FOSS, State College, PA, version 1.63) and ENVI 4.7, respectively. These methods are supposed to reduce background reflectance influence and to enhance absorption spectral features. In order to compare the prediction potential of the original and transformed spectra (FDR, SDR, CR) modified partial least squares regression (MPLSR) was applied as a powerful and full-spectrum based method using WINISI III package (Infrasoft International, LLC. FOSS, State College, PA, version 1.63). Several methods were used to combine the spectral information with USH by ordinary least square regression. To evaluate the potential of hyperspectral data in combination with USH, principle component analysis (PCA) was performed as a hyperspectral compression tool in SAS version 9.2 (SAS Institute, Inc., Cary, NC, USA) to calculate a maximum of 5 principal components explaining 99 % of variance. Furthermore several published vegetation indices (VIs) recently applied to grassland swards (Reddersen et al., 2014) were calculated: normalized difference vegetation index (NDV), red edge inflection point (REIP), soil adjusted vegetation index (SAVI) and water index

(WI). To evaluate the potential of a 2-band vegetation index across the available hyperspectral range, the normalized difference spectral index (NDSI) (Inoue et al. 2008) was applied over the range of 1nm and 50nm spectral bandwidths using all possible combinations of two-band reflectance ratios based on NDVI formula according to Eq 2:

$$\mathrm{NDSI}(b1, b2) = b1 - b2 / b1 + b2 \quad \text{(Eq2)}$$

where, $b1$ and $b2$ = represents spectral bands of reflection signals with $\mathrm{Wavelength}_{b1} > \mathrm{Wavelength}_{b2}$ for either specific narrow bands (1 nm) or broad bands (50 nm).

To test the performance of the multi-spectral approach used in satellites, hyperspectral data were re-combined into 8 broad wavebands according to WorldView-2: coastal (400-450 nm), blue (450-510 nm), green (510-580 nm), yellow (585-625 nm), red (630-690 nm), red edge (705-745 nm), near infrared-1 (770-895 nm) and near infrared-2 (869-900 nm) (http://www.landinfo.com/WorldView2.htm) and 5 broad bands according to RapidEye: blue (440-510 nm), green (520-590 nm), red (630-685 nm), red edge (690-730 nm) and near infrared (760-850 nm) (http://www.satimagingcorp.com/satellite-sensors/other-satellite-sensors/rapideye.htm).

Ordinary least squares regression analysis was performed using the statistical program package R (version 3.0.2) to examine the relationship between the dependent variables (fresh matter yield, dry matter yield and dead material proportion) and USH (Eq3), VIs, satellite bands and PCA-derived components exclusively (Eq 4 and 5) and as a combination of USH with variables calculated from hyperspectral data (Eq 6 and 7) to compare their potential for sensor fusion. After having examined the data and verified, that saturation effects could be excluded, it was assumed, that squared variables would sufficiently represent possible non-linear effects. Even though, due to a limited sample size of $n \leq 54$ squared satellite band variables and squared PCA-derived components were omitted in the regressions to reduce the risk of over-fitting.

Exclusive ultrasonic sward height

$$Y = \mathrm{USH} + \mathrm{USH}^2 \quad (3)$$

Exclusive vegetation index

$$Y = \mathrm{VI} + \mathrm{VI}^2 \quad (4)$$

Exclusive satellite bands or PCA-derived components

$$Y = X1 + X2 + \cdots + Xn \quad (5)$$

Combination of ultrasonic sward height and vegetation index

$$Y = USH + VI + USH * VI + USH^2 + USH^2 * VI + VI^2 + USH * VI^2 + USH^2 * VI^2 \quad (6)$$

Combination of ultrasonic sward height (USH) and satellite bands or PCA-derived components

$$Y = USH + USH^2 + X1 + X2 + \cdots + Xn + USH * X1 + \cdots + USH * Xn + USH^2 * X1 + \cdots + USH^2 * Xn \quad (7)$$

where:

Y = fresh matter yield (FMY) (gm^{-2}), dry matter yield (DMY) (gm^{-2}) or dead material proportion (DMP) (% of DMY), respectively.

USH = ultrasonic sward height (mm)

VI = vegetation index derived from hyperspectral data

X = satellite bands or PCA derived components

To determine the best NDSI wavebands having maximum r^2, a wavelengths selection was first conducted according to Eq 4 and Eq 6 for each target parameter. Thus, all possible 2-band NDSI combinations, in all a total of 1,267,876 indices, were individually used in linear regression models for each sensor combination. The best fit wavelengths for the full models were then used to develop regression models. According to the rules of hierarchy and marginality (Nelder, 1994), non-significant effects were excluded from the models, but were retained if the same variable appeared as part of a significant interaction at α-level of 5%. Models were validated by a four-fold cross validation method (Diaconis and Efron, 1983).

3.3 Results and discussion

3.3.1 Sward characteristics

Biomass as FMY and DMY varied from 68.8 to 3207 g m^{-2} and from 29.2 to 691.9 g m^{-2} with an overall mean value of 823.9 g m^{-2} and 276.4 g m^{-2}, respectively, for all sampling dates (Table 3.1). The second sampling date (date 2) at the beginning of June exhibited the highest biomass (mean value of 1240 g m^{-2} and 314.5 g m^{-2} for FMY and DMY, respectively), whereas the date 4 showed the lowest biomass (mean value of 567.5 g m^{-2} and 237.6 g m^{-2} for FMY and DMY, respectively). USH ranged from 7 to 646 mm during the growing season and lowest sward heights were found at date 1 (mean value = 136 mm). A wide range of DMP (1.4 to 83.6% of DM; sd = 20.5) was observed throughout the growing season. The highest variability of DMP was observed at more

advanced developmental stages of swards (date 3 and 4; sd = 18.8 and 17.7% of DMY, respectively) which also delivered the highest mean values of DMP (45.7 and 40% of DMY, respectively). Grass proportion was always considerably higher than proportions of legumes and herbs. Moss proportion was negligible (overall mean value 1.9%). In total, 48 species were identified in the sampling plots (Table 3.2). Most important species were *Dactylis glomerata* (Constancy, C = 89.7%), *Lolium perenne* (C = 70.1%) among the grasses, *Trifolium repens* (C = 39.7%) and *Trifolium pratense* (C = 17.8%) among the legumes, and *Taraxacum officinale* (C = 57.5%) and *Galium mollugo* (C = 40.7%) among the herbs.

Table 3.1 Descriptive statistics of dry matter yield, fresh matter yield, ultrasonic sward height and proportion of mosses grasses, legumes, herbs and dead materials for common and date-specific swards.

	N	Min	Max	Mean	sd[e]	Min	Max	Mean	sd
			Dry matter yield (g m-²)				Fresh matter yield (g m-²)		
Common	214	29.2	691.9	276.4	145.5	68.8	3207.0	823.9	554.6
Date 1 [a]	54	51.9	612.1	248.8	130.0	140.0	1883.0	739.6	416.9
Date 2 [b]	54	31.9	691.9	314.5	180.2	107.2	3207.0	1240.0	785.6
Date 3 [c]	52	68.2	654.8	305.7	138.1	148.0	1822.0	745.4	337.0
Date 4 [d]	54	29.2	468.8	237.6	112.7	68.8	1325.0	567.5	281.7
			Ultrasonic sward height (mm)				Grass proportion (% of DM)		
Common	214	7	646	252	151	8.0	93.7	50.6	23.9
Date 1	54	7	438	136	99	12.9	81.1	44.9	16.8
Date 2	54	31	646	364	174	8.2	93.7	72.2	19.0
Date 3	52	105	615	268	119	8.8	92.9	41.9	24.8
Date 4	54	48	576	240	107	8.0	85.3	43.1	20.6
			Legume proportion (% of DM)				Moss proportion (% of DM)		
Common	214	0.0	39.6	2.9	6.8	0.0	27.5	1.9	4.4
Date 1	54	0.0	36.4	4.7	8.2	0.0	21.3	4.9	6.1
Date 2	54	0.0	39.6	4.1	9.0	0.0	14.7	0.7	2.4
Date 3	52	0.0	31.2	1.9	5.0	0.0	27.5	1.6	4.4
Date 4	54	0.0	7.1	0.6	1.6	0.0	5.8	0.3	0.9
			Herb proportion (% of DM)				Dead material proportion (% of DM)		
Common	214	0.0	63.7	13.1	12.9	1.4	83.6	31.6	20.5
Date 1	54	0.0	44.6	13.6	12.7	2.5	70.3	31.9	14.9
Date 2	54	0.0	63.7	13.9	15.0	1.4	37.6	9.2	6.4
Date 3	52	0.0	47.5	14.6	12.8	3.9	76.3	40.0	18.8
Date 4	54	0.0	42.1	10.3	10.8	10.5	83.6	45.7	17.7

[a] Date 1: 25th April-2nd May 2013 ; [b] Date 2: 3rd-5th June 2013; [c] Date 3: 21st-23rd August 2013; [d] Date 4: 30th September-2nd October 2013. [e] sd: standard deviation.

Table 3.2 List of pasture species identified in 214 sampling plots in 2013 with their minimum, maximum and mean values of dry matter contribution estimated according to the Klapp and Stählin method. Constancy (Const.) refers to the relative proportion of plots containing the respective species.

Species	Min	Max	Mean	Const. (%)	Species	Min	Max	Mean	Const. (%)
Grasses					**Herbs**				
Agrostis stolonifera	0.0	79.4	9.22	54.2	*Achillea millefolium*	0.0	85.0	0.92	5.1
Alopecurus pratensis	0.0	95.0	3.83	13.6	*Anthriscus sylvestris*	0.0	28.0	0.13	0.5
Arrhenatherum elatius	0.0	1.0	0.00	0.5	*Bellis perennis*	0.0	59.0	0.31	2.3
Bromus mollis	0.0	7.0	0.10	3.7	*Centaurea jacea*	0.0	1.0	0.00	0.5
Cynosurus cristatus	0.0	59.6	1.77	10.3	*Cerastium holosteoides*	0.0	4.0	0.23	19.6
Dactylis glomerata	0.0	94.0	25.68	89.7	*Cirsium arvense*	0.0	40.0	1.14	9.3
Deschampsia caespitosa	0.0	90.0	0.59	0.9	*Cirsium vulgare*	0.0	15.0	0.30	7.0
Elymus repens	0.0	80.0	5.82	36.9	*Convolvulus arvensis*	0.0	28.6	0.39	6.1
Festuca pratensis	0.0	85.0	0.71	5.6	*Crepis capillaris*	0.0	20.0	0.38	6.1
Festuca rubra	0.0	95.4	4.85	21.0	*Erophila verna*	0.0	4.0	0.04	4.7
Lolium perenne	0.0	88.6	15.64	70.1	*Epilobium spec.*	0.0	16.0	0.20	4.7
Phleum pratense	0.0	4.0	0.06	2.3	*Galium mollugo*	0.0	88.0	9.67	40.7
Poa annua	0.0	1.0	0.01	0.9	*Geranium dissectum*	0.0	13.0	0.20	13.6
Poa pratensis	0.0	45.0	2.32	27.6	*Geum urbanum*	0.0	30.0	0.19	3.3
Poa trivialis	0.0	16.0	1.28	25.2	*Hieracium pilosella*	0.0	0.2	0.00	0.5
					Lamium purpureum	0.0	38.0	0.21	2.3
Legumes					*Leontodon hispidus*	0.0	2.0	0.02	1.9
Medicago lupulina	0.0	5.0	0.03	0.9	*Plantago lanceolata*	0.0	35.0	0.56	10.7
Trifolium campestre	0.0	20.0	0.17	1.9	*Plantago major*	0.0	3.0	0.01	0.5
Trifolium dubium	0.0	25.0	0.18	3.7	*Taraxacum officinale*	0.0	83.0	5.89	57.5
Trifolium pratense	0.0	61.0	1.50	17.8	*Ranunculus acris*	0.0	10.0	0.20	6.5
Trifolium repens	0.0	49.6	2.49	39.7	*Ranunculus repens*	0.0	71.8	1.35	23.8
Vicia cracca	0.0	1.0	0.00	0.5	*Rosa spec.*	0.0	5.0	0.04	0.9
					Rumex acetosa	0.0	4.0	0.03	1.4
					Urtica dioica	0.0	84.0	1.09	2.8
					Veronica chamaedrys	0.0	4.0	0.03	1.9
					Veronica serpyllifolia	0.0	35.0	0.19	1.9

3.3.2 Exclusive use of ultrasonic sward height

Prediction accuracies for DMY and FMY varied significantly between sampling dates and were predominately low (Tables 3.3 and 3.4). Higher accuracies were achieved at date 1 both for DMY and FMY (r^2 = 0.74 and 0.81 respectively) where sward heights were much lower than at later dates. Lowest r^2 values were found at date 3 and 4 (<0.45). With advancing grazing season, height of swards seems to be a poor indicator of biomass, as partly utilized patches were short but biomass was denser. In addition, some species like Dactylis glomerata and Festuca rubra frequently grow in dense tussocks and produce high biomass at low height, which is results in an underestimation of biomass (Figure. 3.1). In some patches rejected by animals, very tall and mature species like Cirsium arvense, elongated stems of Galium mollugo or very tall and sparse individuals of Phleum pratensis at inflorescence stage, probably boosted USH measures although the amount of biomass was not very high. Sward types like this may tend to be over-estimated (Figure 3.1). This influence was also observed by Fricke et al. (2011), who further showed that the relationship between forage mass and USH could also be influenced by weed proportion, as some weeds grow higher than the sown species. Beside the heterogeneity of canopy structure, variation in leaf angles among plant species and movements of swards during measurement due to wind may have further affected the reflection of ultrasonic signal (Hutchings et al., 1990; Hutchings, 1992). DMP had very weak or no correlation with USH and, thus, data were not shown. It can be summarized that exclusive USH measurements only produced low prediction accuracies for yield parameters in heterogeneous pastures.

Table 3.3 Regression and cross validation (CV) results for a range of sensor models used for prediction of dry matter yield (DMY) in exclusive application or as combination of ultrasonic sward height (USH) with a selection of relevant spectral variables on common and date-specific swards.

	Exclusive				combination with USH			
	SE [a]	r^2 [b]	RMSEcv[c]	r^2cv [d]	SE	r^2	RMSEcv	r^2cv
Common (N [e] = 214)								
USH	109.9	0.43	112.0	0.42				
MPLSR [g]	94.0	0.56	101.5	0.48				
PCA [h]	130.0	0.21	131.5	0.19	97.6	0.57	99.7	0.49
WV2 [i]	137.0	0.13	137.5	0.09	93.3	0.62	96.5	0.48
NDSI [j]	121.0	0.31	121.5	0.30	98.4	0.55	99.3	0.52
Date 1 [k] (N = 54)								
USH	67.5	0.74	68.8	0.73				
MPLSR	52.4	0.80	80.3	0.63				
PCA	97.1	0.46	99.4	0.44	55.6	0.84	73.8	0.56
WV2	96.6	0.48	97.2	0.41	53.5	0.88	84.20	0.61
NDSI	81.2	0.62	82.7	0.61	48.5	0.88	55.9	0.80
Date 2 [l] (N = 54)								
USH	133.0	0.47	134.1	0.45				
MPLSR	79.9	0.80	90.1	0.79				
PCA	106.0	0.67	109.7	0.59	92.4	0.77	103.8	0.63
WV2	109.0	0.65	114.4	0.60	84.6	0.83	97.8	0.60
NDSI	95.7	0.72	95.9	0.70	81.5	0.80	83.4	0.77
Date 3 [m] (N = 52)								
USH	111.8	0.36	112.0	0.31				
MPLSR	100.3	0.47	130.5	0.15				
PCA	n.s.[f]	n.s.	n.s.	n.s.	108.0	0.44	108.2	0.19
WV2	116.0	0.36	124.8	0.18	102.0	0.54	120.4	0.25
NDSI	104.9	0.43	106.4	0.38	86.6	0.66	110.9	0.11
Date 4 [n] (N = 54)								
USH	86.8	0.42	91.9	0.37				
MPLSR	52.5	0.76	57.5	0.76				
PCA	86.2	0.46	94.5	0.35	72.3	0.69	95.3	0.45
WV2	86.5	0.44	88.8	0.34	69.0	0.73	194.5	0.46
NDSI	77.6	0.55	82.5	0.41	65.0	0.72	90.3	0.46

[a] SE: Standard error of regression (g m^{-2}).
[b] r^2: Regression coefficient of determination.
[c] RMSEcv: Root mean square error of cross validation (g m^{-2}).
[d] r^2cv: Cross validated coefficient of determination.
[e] N: Number of sampling plots.
[f] n.s.: Non-significant effect.
[g] MPLSR: Modified partial least square regression comprising the whole range of hyperspectral data.
[h] PCA: Principle component analysis derived components.
[i] WV2: WorldView2 satellite broad bands.
[j] NDSI: Narrow band normalized spectral vegetation index.
[k] Date 1: 25th April-2nd May 2013; [l] Date 2: 3rd-5th June 2013; [m] Date 3: 21st-23rd August 2013; [n] Date 4: 30th September-2nd October 2013.

Table 3.4 Regression and cross validation (CV) results for a range of sensor models used for prediction of fresh matter yield (FMY) in exclusive application or as combination of ultrasonic sward height (USH) with a selection of relevant spectral variables on common and date-specific swards.

	exclusive				combination with USH			
	SE [a]	r^2 [b]	RMSEcv[c]	r^2cv [d]	SE	r^2	RMSEcv	r^2cv
Common (N [e] = 214)								
USH	417.0	0.44	424.9	0.42				
MPLSR [g]	281.5	0.69	290.2	0.67				
PCA [h]	444.0	0.37	448.4	0.35	278.0	0.76	285.7	0.66
WV2 [i]	482.9	0.25	486.3	0.24	288.0	0.74	296.7	0.62
NDSI [j]	349.5	0.61	350.7	0.59	288.4	0.74	299.5	0.63
Date 1 [k] (N = 54)								
USH	184.0	0.81	187.7	0.80				
MPLSR	154.8	0.86	216.2	0.78				
PCA	269.0	0.61	288.3	0.57	152.0	0.88	169.0	0.84
WV2	288.0	0.55	299.2	0.46	140.0	0.91	147.92	0.83
NDSI	253.8	0.64	274.8	0.60	122.6	0.92	132.2	0.90
Date 2 [l] (N = 54)								
USH	586.0	0.46	617.5	0.40				
MPLSR	257.7	0.89	319.0	0.86				
PCA	378.0	0.78	419.8	0.73	336.0	0.83	377.3	0.76
WV2	426.0	0.72	444.1	0.67	318.0	0.86	338.5	0.74
NDSI	362.8	0.79	377.1	0.77	344.2	0.82	340.0	0.75
Date 3 [m] (N = 52)								
USH	303.0	0.21	306.5	0.12				
MPLSR	221.9	0.57	306.1	0.33				
PCA	n.s.[f]	n.s.	n.s.	n.s.	246.0	0.51	257.6	0.30
WV2	272.0	0.40	287.9	0.25	239.0	0.57	257.5	0.32
NDSI	258.1	0.42	262.2	0.37	204.4	0.68	257.6	0.40
Date 4 [n] (N = 54)								
USH	214.0	0.45	231.2	0.39				
MPLSR	147.35	0.65	158.3	0.68				
PCA	225.0	0.39	240.8	0.35	209.0	0.47	216.8	0.44
WV2	220.0	0.43	226.7	0.32	184.0	0.68	243.9	0.43
NDSI	217.8	0.41	229.4	0.36	184.1	0.63	236.1	0.38

[a] SE: Standard error of regression (g m^{-2}).
[b] r^2: Regression coefficient of determination.
[c] RMSEcv: Root mean square error of cross validation (g m^{-2}).
[d] r^2cv: Cross validated coefficient of determination.
[e] N: Number of sampling plots.
[f] n.s.: Non-significant effect.
[g] MPLSR: Modified partial least square regression comprising the whole range of hyperspectral data.
[h] PCA: Principle component analysis derived components.
[i] WV2: WorldView2 satellite broad bands.
[j] NDSI: Narrow band normalized spectral vegetation index.
[k] Date 1: 25th April-2nd May 2013; [l] Date 2: 3rd-5th June 2013; [m] Date 3: 21st-23rd August 2013; [n] Date 4: 30th September-2nd October 2013.

3.3.3 Exclusive use of spectral data

MPLSR analysis revealed that the unprocessed reflectance data showed better correlation with the target parameters than the transformed reflectance data (FDR, SDR, CR). Therefore, original reflectance data were used for further analysis. Models developed with published VIs gave low r^2-values and so the results are not presented here. Poor prediction of published VIs has also been found in other studies (Cho et al., 2007; Biewer et al., 2009a; Duan et al., 2014). Obviously, a reduction of spectral information to only two or three wavelengths, as with published VIs, does not suffice to cover the high variability within pastures. The location of best fit wavelengths using NDSI for 1 nm bandwidths were mostly the same as for the 50 nm band widths for DMY and FMY in common, date 1 and 2 dataset, as well as for DMP in common and date-specific swards. This finding is in line with results of Reddersen et al. (2014) for prediction of biomass using NDSI as exclusive parameter or in combination with USH and leaf area index. However, best fit narrow and broadband wavelengths were not identical for FMY and DMY at date 3 and 4. Maximum r^2 of full models based on 1 nm bandwidth was up to 19% higher than with 50 nm. This result does not correspond with findings of Fricke and Wachendorf (2013) who found no substantial losses in prediction accuracy with increasing bandwidths for high yielding legume/grass mixtures. However, this corresponds with other findings (Thenkabail et al., 2000; Mutanga and Skidmore, 2004; Peng Gong et al., 2003) where narrow bands performed better than broad bands. Therefore, NDSI indices based on narrow bands were chosen to develop sensor models. Maximum prediction accuracy based on exclusive narrow band NDSI were found mostly with bands between 1035 and 1139 nm, i.e. the ascending slope of the first water absorption band and the descending slope of the second water absorption band. The ascending slope of the second water absorption band (1188 to 1305 nm) was found the most important part of the spectrum for prediction of DMP (Table 3.5). Among exclusive sensor procedures, MPLSR prediction accuracy was best both for DMY (r^2 of 0.56 for common and 0.47 - 0.80 for date-specific models) and FMY (0.69 and 0.57 - 0.89 respectively) (Tables 3.3 and 3.4). This approach integrates spectral information of the whole hyperspectral range and has also been addressed to be successful in other studies for measuring grassland properties (Biewer et al., 2009a; Marabel and Alvarez-Taboada, 2013; Pellissier et al., 2015; Thulin et al., 2012). Although MPLSR is a robust method to adequately predict biomass, it is not feasible for a livestock manager to implement the technique, as purchasing a full range hyperspectral radiometer is far too expensive (Starks et al., 2006). In order to reduce the number of wavebands, PCA was adopted to the spectra and five principal components (PC) were identified accounting for

99% of the variation in data. Remarkably, PCs showed weak relationships with DMY ($r^2 = 0.21$), FMY ($r^2 = 0.37$) and DMP ($r^2 = 61$) for common dataset. Prediction accuracy did not exceed r^2 0.67 by separation of dataset into sampling dates. No significant correlation was found between FMY or DMY and PCA derived components at date 3. For the other dates, accuracy of PCA was always below NDSI but well above RapidEye satellite bands (RE; data not shown). Although the predictive power of WorldView2 (WV2) bands (r^2 0.13 - 0.55) was slightly better than RE bands (r^2 of 0.13 - 0.48) results obtained were not satisfactory.

Most spectral variables gave better prediction accuracies than exclusive USH measurements. This finding does not match with that of Fricke and Wachendorf (2013) and Reddersen et al. (2014) who reported that exclusive USH always achieved better results than exclusive narrow and broad band VIs for prediction of biomass in more homogeneous grasslands. Contrary to yields, separation of the common dataset into date specific subsets did not improve prediction accuracy for DMP based on spectral information (Table 3.6). Yang and Guo (2014) found that the relationship between dead material cover and VIs is a function of the amount of dead material and they concluded that spectral VIs could be used for estimating dead material cover which is greater than 50% in mixed grasslands. In this respect, the lower model accuracies for yield at later dates may be partly attributed to the higher amount of dead material at this time. The higher proportion of explained variance in DMP by spectral variables may reflect the impact of dead materials on the canopy reflectance at date 3 ($r^2 = 0.50$-0.70) and, to a lesser degree, at date 1 ($r^2 = 0.32$-0.67) and date 4 ($r^2 = 0.41$-0.68). In contrast, DMP is much lower at date 2, which corresponds to lower R^2 values for DMP prediction (0.16-0.25) (Table 3.6), but allows higher accuracies for yield prediction, as low levels of DMP are inversely related to higher proportions of green plant material. This is consistent with findings by Chen et al. (2010), who pointed out that spectral indicators usually collect data over green vegetation rather than mature and dry vegetation. To summarize, yield of pastures with complex sward structures could barely be predicted using exclusive sensor measurements as conducted in this study.

Table 3.5 Wavelength positions of best fit band combination (b1, b2) and maximum r^2 values (r^2 of full model) for the normalized difference spectral index (NDSI) as narrow (1 nm) and broad (50 nm) bands, exclusively and in combination with ultrasonic sward height (USH) to predict target parameters.

	Common (n=214)			Date 1[a] (n=54)			Date 2[b] (n=54)			Date 3[c] (n=52)			Date 4[d] (n=54)		
	r^2	b1	b2	r^2	b1	b2	r^2	b1	b2	r^2	b1	b2	r^2	b1	b2
Dry matter yield (g m^{-2})															
$NDSI_{1nm}$	0.31	1035	1051	0.62	389	609	0.73	1097	1139	0.44	1122	1128	0.55	769	778
$NDSI_{50nm}$	0.28	1018-1068	1019-1069	0.55	377-427	572-622	0.71	1093-1143	1094-1144	0.25	377-427	455-505	0.45	454-504	467-517
USH + $NDSI_{1nm}$	0.55	521	578	0.88	1215	1225	0.81	1024	1031	0.67	1116	1118	0.72	1622	1633
USH + $NDSI_{50nm}$	0.55	498-548	552-602	0.85	1174-1224	1175-1225	0.78	733-783	734-784	0.56	710-760	954-1004	0.63	894-944	900-950
Fresh matter yield (g m^{-2})															
$NDSI_{1nm}$	0.61	1117	1134	0.64	1040	1073	0.80	1080	1104	0.43	1122	1128	0.42	751	782
$NDSI_{50nm}$	0.58	1101-1151	1102-1152	0.58	633-683	643-693	0.78	1091-1141	1092-1142	0.33	499-549	669-719	0.45	454-504	467-517
USH + $NDSI_{1nm}$	0.74	1077	1086	0.93	996	1005	0.83	536	564	0.70	1122	1135	0.65	1621	1633
USH + $NDSI_{50nm}$	0.72	1044-1094	1241-1291	0.90	996-1046	997-1047	0.82	521-571	531-581	0.64	1582-1632	1583-1632	0.62	709-759	907-957
Dead material proportion (% of dry matter yield)															
$NDSI_{1nm}$	0.65	1242	1305	0.54	1231	1285	0.43	1188	1202	0.69	1236	1281	0.70	1187	1206
$NDSI_{50nm}$	0.65	1242-1292	1243-1293	0.53	1166-1216	1260-1310	0.33	1166-1216	1167-1217	0.50	1169-1219	1260-1310	0.63	1166-1216	1168-1218

[a] Date 1: 25th April-2nd May 2013 ; [b] Date 2: 3rd-5th June 2013; [c] Date 3: 21st-23rd August 2013; [d] Date 4: 30th September-2nd October 2013.

Table 3.6 Regression and cross validation (CV) results for prediction of dead material proportion (DMP) using modified partial least square regression (MPLSR) and a set of spectral predictor variables as narrow band normalized spectral vegetation index (NDSI), WorldView2 (WV2) bands and principle component analysis (PCA) derived components on common and date-specific swards.

	SE [a]	r^2 [b]	RMSEcv [c]	r^2cv [d]
Common (N [e] = 214)				
MPLSR	10.1	0.76	10.4	0.74
PCA	13.0	0.61	13.2	0.58
WV2	11.7	0.68	12.0	0.66
NDSI	12.2	0.65	12.3	0.64
Date 1 [f] (N = 54)				
MPLSR	8.0	0.67	10.6	0.46
PCA	12.6	0.32	12.9	0.17
WV2	11.9	0.42	12.6	0.26
NDSI	10.3	0.54	10.7	0.49
Date 2 [g] (N = 54)				
MPLSR	4.5	0.21	4.6	0.19
PCA	5.7	0.25	6.0	0.07
WV2	5.9	0.16	6.1	0.09
NDSI	4.7	0.43	5.2	0.24
Date 3 [h] (N = 52)				
MPLSR	13.37	0.50	14.2	0.43
PCA	11.1	0.66	11.5	0.63
WV2	10.8	0.70	11.5	0.64
NDSI	11.0	0.66	11.5	0.64
Date 4 [i] (N = 54)				
MPLSR	13.6	0.41	13.9	0.39
PCA	12.2	0.54	12.1	0.50
WV2	11.9	0.58	12.8	0.51
NDSI	10.2	0.68	10.5	0.66

[a] SE: Standard error of regression (% DMY).
[b] r^2: Regression coefficient of determination.
[c] RMSEcv: Root mean square error of cross validation (% DMY).
[d] r^2cv: Cross validated coefficient of determination.
[e] N: Number of sampling plots.
[f] Date 1: 25th April-2nd May 2013; [g] Date 2: 3rd-5thJune 2013; [h] Date 3: 21st-23rd August 2013; [i] Date 4: 30th September-2nd October 2013.

3.3.4 Sensor data fusion using combinations of USH and spectral variables

Compared to exclusive use of USH, prediction accuracy of combinations of USH and published VIs showed only minor or no improvement at all (data not shown), which was confirmed by Reddersen et al. (2014) who also found no improvement for such combinations in grasslands applied to three sward types with greater homogeneity comprising a pure stand of reed canary grass (Phalaris aruninacea), a legume grass mixture and a diversity mixture with thirty-six species in an extensive two cut management system.

Combination of USH with the applied spectral variables increased r^2-values for common swards from 0.43 (exclusive USH) to a maximum of 0.62 (WV2 combined with USH) for DMY and from 0.44 (exclusive USH) to a maximum of 0.76 (PCA combined with USH) for FMY in common swards (Tables 3.3 and 3.4). Irrespective of spectral sensor configuration, date-specific calibrations of yield parameter for date 1 and 2 performed better than for date 3 and 4. Obviously, sward structure is so complex at later stages of the grazing season that even sensor combinations did not produce adequate results. Considering the consequences of these limitations for the implementation of sensor data fusion in precision agriculture, it should be noted that the productivity of cool-season pastures is usually highest in the first half of the growing season (Gherbin et al., 2007) when the best results with combined sensor data were obtained. Thus, sensor data fusion gain more importance in this part of the vegetation period, when efficient and timely estimates of available biomass is an important support of grazing management decisions. Further, major management measures (e.g. fertilization; evaluation of botanical sward composition) are also scheduled mainly before summer, where pasture growth is frequently limited by water scarcity or progressively reduced day lengths. Most remarkably, PCA generally performed worse than multi-spectral calibrations, although principal components represented most of the variation in total spectral data. On the other hand, combination of USH and NDSI consistently produced best results both in common and date-specific calibrations. Dominant bands of NDSI were mostly located at water absorption bands similar to exclusive use, i.e. the ascending slop of the first absorption band (between 996 to 1086 nm) and the ascending slope of the second water absorption band (1215 to 1225 nm) as well as the green region in the visible spectrum (521 to 578 nm) (Table 3.5). The dominance of water absorption bands can be explained by the strong relationship between biomass and canopy water content (Anderson et al., 2004; Mutanga and Skidmore, 2004). The importance of water absorption bands for estimating biomass is also confirmed by other investigations (Psomas

et al., 2011; Fricke and Wachendorf, 2013). Numata et al., (2008) found that water absorption features derived from hyperspectral sensors were better measures for estimating pasture biomass compared to VIs, such as Normalized Difference Vegetation Index and Normalized Difference Water Index. Figure 3.1 shows example plots of fit for DMY prediction based on USH and NDSI and provides a comprehensive insight into the effects of sensor combination. It becomes clear that with exclusive sensors, calibration models led to an over-estimation at low levels of DMY, whereas higher values were under-estimated. An improvement of fit by the combination of sensors is obvious for all sampling dates and is presented by a higher r^2-value and a convergence of the regression line to the bisector. Yield predictions in heterogeneous pastures as presented in this study partly show a complex interaction between USH, NDSI and DMP (Figure 3.2). At higher levels of NDSI, DMY and FMY basically follow a linear increase with USH gain, regardless of DMP. In contrast, at low levels of NDSI, DMY and FMY curves show differing trends. While DMY (Figure 3.2A) just shows a parallel shift to lower yield levels, FMY (Figure 3.2B) in swards with high DMP shows a saturated curve, suggesting that high DMP might consist of both compacted xeric material leading to higher yield levels at low sward height and sparse high growing mature shoots reaching higher sward layers without much contribution to yield. In contrast, at low DMP, NDSI seems to be more closely linked to pure bulk density of green vegetation. The inter-relationship between selective grazing and species phenology creates a broad variation of sward structures posing an enormous challenge for any sensor applications.

Comparable to NDSI, WV2 bands also proved to be an effective spectral information in combination with USH. This is of particular interest, as this finding points to the potential of the WordView-2 ® satellite system to provide large-scale images with an acceptable spatial resolution to assess larger pasture areas in farming practice. The relatively high prediction accuracy of WV2 bands particularly in the major growth period in the first half of the year opens up a perspective for the development of future management assistant tools. Continuous biomass monitoring based on advanced multi-spectral satellite images with high spatial resolution like WorldView® and GeoEye® can be used as a basis for decision support for supporting management decision such as planning grazing time and intervals for cattle on pasture paddocks, site specific re-sowing or targeted cut of less-preferred sub-areas, respectively. However, further research is necessary to evaluate the availability of reliable images at a high repetition rate and their combination with sward height data, as for instance derived from radar satellites.

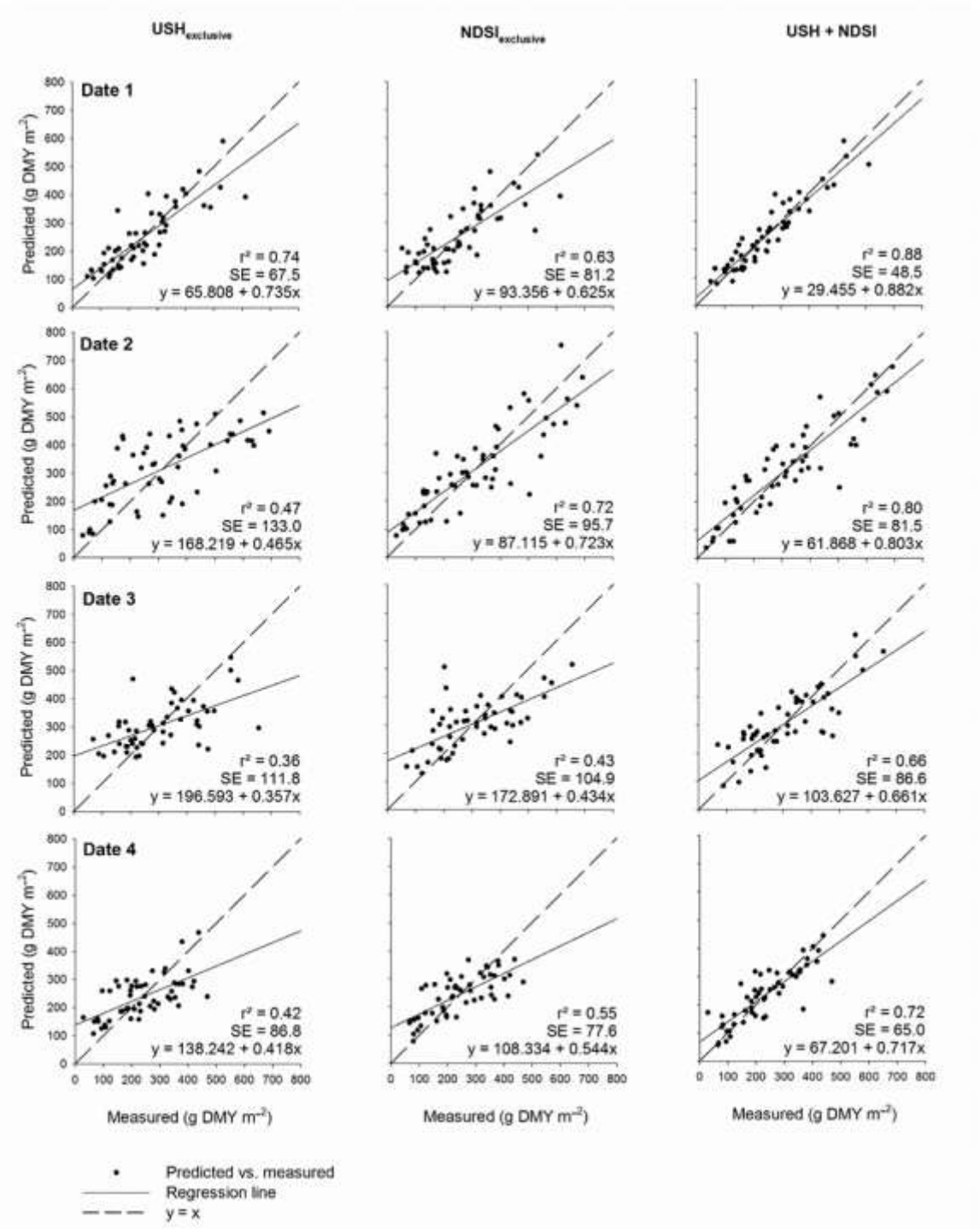

Figure 3.1 Plots of fit between measured and predicted dry matter yield (DMY) for exclusive ultrasonic sward height (USHexclusive), the best fit normalized difference spectral index (NDSIexclusive) and a combination of USH and NDSI (USH + NDSI) applied in date-specific swards: Date 1: 25th April-2nd May 2013, Date 2: 3rd-5th June 2013, Date 3: 21st-23rd August 2013 and Date 4: 30th September-2nd October 2013.

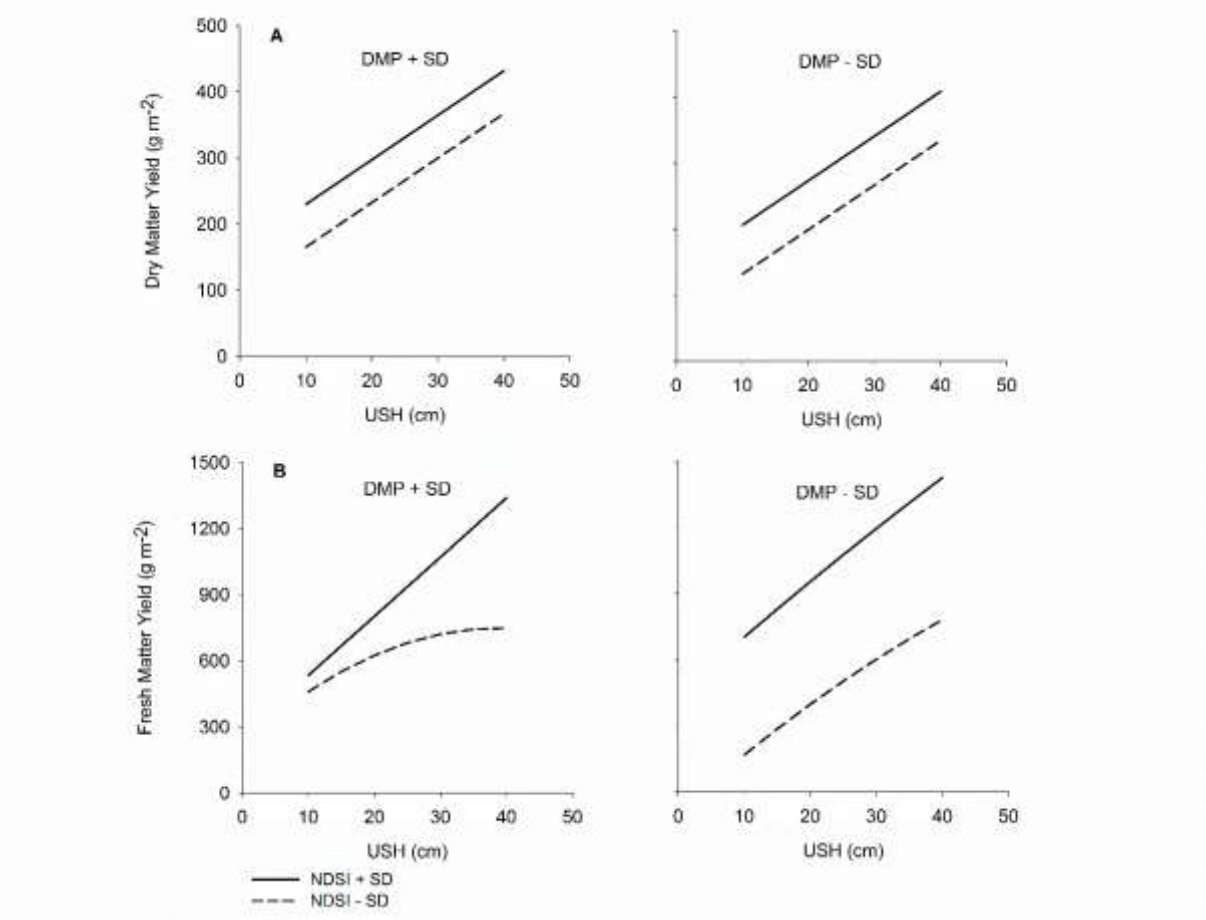

Figure 3.2 Predictions of dry matter yield (DMY) (A) and fresh matter yield (FMY) (B) in common swards based on ultrasonic sward height (USH) and the Normalized Difference Spectral Index (NDSI) as influenced by dead material proportion (DMP) in the range of ± standard deviation (SD). NDSI represents narrow-band reflection values selected in combination with USH for each parameter. For dry matter yield (DMY) (A): $r^2 = 0.57$, SE = 96.98, DMY = 21950 NDSI - 100000 $NDSI^2$ + 41.37 DMP + 6.74 USH - 703.5 NDSI*DMP + 2963 $NDSI^2$*DMP - 1064. For fresh matter yield (FMY) (B): $r^2 = 0.72$, SE = 310.2, FMY = 370.7 + 341100 NDSI + 51920000 $NDSI^2$ - 1.508 DMP + 26.73 USH - 0.067 USH^2 - 7832 NDSI*DMP - 1644000 $NDSI^2$*DP + 3.833 NDSI*DMP*USH^2 + 694.5 $NDSI^2$*DMP*USH^2.

3.4 Conclusions

The main purpose of this study was to explore the potential of sensor data fusion for predicting biomass in heterogeneous pastures. It can be concluded that:

(i) Exclusive ultrasonic sward height or spectral measurement can barely predict yield parameters of heterogeneous pastures.

(ii) Sensor data fusion by combining USH with narrow band NDSI or WV2 satellite broad bands increased the prediction accuracy significantly. These combinations can be on a par or even better than the use of the full hyperspectral information. Spectral regions related to plant water content (996-1225 nm) were found to be most important. Narrow-band NDSI constructed with bands in these spectral regions may be preferred for research purposes where highest accuracy is essential, whereas WV2 provides interesting perspectives for practical implementation, as these bands are already implemented on satellite platforms.

(iii) The presence of a high proportion of senesced material in pastures influences the performance of the sensor systems and may limit the applicability of such concepts in the second half of the growing season. More advanced sensor systems are required to overcome these limitations.

(iv) The present study documents the promising potential of ultrasonic and hyper-spectral sensor data fusion for the prediction of biomass in pastures with high structural diversity, which provides an adequate tool needed for future mapping of spatio-temporal dynamics in heterogeneous grassland.

4 Determination of fibre and protein content in heterogeneous pastures using field spectroscopy and ultrasonic sward height measurements

Abstract Feeding of livestock on pastures requires constant monitoring of diet composition to ensure consistent levels of animal production. The widely used but conventional techniques to measure the components of feed are impractical to obtain in-field forage quality status for making real-time decisions. Assessment of forage quality parameters using proximal sensing is of particular interest. The present study aimed to demonstrate the potential of using a combination of ultrasonic and canopy reflectance data to predict forage quality variables of heterogeneous pastures. A field experiment with pastures continuously grazed by cows with three stocking density treatments (moderate, lenient and very lenient stocking) was used to calibrate ultrasonic and hyperspectral reflectance sensors. Hyperspectral analysis by a modified partial least square regression (MPLSR) resulted in maximum accuracy for the prediction of acid detergent fibre (ADF) and crude protein (CP) (R^2calibration = 0.63-0.85). Any reduction of hyperspectral data into vegetation indices based on few specific narrow wavebands or satellite broadbands reduced prediction accuracy significantly. However, prediction of ADF and CP was improved by a combined analysis of ultrasonic sward height and vegetation indices or satellite broadbands, so that most calibration models exceeded an RPD (Ratio of standard deviation and standard error of prediction) value of 1.4, which is considered as an acceptable predicting capability for variable field condition. Our findings showed that combined sensing systems using reflectance and ultrasonic sensors may provide acceptable prediction accuracies for practical application even under extremely heterogeneous pasture conditions.

4.1 Introduction

Feeding of livestock on pastures requires constant monitoring of diet composition to ensure consistent levels of animal production (Deaville and Flinn, 2000). Pasture quality is highly variable within and between paddocks and during the growing season due to differences in species composition, sward maturity, soil type and topography as well as climatic factors (Pullanagari et al., 2012a). Management decisions such as grazing intensity can also influence pasture quality (Pavlů et al., 2006). The widely used but conventional techniques of wet chemistry and laboratory based VIS/NIR techniques to measure the components of feed quality are expensive, destructive,

and labour and time consuming (Zhao et al., 2007). Moreover, these methods are impractical to determine the in-field forage quality status for making real-time decisions. Ground based (proximal) remote sensing technologies have been recognized as practical means to estimate various biophysical and biochemical properties of vegetation at the field scale (Starks et al., 2006). Assessment of forage quality parameters using proximal sensing of pasture canopy reflectance is of particular interest. While broadband multispectral sensors are considered to have limitations in providing accurate estimates of vegetation characteristics (Thenkabail, 2012), hyperspectral sensors with narrow and near-continuous spectra allow much more detailed spectral information and offer significant improvements over broadband sensors. Partial least square regression (PLSR) is a technique for analysing spectral datasets that employs the whole range of hyperspectral data in the analysis. Several studies have shown that PLSR is a powerful tool to accurately predict forage quality constituents under field conditions (Biewer et al., 2009b; Starks et al., 2004; Li et al., 2014a). However, due to costs and complexity of hyperspectral data, reducing the spectral data range and identification of the best spectral features of hyperspectral information would facilitate simple sensor applications in the field (Biewer et al., 2009b; Li et al., 2014b; Reddersen et al., 2014). One option is the selection of optimal wavebands that provide the best information by developing two-wavelength reflectance ratios from hyperspectral data. Comparisons between traditional vegetation indices (VIs) (which commonly use average spectral information over predetermined broad-band wavelengths) and hyperspectral narrowband VIs showed a lower accuracy of traditional VIs than for narrowband VIs derived from hyperspectral measurements for various vegetation characteristics (Thenkabail et al., 2000; Mutanga and, Skidmore, 2004; Inoue et al., 2008a; Fricke and Wachendorf, 2013).VIs based on visible and NIR reflectance indicate saturation at high biomass values which limit their sensitivity to further changes in biomass accumulation (Cammarano et al., 2014). As selection of specific narrow wavelengths or reducing the hyperspectral range may lead to a loss of spectral information, combining spectral data with information from other sensors may be effective. Sward height measured by ultrasonic distance sensor (referred as ultrasonic sward height (USH)) may provide useful information, as forage quality is known to be negatively correlated with the growth height of the plants (Hofmann et al., 2001; Pavlů et al., 2006; Summers and Putnam, 2008).The combination of ultrasonic and spectral sensors has been previously utilized for the prediction of biomass in sown grasslands with acceptable accuracies (Fricke and Wachendorf, 2013; Reddersen et al., 2014; Pittman et al., 2015).

However, the benefit of such a combined sensing technique for a non-destructive determination of forage quality in heterogeneous pastures has yet to be verified.

In order to reduce hyperspectral information to few variables we tested several approaches, such as normalized difference spectral indices (NDSIs) using narrowband reflectance combination (according to the normalized difference vegetation index (NDVI) type formula), multi-spectral satellite bands (according to 8 broadbands of WorldView2 satellite) and principle component analysis (PCA) derived components. Thus, the goal of this study was to test the performance of those spectral variables derived from hyperspectral data exclusively and in combination with USH and compare it to modified partial least square regression (MPLSR) models for predicting crude protein (CP) and acid detergent fibre (ADF) of heterogeneous pastures, which were continuously stocked by cows with differing stocking density.

4.2 Materials and methods

4.2.1 Study area and site characteristics

The research was conducted on a heterogeneous permanent pasture at the experimental farm Relliehausen of the University of Goettingen in the Solling uplands, Lower Saxony (51°46′55″N, 9°42′13″E, 180-230 m above mean sea level). The site has been described in detail by Wrage et al. (2012). Briefly, the soil was characterized as pelosol-brown with pH of 6.3. Average annual rainfall was 879 mm with an average temperature of 8.2°C. The grassland was a moderately species-rich *Lolio-Cynosuretum*. The one hectare paddocks were continuously stocked by Simmental cows with three stocking density treatments as follow: a) moderate stocking, average of 3.4 standard livestock units (SLU, i.e. 500 kg live weight) per hectare, b) lenient stocking, average of 1.8 SLU per hectare, c) very lenient stocking, average of 1.3 SLU per hectare. Treatments were replicated 3 times and the grazing season lasted from May to October, usually interrupted by breaks in July or August due to insufficient sward productivity.

4.2.2 Field measurements and plant sampling

Field measurements were carried out within one paddock of each stocking density at three sampling dates in 2013 ((i) 3rd to 5th June, (ii) 21st to 23rd August and (iii) 30th September to 2nd October) and 2014 ((i) 20th to 22nd May, (ii) 15th to 17th July and (iii) 23rd to 30th September). For sensor

measurements and plant sampling subplots with the area of 0.25 m^2 were selected and marked in each paddock representing the range of sward compositions and structures. A Trimble GPS device with ASCOS reference data correction (mean horizontal accuracy = 10 cm) was used to avoid repeated subplot locations during two year measurements. Canopy hyperspectral reflectance was acquired at each sampling location using a hand-held spectroradiometer (Portable HandySpec Field VIS/NIR, Tec-5 AG, Germany) in the range from 305 to 1700 nm (Figure 4.1) with 1 nm reading intervals and a field of view (FOV) of 25 ˚. The spectrometer head was held approximately 1 m above the canopy. A gray Spectralon reference panel was used at fixed intervals to calibrate the spectral measurements.

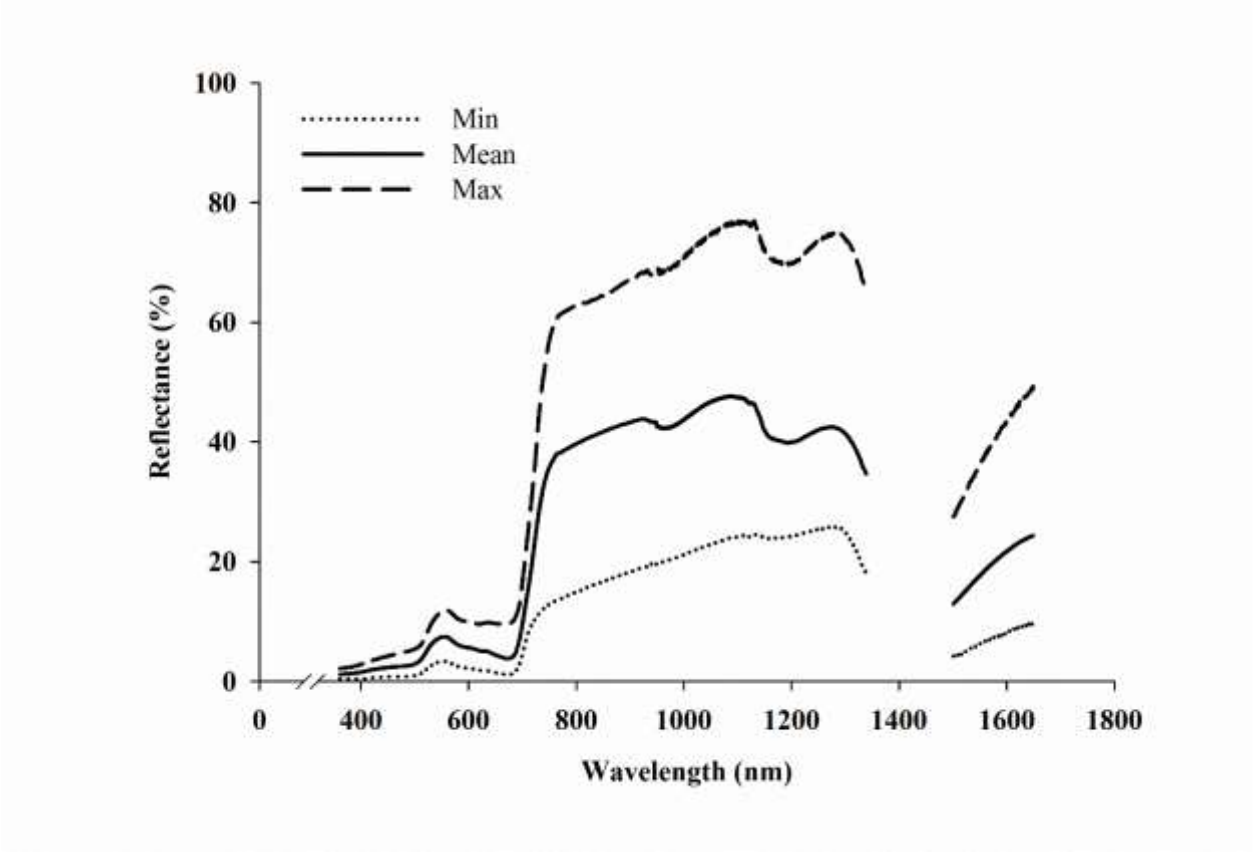

Figure 4.1 Canopy hyperspectral mean, minimum and maximum reflectance derived from each 1nm wavelength calculated for all samples (common swards, N=323).

An ultrasonic distance sensor of type UC 2000-30GM-IUR2-V15 (Pepperl and Fuchs, Mannheim, Germany) was used to gather USH measurements. The beam angel of the device was about 25° and the sensing distance ranged from 0.8 to 200 cm (Pepperl and Fuchs, 2010). The ultrasonic echo was converted into an output voltage linear to the measured distance and subsequently transformed

by an A/D converter into numerical values, logged on a personal computer and finally converted into sward height values using the linear regression EQ 1.

$$y = a - 159.03 + 0.08756\ x \quad \text{(EQ 1)}$$

Where, a = mount height of the ultrasonic sensor above soil surface (cm), x = values from AD/converter (proportional to distance related voltage output), and y = ultrasonic sward height (cm).

At each subplot, five measurements were recorded with the ultrasonic sensors placed at five positions on a frame at a height of about 1 m. The estimated USH for the subplot was calculated as the average value of the five measurements. A detail description of USH device and methodology can be found in Fricke et al. (2011). After sensor measurements were made in each sampling location, all vegetation in the 0.25 m^2 area was clipped at ground surface level. For botanical analysis, a subsample of herbage was separated into fractions of grasses, legumes, herbs, mosses and dead material and dried at 105ºC for 48 h to determine the dry matter (DM) proportion of each functional group.

4.2.3 Assessment of forage quality data

Approximately 100-500 g of sample fresh matter was dried at 65°C for 72 h and were ground with a 1-mm sieve. Subsequently, about 4-10 g of the material was used to determine the spectral signature by lab near-infrared spectroscopy (NIRS).

Nitrogen (N) concentration was determined using an elemental analyser (vario MAX CHN, Elementar Analysesysteme GmbH, Hanau, Germany). The crude protein content was calculated by multiplying N content with 6.25, as protein was assumed to contain 16 % nitrogen on average. ADF content was determined using an ANKOM 200 Fibre Analyzer (ANKOM A200 filter bag technique, ANKOM Company, Macedon, NY). ADF samples were then combusted in a muffle furnace at 550°C for 12 h to measure ash-free acid detergent fibre content. Due to limited lab resources a subdivision of only 176 samples (104 samples in 2013 and 72 samples in 2014) was analysed. Samples were selected by spectral Mahalanobis distance to obtain a representative cross section for the whole dataset. Reflectance spectra of NIRS measurement were obtained using a XDS-spectrometer (Foss NIRSystems, Hillerød, Denmark). With the resulting calibration model (R^2 = 0.97 and 0.96, SE_{CV}= 1.41 and 1.50 % of DM for ADF and R^2 = 0.99 and 0.97, SE_{CV}= 0.08 and 0.10 % of DM for CP in 2013 and 2014, respectively) CP and ADF contents of the remaining

147 samples were predicted. The calculation was done with the WinISI software (version 1.63, Foss NIRSystems/Tecator Infrasoft International, LLC, Silver Spring, MD, USA), using the range between 1100 and 2498 nm.

4.2.4 Data analysis

Prior to analysis, spectral data in the wavelength 305-360 nm, 1340-1500 nm and 1650-1700 nm were eliminated because of visually identified significant signal-noise, leaving 1126 spectral bands between 360 and 1650 nm. Data analysis was performed for four different datasets: a common dataset (N = 323), which comprises data from all levels of stocking density and sampling dates and three subsets for each sampling date from both years, representing the whole range of growth characteristics and plants phenology along the progressing vegetation period (each with N = 108). As a first step, prediction models were developed by applying MPLSR analysis to the original reflectance (raw spectra) and to the first and second derivative transformations of the original reflectance over the whole measured range of the spectrum (360-1650nm) using WINISI III package (Infrasoft International, LLC. FOSS, State College, PA, version 1.63). The number of outlier elimination passes was set to zero in order not to overrate the potential of MPLSR. Derivative spectra were used to reduce the influence of background reflectance and to enhance absorption spectral features for the purpose of creating more robust calibration models. Several approaches were used to reduce the hyperspectral information to few variables which could be combined with USH: the normalized difference spectral index (NDSI) (Inoue et al. 2008) was applied over the range of 1nm spectral bandwidths using all possible combinations of two-band reflectance ratios across the available hyperspectral range based on the NDVI formula:

$$NDSI\ (b1, b2) = b1 - b2 / b1+b2 \qquad (EQ2)$$

Where b1 and b2 are specific narrow band (1 nm) reflection signals with $Wavelength_{b1} > Wavelength_{b2}$.

Hyperspectral data were also re-combined into 8 broad wavebands according to WorldView-2 (WV2) satellite broadbands by calculating an arithmetic mean of the measured reflectance values within each broadband range: coastal (400-450 nm), blue (450-510 nm), green (510-580 nm), yellow (585-625 nm), red (630-690 nm), red edge (705-745 nm), near infrared-1 (770-895 nm) and near infrared-2 (869-900 nm) (http://www.landinfo.com/WorldView2.htm). Finally, principle

component analysis (PCA) was performed to obtain a maximum of 5 principal components explaining 99 % of variance.

Prediction models for acid detergent fibre (ADF) and crude protein (CP) with sensor response variables were generated by multiple linear regression using the lm () of the R software package (R Development Core Team, 2013). ADF and CP were accounted as dependant variables and USH, NDSI, WV2 bands and PCA derived components were accounted for the independent sensor variable in an exclusive approach (EQs 3-5) or in combination with USH (EQs 6 and 7). The starting models included all possible interactions and quadratic terms.

Exclusive ultrasonic sward height

$$y = USH + USH^2 \quad \text{(EQ3)}$$

Exclusive vegetation index

$$Y = NDSI + NDSI^2 \quad \text{(EQ4)}$$

Exclusive satellite bands or PCA derived components

$$Y = X_1 + X_2 + \ldots + X_n \quad \text{(EQ5)}$$

Combination of USH and vegetation index

$$Y = USH + NDSI + USH*NDSI + USH^2 + USH^2*NDSI + NDSI^2 + USH*NDSI^2 + USH^2*NDSI^2 \quad \text{(EQ6)}$$

Combination of USH and WV2 satellite bands or PCA derived components

$$Y = USH + USH^2 + X_1 + X_2 + \cdots + X_n + USH*X_1 + \cdots + USH*X_n + USH^2*X_1 + \cdots + USH^2*X \quad \text{(EQ7)}$$

Where:

Y = ADF (% of DM) or CP (% of DM)

X = WV2 satellite bands or PCA derived components.

n = number of WV2 satellite bands or PCA derived components

USH = ultrasonic sward height (cm)

NDSI = best fit narrowband normalized difference spectral index derived from hyperspectral data.

Saturated starting models included all possible quadratic terms and two-way interactions and were subjected to a stepwise exclusion of non-significant effects at α-level of 5% in agreement with the rules of hierarchy and marginality (Nelder, 1994). All the regression models were cross-validated (CV) according to the four-fold cross-validation method (Diaconis and Efron, 1983). This approach is implemented by dividing the dataset into four groups (folds) of similar size selected randomly, leaving out one of four folds for validation and fitting the models on the other three and then predicting on the held-out data. The procedure is repeated until every fold has been left out once.

The coefficients of determination R^2_c for calibration and R^2_{cv} for cross-validation as well as the root mean squared error (SE_c and SE_{cv}, respectively, were calculated to assess the prediction accuracy. In addition, the residual predictive value (RPD) was determined by dividing the standard deviation of the measured values by the SE_{cv} to compare the performance of all calibrations, irrespective of the units of the parameters (Park et al., 1998). An RPD greater than 2 is considered to be most useful for measurement purposes using infrared spectroscopy in the laboratories. However at variable field conditions lower values of RPD may also be acceptable (Biewer et al., 2009b). Chang et al. (2001) suggested values of RPD larger than 2.0 were excellent, between 1.4 and 2.0 were good and below 1.4 were unreliable to predict diverse soil properties in the laboratory. Aliah Baharom et al. (2015) considered such classification for evaluating the performance of the calibration models to provide quantitative prediction and mapping of the soil properties at the field scale.

4.3 Results and Discussion

4.3.1 Sward characteristics

Across all sampling dates, acid detergent fibre (ADF) and crude protein (CP) in the grassland biomass varied from 9 to 46.9 % of DM and from 5 to 22.6 % of DM with a mean value of 32.7 % of DM and 11.4 % of DM, respectively (Table 4.1). Average ADF content was highest in summer (34.4 % of DM), where a wide range of dead material was found (19.2 % of DM on average) and lowest in spring with 30.5 % of DM, where the least amount of dead material was observed (10.8 % DM on average). CP content showed slightly higher values in autumn (12.6 % of DM) than in other seasons, however, a wider range was observed in the summer (5 to 22.6 % of DM), which may be attributed to the effects of summer grazing. Grazing during the growing season interrupts sward maturation and the associated decline in forage quality. As a result plant developmental changes are postponed and autumn regrowth contains higher than normal levels of nutrients (Rhodes and Sharrow 1990). Contribution of grasses was highest in spring (mean value of 71 % of DM) where they develop fertile tillers and cause increased sward heights, which is also captured by maximum ultrasonic height measurements (33.1 cm). Contrary, growth of grasses in summer was influenced by drought and photoperiodic conditions did not allow the development of fertile tillers, which resulted in lower grass contents (42.6 % of DM on average) and reduced sward height.

Table 4.1 Descriptive statistics of acid detergent fibre (ADF), crude protein (CP), ultrasonic sward height (USH) and proportion of grasses (G), legumes (L), herbs (H) and dead materials (D) in heterogeneous pastures in the common (N=323) and date-specific dataset (N=108).

		Range	Mean (±SD)
ADF (% of DM)	C[a]	9.0-46.9	32.7 (±5.9)
	Sp[b]	20.5-40.5	30.5 (±4.2)
	Sm[c]	9.9-46.9	34.4 (±6.3)
	Au[d]	9.0-46.3	33.2 (±6.4)
CP (% of DM)	C	5.0-22.6	11.4 (±3.1)
	Sp	7.3-17.5	10.6 (±1.9)
	Sm	5.0-22.6	10.8 (±3.6)
	Au	5.5-20.0	12.7 (±3.1)
USH (cm)	C	2.0-64.1	28.1 (±14.0)
	Sp	3.1-64.6	33.1 (±15.8)
	Sm	2.0-61.7	28.2 (±12.5)
	Au	4.0-57.6	23.1 (±11.5)
G (% of DM)	C	7.9-96.3	52.6 (±23.2)
	Sp	8.2-96.3	71.0 (±17.7)
	Sm	8.6-93.0	42.6 (±20.9)
	Au	7.9-85.3	44.1 (±18.9)
L (% of DM)	C	0.0-57.5	3.2 (±7.4)
	Sp	0.0-39.6	3.6 (±7.6)
	Sm	0.0-57.5	3.0 (±8.1)
	Au	0.0-27.4	3.0 (±6.3)
H (% of DM)	C	0.0-84.0	14.4 (±14.2)
	Sp	0.0-63.7	14.0 (±14.0)
	Sm	0.0-84.0	16.6 (±15.7)
	Au	0.0-57.8	12.4 (±12.5)
D (% of DM)	C	1.4-83.6	29.0 (±19.2)
	Sp	1.4-37.6	10.8 (±6.6)
	Sm	3.9-86.3	36.7 (±17.3)
	Au	10.5-83.6	39.5 (±16.3)

[a] C: common dataset; [b] Sp: spring dataset; [C] Sm: summer dataset; [d] Au: autumn dataset

4.3.2 Exclusive use of ultrasonic sward height

Prediction of ADF and CP using exclusive USH resulted in very poor prediction accuracies (Table 4.2). However, higher R^2_c values were achieved for ADF (0.25 to 0.53) compared to CP (0.03 to 0.07). Exclusive USH measurements estimated ADF better in spring (R^2_c = 0.53) probably due to a wider range of USH values. Further, it was only at this time that a positive linear relationship was revealed between USH and ADF. The main limitation of ultrasonic techniques is that signals are reflected predominantly from the upper canopy layers (Fricke and Wachendorf, 2013) and the measured USH might not be an appropriate representative of the whole biomass underneath the surface. Our results confirm the results of Fricke et al. (2011) and Reddersen et al. (2014), who found lower accuracies for biomass prediction when only USH information was available. Overall, the results of the present study indicate that for heterogeneous pasture vegetation it may be difficult to predict ADF and CP accurately only based on canopy height measurements.

Table 4.2 Calibration (C) and cross validation (CV) results for prediction of acid detergent fibre (ADF) and crude protein (CP) in the biomass of heterogeneous pastures from ultrasonic sward height (USH) for common (N=323) and date-specific dataset (N=108).

		R^2_c	SE_c	R^2_{cv}	SE_{cv}	RPD	Md[e]
ADF (% of DM)	C[a]	0.25	5.2	0.23	5.21	1.14	q***
	Sp[b]	0.53	2.90	0.50	2.95	1.43	l***
	Sm[c]	0.31	5.27	0.29	5.33	1.18	q***
	Au[d]	0.30	5.36	0.28	5.34	1.19	q***
CP (% of DM)	C	0.03	3.01	0.03	3.02	1.01	l***
	Sp	0.07	1.83	0.03	1.89	0.99	q*
	Sm	0.04	3.50	0.03	3.59	0.99	q*
	Au	-	-	-	-	-	n.s[f]

[a] C: common dataset; [b] Sp: spring dataset; [C] Sm: summer dataset; [d] Au: autumn dataset. [e] Md: type of regression model: l = linear, q = quadratic; significant at * = 0.05, ** = 0.01, *** = 0.001 probability level. [f] n.s: not significant

4.3.3 Modified partial least square regression analysis of hyperspectral data

The MPLSR analysis revealed that the original reflectance data showed better correlation with the quality parameters than the first and second order derivatives (data not shown). Therefore, only the original reflectance data were used for further analysis. Analysis of the full spectral data using

MPLS regression explained 0.75 and 0.76% of the total variance in the common dataset with SE_{cv} values of 3.47 and 1.79 for ADF and CP, respectively (Table 4.3). However, with RPD values of 1.71 both for ADF and CP the level of accuracy was identical. The RPD values for ADF prediction did not improve by the separation of data into sampling seasons. For prediction of CP an R^2_c value of 0.85 was achieved during the summer and the RPD value exceeded 2.0. Lowest accuracies were achieved for both quality parameter with the autumn dataset. The high amount of accumulated dead material at the end of the grazing season may have impacted spectral reflectance characteristics. Biewer et al. (2009b) received better calibration results and RPD values for the prediction of CP and ADF using MPLSR (R^2_c: 0.70 to 0.93; RPD 1.6 to 3.2) compared to our study, which may be due to the higher level of sward heterogeneity in the present study. A significant number of outliers were excluded during the MPLSR procedure in their analysis, which may have further improved the performance of regression models. The MPLSR results from the present study suggest the potential of a good to approximate estimation of CP and ADF in extremely heterogeneous pastures. Thus, this method may be a useful tool when there is no practical need to limit the number of measured factors in the prediction models (Tobias, 1995). But quite often there exist resource limitations, which restrict the availability of hyperspectral information and suggest the use of a limited set of informative spectral wavelengths.

Table 4.3 Calibration (C) and cross validation (CV) results for prediction of acid detergent fibre (ADF) and crude protein (CP) in the biomass of heterogeneous pastures with the modified partial least square (MPLS) regression for common (N=323) and date-specific dataset (N=108).

		R^2_c	SE_c	R^2_{cv}	SE_{cv}	RPD
ADF (% of DM)	C[a]	0.75	2.96	0.66	3.47	1.71
	Sp[b]	0.75	2.09	0.62	2.60	1.62
	Sm[c]	0.72	3.30	0.65	3.73	1.69
	Au[d]	0.63	3.87	0.50	4.57	1.39
CP (% of DM)	C	0.76	1.51	0.66	1.79	1.71
	Sp	0.70	1.03	0.52	1.30	1.45
	Sm	0.85	1.37	0.77	1.70	2.09
	Au	0.64	1.85	0.63	1.88	1.64

[a] C: common dataset; [b] Sp: spring dataset; [C] Sm: summer dataset; [d] Au: autumn dataset.

4.3.4 Multispectral analysis and combined analysis of multispectral and USH data

The results of models using best fit NDSI and WV2 wavebands exclusively and in combination with USH are presented in Table 4.4 and 4.5. With exclusive use of NDSI and WV2, R^2_c values were mostly below 0.60 showing CP and ADF of heterogeneous pastures could hardly be predicted using solely those spectral variables. Poor performance of two-waveband narrow reflectance ratios for the prediction of quality parameters were also reported in other studies with forage crops (Zhao et al., 2007; Biewer et al., 2009b). With the inclusion of USH in the regression models accuracy of both ADF and CP prediction was mostly improved (RPD values $\geq$ 1.4), however, the improvement was more pronounced for ADF. Prediction models using combined NDSI and USH were not significant for CP during summer and autumn, when the contribution of dead material in the canopies was high and where exclusive spectral calibrations already reached accuracy levels of the combined applications from spring or far above it. Models combining WV2 and USH also showed a minor improvement (only 2% increase in R^2_c) compared to exclusive use of WV2 bands at this time. Therefore, less enhancement in prediction accuracy can be expected from these combined sensor approaches for prediction of CP in such vegetation.

Table 4.4 Calibration (C) and cross validation (CV) results for prediction of acid detergent fibre (ADF) and crude protein (CP) in the biomass of heterogeneous pastures from best-fit normalized difference spectral index (NDSI) exclusively and as a combination with ultrasonic sward height (USH) for common (N=323) and date-specific dataset (N=108).

			R^2_c	SE_c	R^2_{cv}	SE_{cv}	RPD	Best-fit wavelengths	NDSI	USH
ADF (% of DM)	C[a]	ex[e]	0.49	4.24	0.48	4.27	1.39	1222, 1281	l***	-
		co[f]	0.62	3.70	0.58	3.79	1.56	1236, 1281	q***	q**
	Sp[b]	ex	0.47	3.08	0.45	3.12	1.35	905, 922	l***	-
		co	0.76	2.12	0.68	2.19	1.92	1011, 1012	q***	l*
	Sm[c]	ex	0.64	3.83	0.63	3.90	1.61	1192, 1258	q***	-
		co	0.70	3.53	0.66	3.79	1.66	1173, 1258	q*	l***
	Au[d]	ex	0.49	4.57	0.46	4.55	1.40	1204, 1225	l***	-
		co	0.65	3.85	0.61	3.82	1.66	1179, 1206	q***	q***
CP (% of DM)	C	ex	0.58	1.99	0.56	2.02	1.51	698, 1339	q***	-
		co	0.63	1.88	0.60	1.91	1.60	434, 645	q***	l***
	Sp	ex	0.48	1.37	0.41	1.41	1.33	1219, 1282	q***	-
		co	0.55	1.32	0.45	1.39	1.35	373, 631	q*	q*
	Sm	ex	0.85	1.40	0.84	1.42	2.51	703, 1148	q***	-
		co			n.s					
	Au	ex	0.61	1.93	0.60	1.95	1.58	481, 684	l***	-
		co			n.s					

[a] C: common dataset; [b] Sp: spring dataset; [C] Sm: summer dataset; [d] Au: autumn dataset. [e] ex: exclusive NDSI; [f] co: combination of USH and NDSI. [g] n.s: not significant. Type of regression model: l = linear, q = quadratic; significant at * = 0.05, ** = 0.01, *** = 0.001 probability level.

Table 4.5 Calibration (C) and cross validation (CV) results for prediction of acid detergent fibre (ADF) and crude protein (CP) in the biomass of heterogeneous pastures from WorldView2 satellite bands exclusively and as a combination with ultrasonic sward height (USH) for common (N=323) and date-specific swards (N=108).

			R^2_c	SE_c	R^2_{cv}	SE_{cv}	RPD	Significant wavebands
ADF (% of DM)	C[a]	ex[e]	0.36	4.81	0.32	5.05	1.17	B1,B2,B3,B4,B5,B7,B8
		co[f]	0.69	3.42	0.55	3.66	1.62	B1,B2,B3,B4,B5,B6, B7,B8
	Sp[b]	ex			n.s[g]			
		co	0.68	2.49	0.59	2.70	1.56	B1,B2,B5,B7
	Sm[c]	ex	0.52	4.47	0.47	4.77	1.32	B1,B2,B3,B4,B6
		co	0.75	3.44	0.61	3.84	1.64	B1,B2,B3,B4,B5,B7,B8
	Au[d]	ex	0.59	4.21	0.53	4.31	1.48	B3,B4,B5,B6,B7,B8
		co	0.73	3.58	0.59	3.88	1.64	B1,B2,B3,B4,B5,B6,B7,B8
CP (% of DM)	C	ex	0.52	2.14	0.49	2.17	1.41	B1,B2,B3,B6
		co	0.63	1.90	0.57	1.97	1.55	B1,B2,B3,B4,B5,B7
	Sp	ex	0.37	1.51	0.27	1.61	1.17	B1,B4,B6
		co	0.69	1.16	0.29	1.31	1.43	B1,B2,B3,B4,B5,B6,B7,B8
	Sm	ex	0.86	1.35	0.84	1.39	2.56	B2,B3,B7
		co	0.88	1.27	0.84	1.32	2.70	B1,B2,B3,B7
	Au	ex	0.58	2.03	0.55	2.08	1.48	B2,B3,B4,B5,B6
		co	0.60	2.02	0.54	2.08	1.48	B2,B3,B4,B5,B7

[a] C: common dataset; [b] Sp: spring dataset; [C] Sm: summer dataset; [d] Au: autumn dataset. [e] ex: exclusive satellite bands; [f] co: combination of USH and satellite bands. [g] n.s: not significant.
WorldView2 satellite broad bands as independent variables; B1-B8: the first to eighth broad-bands of WV2. B1: coastal (400-450 nm), B2: blue (450-510 nm), B3: green (510-580 nm), B4: yellow (585-625 nm), B5: red (630-690 nm), B6: red edge (705-745 nm), B7: near infrared-1 (770-895 nm) and B8: near infrared-2 (869-900 nm)

Scatter plots were used to further compare ADF and CP values predicted by the exclusive and combined sensors with laboratory measurements (Figures 4.2 and 4.3). It becomes clear that with calibration models based on exclusive NDSI or WV2 both ADF and CP were overestimated at low levels of laboratory-measured values and underestimated when these reference values were high. The improvement of fit by the combined use of sensor variables is reflected by higher R^2-values, lower SE-values and a convergence of the regression line to the bisector.

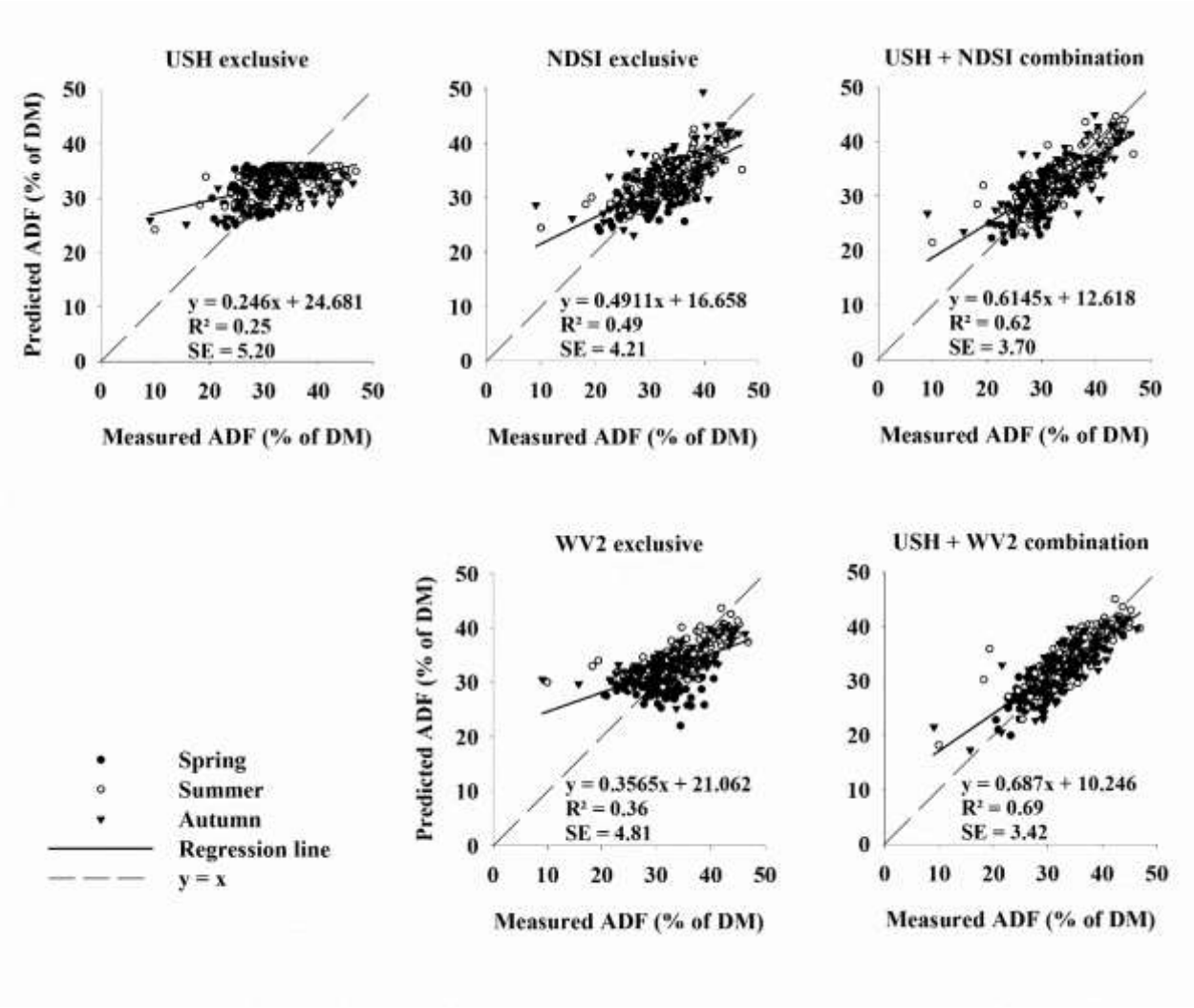

Figure 4.2 Plot of fit between measured and predicted acid detergent fibre (ADF) for exclusive ultrasonic sward height (USH exclusive), exclusive best fit normalized difference spectral index (NDSI exclusive) and exclusive Worldview-2 (WV2 exclusive) as well as for combinations of USH with NDSI and WV2 applied in common swards.

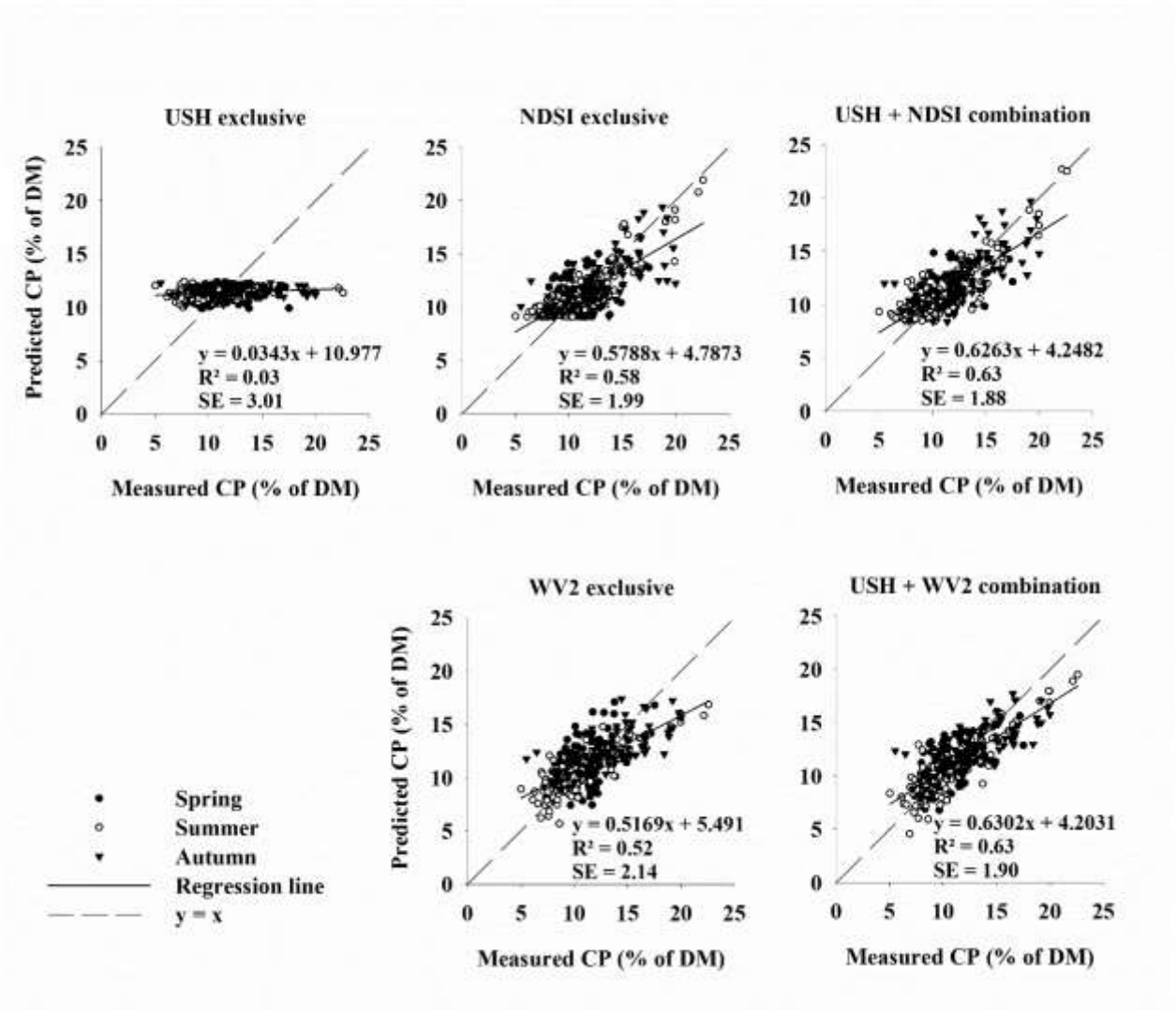

Figure 4.3 Plot of fit between measured and crude protein (CP) for exclusive ultrasonic sward height (USH exclusive), exclusive best fit normalized difference spectral index (NDSI exclusive) and exclusive Worldview-2 (WV2 exclusive) as well as for combinations of USH with NDSI and WV2 applied in common swards.

The interpretation of coefficients in models including USH and NDSI is difficult, as they comprise various quadratic terms and interactions (see Appendix Table A.7). Thus, the significant effects of the models for ADF and CP of the common dataset were presented graphically (Figure 4.4). Generally, ADF increased and CP declined with increasing USH, which could be expected, as with increasing maturity of plants rejected by cows, fibrous components are accumulated at the costs of protein and mineral concentration in plants tissue (Bakker et al., 1984; Hobbs and Swift, 1988; Milchunas et al., 1995). The reverse effect of the spectral index NDSI to ADF and CP, respectively,

is caused by the band locations on ascending (ADF) or descending slopes (CP) on the hyperspectral curve (see also Figure 4.1 and Table 4.4). These results correspond well with findings of Guo et al. (2010), who found higher negative correlation in absorption regions and higher positive correlations in reflectance regions for protein content in a mixed grass ecosystem.

Predictions depict a changing NDSI effect along the sward height gradient for both forage quality parameters with less distinct differentiation in higher swards (Figure 4.4). One reason might be a reduced representation of reflectance characteristics of subordinate layers in high swards due to limited light transmission with increasing leaf density (Jacquemoud and Baret, 1990). Thus, in high swards the variation of ADF and CP predictions might be predominantly caused by the fraction of mature plants, which protrude over the surrounding canopy. Contrary, variation of predicted forage quality in low swards may result either from different contributions of young leafy material (indicating intensively grazed areas) or from high fractions of stubbles and compacted senescent plant material (representing areas which were less preferred by animals).

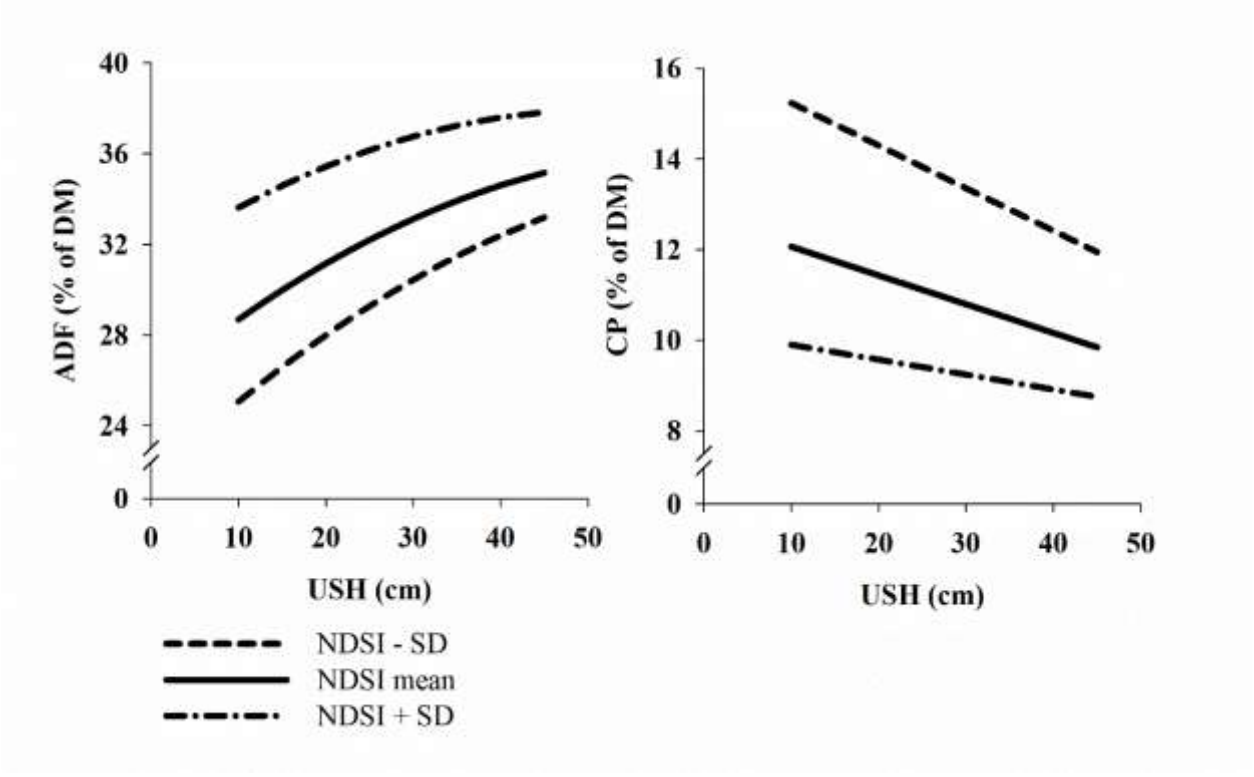

Figure 4.4 Predictions of acid detergent fibre (ADF) and crude protein (CP) in common swards based on ultrasonic sward height (USH) and the Normalized Difference Spectral Index (NDSI) in the range of mean values ± standard deviation. NDSI represents reflection values calculated on basis of 1 nm band selected in combination with USH.

In view of exclusive and combined sensor applications it was found that the prediction accuracy of 2-band NDSI, mostly located beyond 900 nm wavelength, reached the same or even better levels than WV2-based models. This is especially pronounced for ADF, while for CP best fits were found also in visible regions of blue and red (Table 4.4 and Table 4.5). The importance of visible-near infrared region for estimating quality parameters is also confirmed by other investigations (Biewer et al., 2009b; Pullanagari et al., 2012a). The spectrometer used in this study could provide canopy hyperspectral reflectance information up to 1700 nm. However, previous studies indicated that the wavelengths region between 1700 to 2400 nm in the shortwave infrared region was also important for measuring forage quality in the field (Guo et al., 2010). Therefore, using a spectroradiometer that can obtain reflectance measurements for additional wavelengths may further improve the prediction accuracy.

To include more spectral information from the hyperspectral dataset and to accomplish a combination with USH in the calibration analysis, PCA derived components were extracted. Their accuracy in both, exclusive or in combination with USH, was always below NDSI and WV2 wavebands, although principal components represented most of the variation in total spectral data (>0.98 %). Obviously, compared to MLPR analysis, which considers both spectral and reference values during calculation, extracting only the spectrally most informative components does not allow acceptable accuracies. Thus, the results were not presented here. A two-step multivariate calibration method using PCA components was also applied by Pullanagari et al. (2012a) for predicting pasture quality parameters. They also found weak relationships with R^2 values of 0.15 to 0.45. Hence, they considered PCA useful for recognising major sources of variance in the vegetation spectral data (e.g. green and dead vegetation) rather than chemical concentrations with small variances.

It also should be noted that ADF and CP values in the present study were measured by laboratory near infrared spectroscopy (NIRS) and, thus, included prediction errors by themselves. Hence, the prediction models may further improve, if all reference values were determined by exact laboratory chemical analysis.

4.4 Conclusions

The present study aimed to demonstrate the potential of using a combination of ultrasonic and canopy reflectance data to predict forage quality variables in extremely heterogeneous pastures. Hyperspectral analysis by MPLS, which can be considered a reference method, as it exploits the utmost spectral information, resulted in maximum accuracy for the prediction of ADF and CP in grazed grasslands. Any reduction of hyperspectral data into vegetation indices based on few specific narrow wavebands or satellite broadbands reduced prediction accuracy significantly. However, prediction of ADF and CP was improved by a combined analysis of ultrasonic sward height and vegetation indices or satellite broadbands, so that most calibration models exceeded an RPD value of 1.4, which is considered an acceptable predicting capability for variable field condition.

As grazing by cows creates spatially and temporally extremely dynamic environments, forage quality prediction using proximal remote sensing is more challenging than in well managed, homogeneous experimental forage swards usually used for the testing of sensing methods. To summarize, though the performance of models developed in this study is somewhat lower than reported elsewhere, our findings show that combined sensing systems using reflectance and ultrasonic sensors may provide acceptable prediction accuracies for practical application even under extremely heterogeneous pasture conditions. However, further research needs to be carried out into new sensor techniques and practical applications in grassland farming.

5 Comparing mobile and static assessment of biomass in heterogeneous grassland with a multi-sensor system

Abstract The present study aimed to test a mobile device equipped with ultrasonic and spectral sensors for the assessment of biomass from diverse pastures and to compare its prediction accuracy to that from static measurements. Prediction of biomass by mobile application of sensors explained > 63 % of the variation in manually determined reference plots representing the biomass range of each paddock. Accuracy of biomass prediction improved with increasing grazing intensity. A slight overestimation of the true values was observed at low levels of biomass, whereas an underestimation occurred at high values, irrespective of stocking rate and years. Prediction accuracy with a mobile application of sensors was always lower than when sensors were applied statically. Differences between mobile and static measurements may be caused by position errors, which accounted for 8.5 cm on average. Beside GPS errors (± 1 – 2 cm horizontal accuracy and twice that vertically), position inaccuracy predominantly originated from undirected vehicle movements due to heaps and hollows on the ground surface. However, the mobile sensor system in connection with biomass prediction models may provide acceptable prediction accuracies for practical application, such as mapping. The findings also show the limits even sophisticated sensor combinations have in the assessment of biomass of extremely heterogeneous grasslands, which is typical for very leniently stocked pastures. Thus, further research is needed to develop improved sensor systems for supporting practical grassland farming.

5.1 Introduction

Pasture biomass and its quality is a matter of primary concern in continuous grazing systems (Silvia Cid et al., 1998; Kristensen et al., 2005; Oudshoorn et al., 2013). On-site and on-time information on biomass and its spatial distribution in pastures are needed for site-specific pasture management and can help livestock managers in making critical decisions in terms of planning grazing time, grazing period, grazing interval, stocking rate and inputs such as fertilizers (Suzuki et al., 2012). However, conventional plant sampling techniques are costly, destructive and time consuming, thereby limiting the number of measured samples and being impractical to characterize spatial variability in sward characteristics within fields (Fava et al., 2009). In contrast, real-time mobile sensors, which allow the collection of geographically referenced data have proven to be useful for

in-field monitoring of vegetation characteristics with high spatial resolution (Lan et al., 2009; Muñoz-Huerta et al., 2013; Cozzolino et al., 2015). Mobile automated sensor measurements can provide high sampling density at a relatively low cost to generate maps representing both spatial and temporal variations (Adamchuk et al., 2004). Farooque et al. (2013) developed an integrated automated system comprising an ultrasonic sensor, a digital color camera, a slope sensor and a global positioning system (GPS) to measure plant height, fruit yield, slope and elevation in wild blueberry fields and concluded the developed system was accurate, reliable and efficient to map such characteristics in real-time kinematic. Pittman et al. (2015) examined several types of ground-based mobile sensing strategies (ultrasonic, laser and spectral sensors) to estimate biomass and canopy height in bermudagrass, alfalfa and wheat. They suggested that using mobile sensor-based biomass estimation methods could be an effective alternative to the traditional clipping method for a rapid and accurate in-field biomass estimation. Different types of sensors both in static and mobile application have been used in recent grassland studies (Numata et al., 2008; Biewer et al., 2009a and b; Himstedt et al., 2009; Kawamura et al., 2009; Fricke et al., 2011; Pullanagari et al., 2012a and b; Duan et al., 2014; Rahman et al., 2014; Reddersen et al., 2014). Particularly hyperspectral sensors, which measure reflectance signals over a wide range of wavelengths in discrete bands of 1 to 15 nm width, have raised considerable interest for the prediction of biomass and quality parameters. However, pastures are highly heterogeneous ecosystems due to variations in canopy architecture, botanical composition and phenological stage of plants. Hence, the application of sensors in grazed pastures is more difficult than in cut grassland and there are limitations for each specific sensor technique used for the prediction of sward characteristics (Schellberg et al., 2008; Pullanagari et al., 2012b). An effective method for in-field estimation of biomass must reach an accuracy comparable to the accepted standard of destructive procedure (clipping and weighing) (Pittman et al., 2015). Using a data combination of conceptually different sensing methods holds promise for providing more accurate property estimates (Adamchuk et al., 2011). A sensor fusion approach has been proposed that combines measured sward height with an ultrasonic distance sensor and vegetation indices (VIs) derived from spectral-radiometric reflections to estimate biomass in grasslands with acceptable prediction accuracies (Fricke and Wachendorf 2013; Reddersen et al., 2014; Safari et al., 2015). The guiding idea in this approach is that canopy reflectance provides complementary information to canopy height sensing when estimating biomass. In all studies best prediction accuracies were achieved by a combination of ultrasonic sward height (USH) and sward specific band selection using the normalized spectral vegetation

index (NDSI; uses two spectral bands best suited for estimating biomass according to NDVI formula, i.e. normalized difference vegetation index) with R^2 values of 0.63 to 0.90. The selection of two narrow or broad bands from hyperspectral data has an advantage for practical implementation at field scale, as multispectral measurements are less expensive than hyperspectral ones. Likewise, ultrasonic sensors are simple and cost effective equipment but may provide accurate and real-time information needed by farmers to make on-farm decisions. However, no knowledge exists on how accurate such sensors work when applied on mobile devices and which position accuracy can be achieved under real field conditions.

The overall aim of the present study was to develop and test a mobile sensor system equipped with ultrasonic and spectral sensors and a high precision GPS to assess data in experimental pastures with a large variation of spatial and phenological structures. The following specific research questions were addressed in this study: i) Which overall prediction accuracy for grassland biomass can be achieved? ii) Is there a reduction in prediction accuracy between static and mobile application of sensors? iii) Does the performance of the sensor system depend on the grazing intensity? iv) What are possible position errors associated with mobile sensor measurements?

5.2 Material and Methods

5.2.1 Experimental site and set up

The study was conducted on a long-term pasture experiment (established in 2002) at the experimental farm Relliehausen (51°46′55″ N, 9°42′13″ E, 180-230 m above mean sea level) in Solling Uplands on moderately species rich grasslands, vegetation type *Lolio-Cynosuretum*. Three target paddocks of 1 ha each with different continuous stocking treatments were selected from the experiment. Treatments were a) moderate stocking, average of 3.4 standard livestock units (SLU, i.e. 500 kg live weight) per hectare, b) lenient stocking, average 1.8 SLU per hectare, c) very lenient stocking, average 1.3 SLU per hectare (Wrage et al., 2012). In each paddock one study plot of 30 x 50 m size was established, to represent spatial variability in pastures under different grazing intensities during two year measurements. The location of the study plots were determined prior to field sampling in a Geographic Information System (GIS) environment (ArcGIS 9.2). In a first step aerial photographs of each paddock were obtained in April 2013 using a remotely controlled Hexacopter carrying a small lightweight camera. The photos were georeferenced along GPS-levelled boundaries of each paddock and the area of each paddock was classified into grazed and

ungrazed areas using a visually adapted green/yellow threshold (Figure 5.1). The portion of both areas was then calculated for each paddock (63%, 47% and 38% classified as grazed areas in moderate, lenient and very lenient paddocks respectively). Rectangles of 30 x 50 m, representing the study plots, were moved in the paddock area using GIS until they contained identical portions of grazed and ungrazed areas as in the surrounding paddock. Each study plot was accurately located in the field by differential GPS and marked with corner poles. Field measurements for static and mobile calibration of the sensor system were conducted in 2013 on 3rd to 5th June and 2014 on 20th to 22nd May.

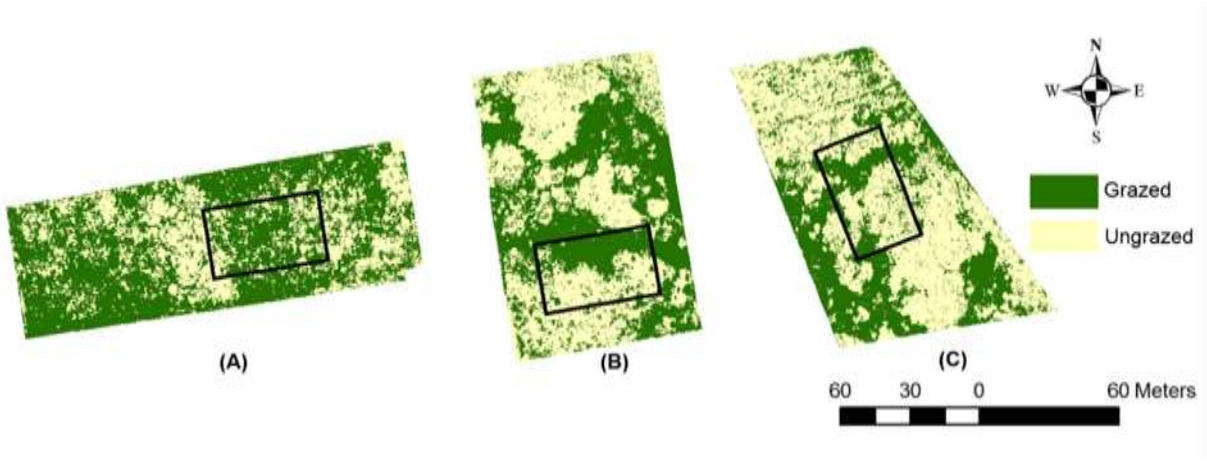

Figure 5.1 Images with digitally classified grazed and ungrazed areas in grassland paddocks of different stocking rate: (A) moderate (B) lenient (C) very lenient. Black boxes indicate the location of 30 x 50 m study plots. Photos were taken in April 2013.

5.2.2 Mobile measurements on the study plots

The multi-sensor system consisted of ultrasonic distance and hyperspectral reflectance sensors. The ultrasonic sensor holds a one-headed system (Pepperl and Fuchs, type UC 2000-30GM-IUR2-V15) operating with a transducer frequency of 180 Hz (Pepperl and Fuchs, 2010). Distances were measured in a range from 80 to 2000 mm within a sound cone formed by an opening angle of about 25°. Ultrasonic sward height (mm) was calculated by subtracting the ultrasonic distance measurement value in mm from the sensor mount height using Eq. (1):

$$USH\ (cm) = Mount\ height\ (cm) - Ultrasonic\ distance\ (cm), \quad (1)$$

Where USH is Ultrasonic sward height.

A HandySpec Field portable spectrometer (Tec5 AG Oberursel, Germany) was used to measure canopy spectral reflectance. The measuring head of the device had two channels measuring incoming and reflected radiation simultaneously between 305 and 1700 nm in 1 nm steps. Spectral calibrations were performed using a grey-standard (Zenith Polymer® Diffuse Reflectance Standard 25%) at fixed intervals. Both sensor systems provided the same opening angle with a field of view (FOV) of 25°. While the spectral sensor measures an integrated value of reflection intensity within the measurement cone, the ultrasonic sensor measure the highest object, creating a reliable reflection within the sound cone.

Mobile measurements where conducted using an electric driven cycle-based 4-wheel-vehicle with a track gauge of 180 cm (Figure 5.2). Both sensors were mounted at front-end center of the vehicle on a frame, allowing measurements along the central track during the vehicle movements. Two more ultrasonic sensors were mounted with 60 cm distance on either side of the central sensor to allow a higher measurement density for future mapping activities. GPS positions of all sensor readings were acquired in 0.1 second intervals using a Leica SR530 dual-frequency geodetic RTK receiver. A GPS AT 502 dual-frequency antenna was mounted on top of a pole close to the sensors. Its geometric position in relation to both the ground and the sensors was recorded and considered in subsequent sensor position calculations including a correction of topographically induced antenna pole skewness. The DGPS correction signals were received from an on-field reference station in a maximum distance of 500 m by a radio modem. Both, reference station and rover were equipped with components of identical technical specifications providing a horizontal positional accuracy of 1-2 cm and 2-3 cm vertical accuracy. For mobile measurements the vehicle was remotely steered along 50 m longitudinal lanes in the study plots at a speed of approximately 0.1-0.3 m s^{-1}. Ultrasonic measurements were triggered at a 0.3 second interval, resulting in a measured point distance of 10 ± 6 cm (mean of all plots). Spectral reflections were continuously assessed, but with a variable data integration time of the spectrometer between 1 and 5 s, measurements were logged discontinuously, corresponding to a measured distance of 43 ± 20 cm between spectral measurement points in each plot (mean of all plots).

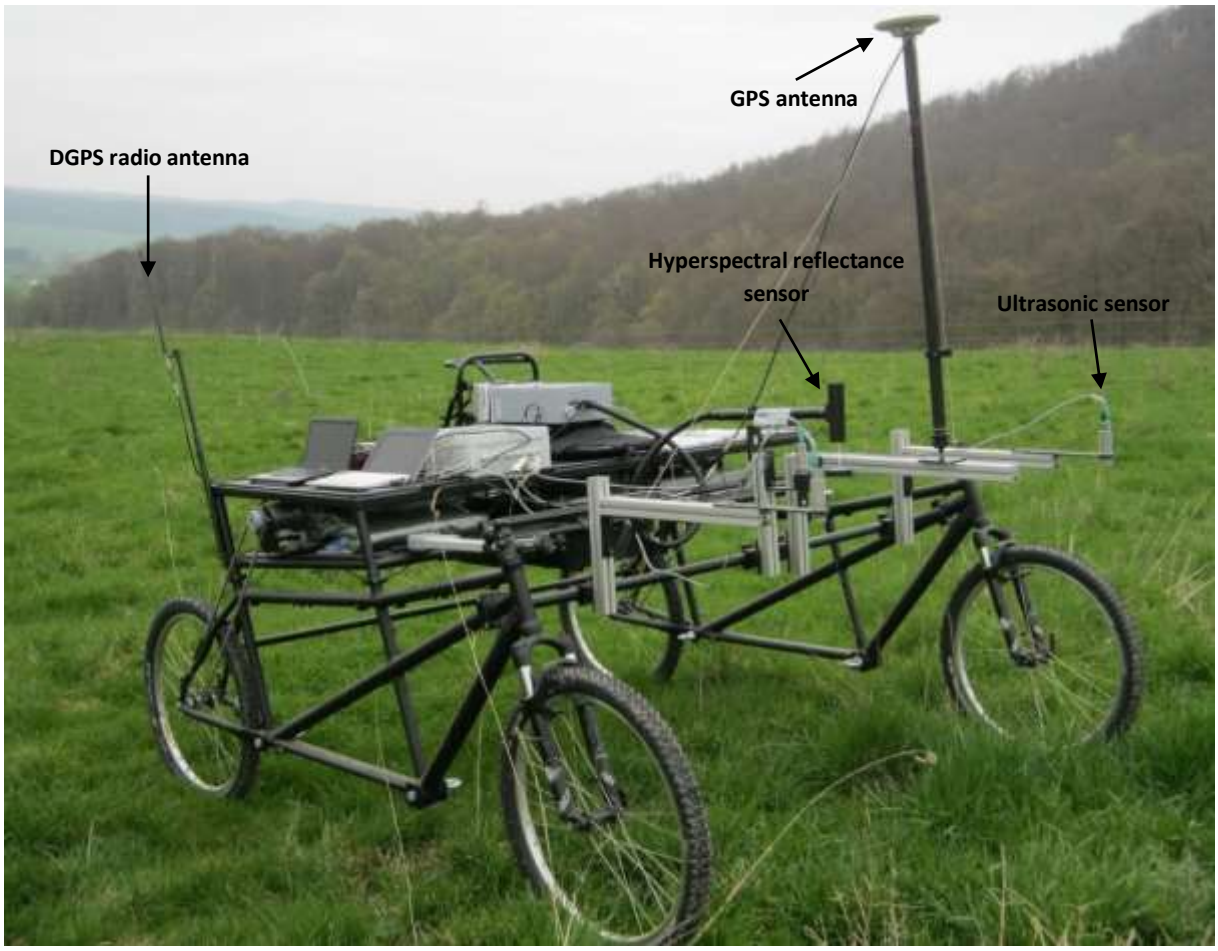

Figure 5.2 Remotely steered sensor vehicle with hyperspectral reflectance and ultrasonic sensors and mounted GPS antenna.

5.2.3 Static measurements on reference plots

Subsequent to the mobile measurement, 18 reference plots (each 50x50 cm) were established within each of the three study plots by positioning them along the central axis between the vehicle tracks to represent the occurring range of available biomass levels and sward structures. Static sensor measurements were conducted on these reference plots using the same sensors as in the mobile measurement and following the methodology as described by Fricke et al. (2011). The total aboveground biomass from each reference plot was clipped at ground surface level after sensor measurements were taken. In the present study grassland biomass is expressed as the amount of fresh matter (FM) in g m^{-2}. To avoid repeated sampling at the same position across time the location of reference plots was determined using DGPS.

5.2.4 Data integration and analysis

Spectral calibration models were developed for each year separately in order to reach the maximum prediction accuracy using biomass data from reference plots. In an attempt to create prediction models with maximum accuracy by using the depth of information of hyperspectral data, narrowband NDSI according to Inoue et al. (2008) were applied over the range of 1nm spectral bandwidths using all possible combinations of two-band reflectance ratios based on NDVI formula according to Eq. (2):

$$NDSI\,(b1, b2) = (b1 - b2) / (b1 + b2), \quad (2)$$

Where b1 and b2 are specific narrow band (1 nm) reflection signals with wavelength b1 > wavelength b2.

All possible two-pair 1nm band combinations in the hyperspectral range from 360 to 1340 nm and 1500 to 1650 nm were tested. Ordinary least square regression analysis was performed using linear model procedure in R (version 3.0.2) (R Development Core Team, 2013) with biomass as the dependent variable and NDSI together with USH as independent variables including interactions and quadratic terms according to Eq. (3):

$$B = USH + NDSI + USH * NDSI + USH^2 + USH^2 * NDSI + NDSI^2 + USH * NDSI^2 + USH^2 * NDSI^2, \quad (3)$$

Where B is biomass (g FM m^{-2}), USH is ultrasonic sward height (cm), NDSI is normalized difference spectral index.

NDSI wavebands were considered adequate when R^2 of the model was maximum. According to the rules of hierarchy and marginality (Nelder, 1994) non-significant effects were excluded from the models, but were retained if the same variable appeared as part of a significant interaction at α-level of 5%. Calibration models were validated by a four-fold cross validation method (Diaconis and Efron, 1983).

5.2.5 Assessment of position accuracy

With the aim to establish a plausibility control for position accuracy of mobile measurements, an additional experiment was set up. Wooden planks of known position and dimension at each end of

the vehicle tracks were measured in spring, before the vegetation started to grow. Thus, higher targets could be clearly distinguished from lower swards. Vehicle measurement were conducted in the same mode as described above. Here, only USH data was used due to its high point density. Measured values were compared to expected values and classified as error if a discrepancy was observed. The distance of an erroneous measurement to the closest apparent target edge (considering target dimensions and sensor properties) was assigned to the respective measurement and used for subsequent spatial analysis. Further information on the methodology is provided in the supplemental material.

5.3 Results and discussion

5.3.1 Relationship between static and mobile sward measurements for use of exclusive sensors

Statically measured USH ranged from 3.1 to 64.6 cm and from 7.2 to 64.0 cm in 2013 and 2014, respectively (Table 5.1). Compared to static measurements higher values of USH were found by mobile application ranging from 4.7 to 75.6 cm and from 11.6 to 67.4 cm in 2013 and 2014, respectively. This may be the effect of a cross bar, which was attached to the rear of the vehicle in a height of about 50 cm for stabilizing purposes and may have compressed higher vegetation during vehicle passage and subsequent static measurements were possibly influenced by that. Pasture with moderate stocking rate exhibited lower USH values (mean value = 21.9 and 26.8 cm in 2013 and 2014 respectively) compared to pastures with lenient stocking rate (mean value = 44.3 and 32.5 cm respectively) and very lenient stocking rate (mean value = 43.1 and 29.8 cm respectively). Swards of the latter two stocking rates showed similar USH levels in both years, although pastures were managed and monitored by the use of a compressed sward height meter (CSH; according Castle, 1976) maintaining levels at 6 cm (moderate), 12 cm (lenient) and 18 cm (very lenient), respectively (Wrage et al., 2012). This disparity may indicate the influence of sward structure on the conducted measurement methods: While CSH reflects the resistance of biomass according to stem density and sward height (Hakl et al., 2012), USH predominantly detects protruding objects regardless of other sward conditions in subordinate layers (Fricke et al., 2011). This fact indicates the limitations of biomass predictions based on pure USH, as it may not directly reflect the biomass, particularly if swards are composed by plants of varying phenology, which is common in leniently grazed swards (Rook and Tallowin, 2003; Wrage et al., 2011).

Table 5.1 Summary statistics of static and mobile measurements of ultrasonic sward height (USH) (cm) and normalized difference spectral index (NDSI) on reference plots of pastures with different stocking rates in 2013 and 2014.

	Static measurements				Mobile measurements			
	2013		2014		2013		2014	
	USH	NDSI	USH	NDSI	USH	NDSI	USH	NDSI
Moderate (n=18 in each year)								
Min	3.1	0.031	9.0	-0.030	4.7	0.032	12.0	-0.032
Mean	21.9	0.046	26.8	-0.017	22.1	0.048	30.0	-0.020
Max	50.6	0.065	64.0	-0.008	60.9	0.063	67.4	-0.015
SD	14.5	0.011	13.6	0.005	14.8	0.010	14.2	0.004
Lenient (n=18 in each year)								
Min	24.8	0.027	16.4	-0.021	22.9	0.030	19.2	-0.020
Mean	44.3	0.038	32.5	-0.015	46.1	0.040	37.3	-0.013
Max	64.0	0.049	55.4	-0.008	75.6	0.057	61.2	-0.007
SD	12.3	0.006	10.6	0.004	16.2	0.008	12.7	0.004
Very Lenient (n=18 in each year)								
Min	10.0	0.032	7.2	-0.020	8.7	0.029	11.6	-0.032
Mean	43.1	0.047	29.8	-0.011	48.9	0.048	36.9	-0.011
Max	64.6	0.065	58	-0.007	75.2	0.070	66.5	-0.005
SD	16.0	0.011	15.8	0.004	19.5	0.009	17.1	0.007
All pastures (n=54 in each year))								
Min	3.1	0.027	7.2	-0.030	4.7	0.029	11.6	-0.032
Mean	36.4	0.044	29.7	-0.014	39.0	0.046	34.7	-0.015
Max	64.6	0.065	64.0	-0.007	75.6	0.070	67.4	-0.005
SD	17.5	0.010	13.5	0.005	20.2	0.010	14.9	0.006

NDSI wavelength locations associated with maximum accuracy of biomass prediction differed between years. Positive NDSI values in 2013 corresponded to the green peak of the spectrum (at 536 and 564 nm, on the ascending slope) while negative values in 2014 corresponded to the descending slope of the second water absorption band (at 1121 and 1133 nm). NDSI values by static measurement ranged from 0.027 to 0.065 with a mean value of 0.044 across all pastures in 2013, which were slightly lower than the values by mobile application (mean value = 0.046). In 2014 a smaller range of NDSI values occurred by both static and mobile application (-0.030 to -0.007), resulting in a mean value of -0.014 (Table 5.1).

USH values from mobile measurements were in good agreement with static values, with $R^2 \geq 0.85$ for all pastures in both years (Figure 5.3). This indicates that reliable and accurate USH information could be acquired by the mobile application of low cost ultrasonic sensors. Moreover, it seems that the performance of the mobile application is not affected by the stocking rate, as R^2 values differed only randomly during the two-year measurements on different pastures.

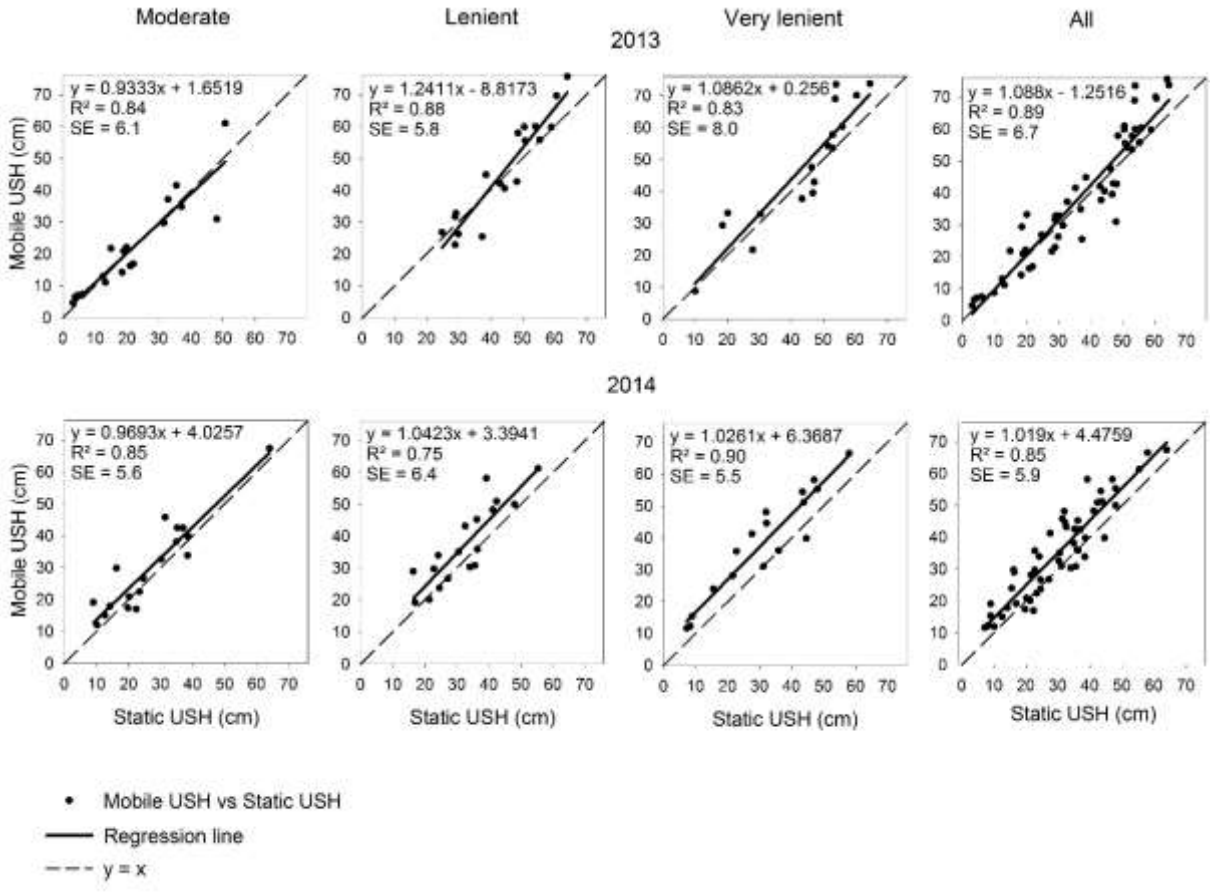

Figure 5.3 Relationship between static and mobile measured ultrasonic sward height (USH) (cm). Both measurements were conducted on reference plots in pastures differently stocked by animals in 2013 and 2014.

The relationship between NDSI values determined on the reference plots by mobile and static application was closer for moderate (R^2 = 0.66 – 91) than for leniently and very leniently grazed pastures (R^2 = 0.59 – 0.72) (Figure 5.4). This may be partly due to a higher proportion of senesced material in pastures at lower grazing intensities. This is supported by results of Safari et al. (2015), which showed a lower accuracy of spectral calibrations for grassland biomass in the second half of the growing season, when senesced material likewise presented greater shares of the grassland canopy. Botanical diversity, which is well known to increase with reduced defoliation intensity through grazing or cutting (Blüthgen et al., 2012; Isselstein et al., 2005), may have further alleviated the relationship between grassland biomass and spectral characteristics. For the biomass of species-poor grasslands, spectral calibrations based on static measurements frequently achieved higher accuracies than for less intensively grazed swards (Biewer et al., 2009a, Reddersen et al., 2014). Compared to ultrasonic measurements, accuracy of spectral calibrations was remarkably lower in both years and at all levels of grazing intensity. One reason may be the lower measurement point density of spectral (1.3 per plot on average) than ultrasonic recordings (5.0 per plot on average), which can be explained by the lower data integration time for the former technique. In pastures with high canopy variability (lenient and very lenient), where extremely short (intensively grazed) and tall (lightly grazed) patches are frequently located in the immediate vicinity of each other, a high measurement point density is of particular benefit. This may explain, why in moderately grazed pastures the accuracy of NDSI is only 7 % lower than USH (averaged over both years), whereas under very leniently grazing accuracy of NDSI is 24 % lower.

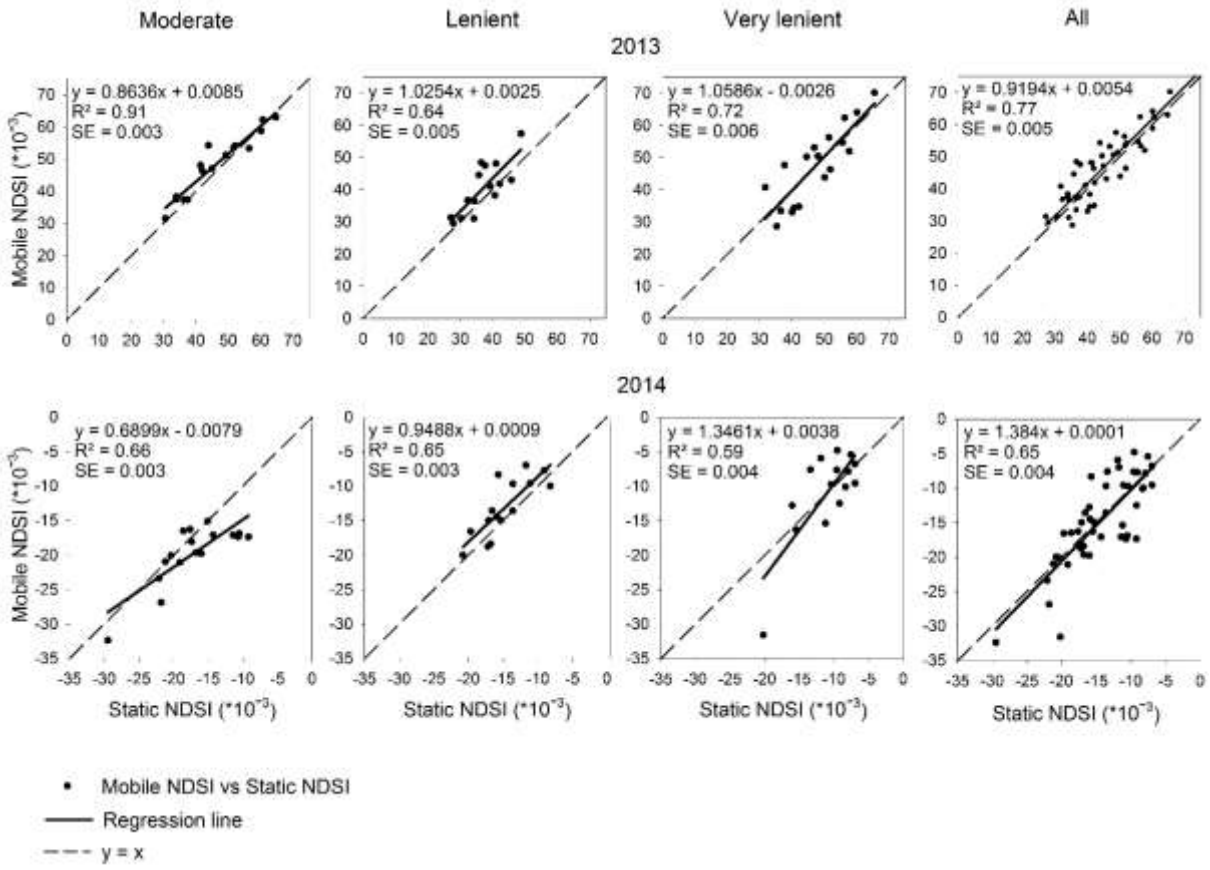

Figure 5.4 Relationship between statically and mobile measured normalized difference spectral index (NDSI). Both measurements were conducted on reference plots in pastures differently stocked by animals in 2013 and 2014.

5.3.2 Relationship between static and mobile sward measurements for sensor combination

Calibrations used in the present study were developed in a recent study by Safari et al. (2015) and showed cross-validation errors for biomass of pastures of 340 and 287 g FM m^{-2} in 2013 and 2014 respectively (Table 5.2). The best-fit two-pair wavelengths for prediction of biomass were located in the visible (2013) and near infrared (NIR) (2014) regions of the spectrum. Several studies have indicated the importance of the visible near infrared range to create models for estimating biomass using narrowband ratios (Numata et al., 2008; Psomas et al., 2011; Fricke and Wachendorf, 2013). The 536 and 564 nm bands from the visible region (2013) can be correlated with chlorophyll content of vegetation (Psomas et al., 2011), while the 1121, 1133 nm from NIR (2014) are related to plant leaf water content (Raymond, 1991).

Table 5.2 Regression and cross validation statistics of prediction models for biomass (B) (g FM m^{-2}) from ultrasonic sward height (USH) (cm) and narrowband normalized difference spectral index (NDSI) during mobile application. Models were derived from static measurements on reference plots according EQs 1 and 2 (see above) (n=54).

Year	b1	b2	R^2	SE (g FM m^{-2})	R^2_{cv}	$RMSE_{CV}$ (g FM m^{-2})	Equation
2013	536	564	0.82	344.2	0.75	340.0	B = 1664.26 - 22748.47 NDSI + 56.82 USH - 991.32 NDSI x USH
2014	1121	1133	0.87	227	0.68	287	B = -271 - 146000 NDSI -9330000 $NDSI^2$ - 29.5 USH + 1.89 USH^2 - 7010 NDSI x USH + 361 NDSI x USH^2 + 11100 $NDSI^2$ x USH^2

b1, b2 = spectral bands
SE = standard error
$RMSE_{CV}$ = random mean square error of cross-validation

Biomass in the reference plots as measured by manual clipping and weighing ranged from 107.2 to 3207.2 and from 360.8 to 2832.0 g FM m^{-2} in 2013 and 2014, respectively (Table 5.3). In 2013 the leniently stocked pasture showed the highest biomass (mean value = 1727.6 g FM m^{-2}) compared to the other pastures, while in 2014 reference plots in moderate pasture had the highest biomass (mean value = 1335.8 g FM m^{-2}) followed by leniently grazed pasture (mean value = 1271.6 g FM m^{-2}). While biomass predicted by static application differed only slightly (<1 %) from manual clipping (mean of all pastures), values predicted by mobile application were somewhat lower with 3.7 and 7.1 % in 2013 and 2014, respectively.

Table 5.3 Summary statistics of measured and predicted biomass (g FM m^{-2}) based on predictions by static and mobile application for pastures with different stocking rates in 2013 and 2014.

	2013			2014		
	Measured	Predicted		Measured	Predicted	
		Static	Mobile		Static	Mobile
Moderate (n=18 in each year)						
Min	107.2	170.4	206.4	645.6	523.6	430.4
Mean	942.8	968.7	831.6	1335.8	1279.5	1252.7
Max	2152.0	2199.6	2028.8	2797.6	2602.7	2615.4
Lenient (n=18 in each year)						
Min	611.2	797.4	354.4	610.4	728.7	686.7
Mean	1727.6	1658.7	1643.2	1271.6	1272.6	1111.1
Max	3207.2	2892.6	3076.0	2832.0	2433.0	2237.2
Very lenient (n=18 in each year)						
Min	250.4	220.9	60.8	360.8	441.6	426.9
Mean	1050.2	1093.1	1112.5	834.1	882.8	779.7
Max	2624.0	2587.0	3109.9	1567.2	1798.4	1349.7
All pastures (n=54 in each year)						
Min	107.2	170.4	60.8	360.8	441.6	426.9
Mean	1240.2	1240.2	1194.7	1147.2	1145.0	1062.5
Max	3207.2	2892.6	3109.9	2832.0	2602.7	2615.4

Biomass prediction by mobile sensors was significantly associated with static sensor predictions and reference data (Figure 5.5). With R^2 values of 0.77 and 0.84 for biomass of all pastures in 2013 and 2014, respectively, the relationship between mobile and static predictions was quite close. Mobile prediction of biomass explained 63 and 76 % of the variation in manually determined reference data of all pastures in 2013 and 2014, respectively. Looking more closely into the data, it becomes apparent that the accuracy of biomass prediction improved with increasing grazing intensity with R^2 values of 0.52, 0.68 and 0.73 (average of both years) for very leniently, leniently and moderately grazed pastures, respectively. Though sensor combinations proved a higher prediction accuracy for grassland yield and quality compared to exclusive ultrasonic or spectral sensors (Safari et al., 2015, 2016), the findings of the present study likewise show the limits even sensor combinations have in the mobile assessment of biomass of extremely heterogeneous grasslands.

Regression lines in Figure 5.5, describing the relationship between actual and mobile predicted biomass, generally exhibit a slope < 1, which indicates an overestimation of the true values at low levels of biomass and an underestimation at high values, irrespective of stocking rate and years. The reason for an overestimation at low levels of biomass may be that the sensor system was not capable to grasp extremely high bulk densities accurately, which obviously occur when low swards exhibit high yields.

In such situations bulk density of upper canopy layers are frequently much less than in lower canopy layers why both sensors may face limitations: On the one side the ultrasonic sensor detects signals reflected predominantly from upper canopy layers (Fricke et al., 2013) largely independent of the actual density of the sward. On the other side the reduction in the amount of radiation penetrating to a greater depth in the canopy can limit reflectance sensors especially in grass dominated canopies, which have their maximum leaf area index close to the soil surface (Goel, 1988).

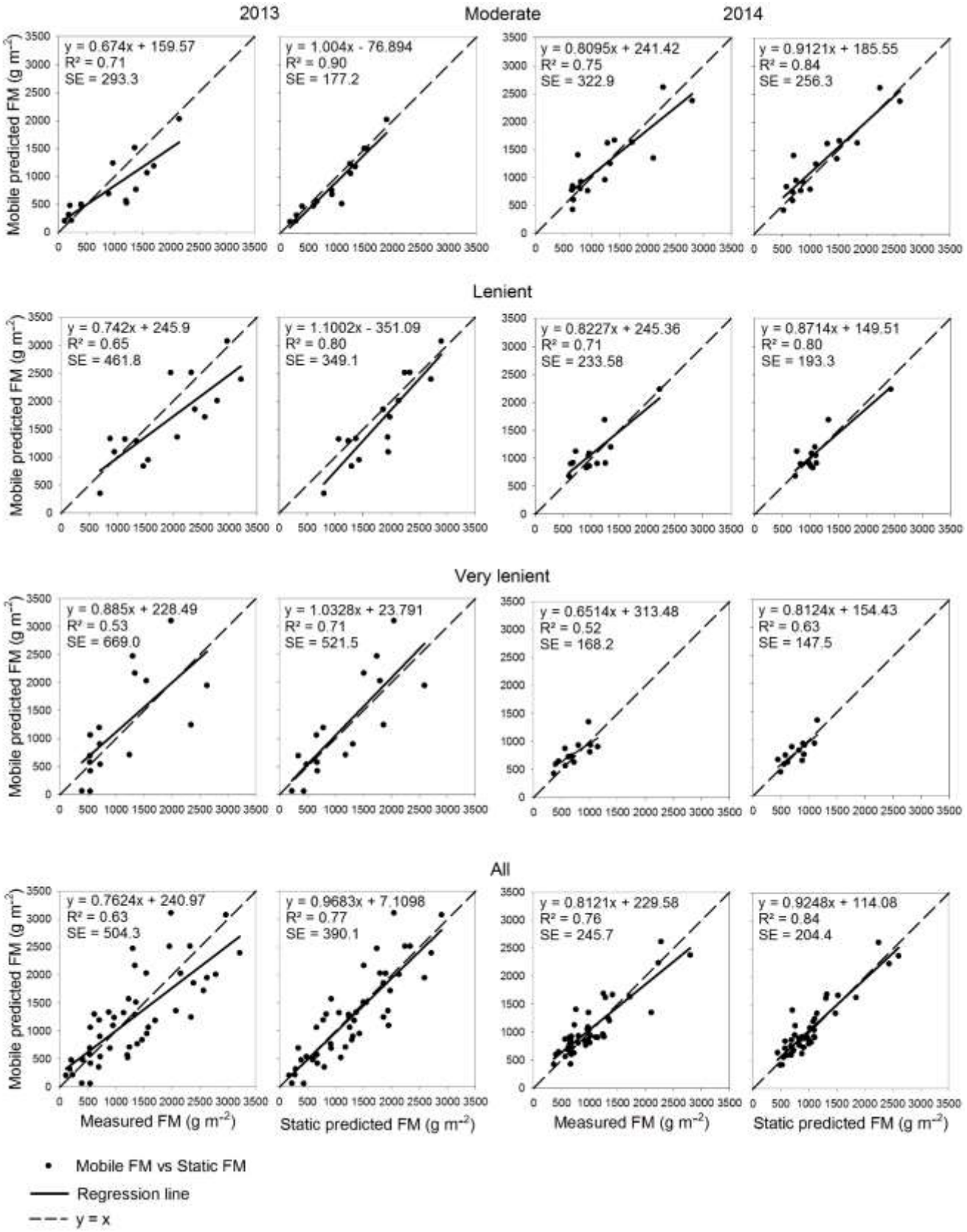

Figure 5.5 Relationship between mobile and static measured biomass (g FM m^{-2}; based on combined sensor data USH and NDSI) and values measured by clipping. All measurements were conducted on reference plots in pastures differently stocked by animals in 2013 and 2014.

5.3.3 Assessment of position accuracy

Though equal sensor calibrations were used, variation occurred between static and mobile measurements (Figure 5.3 and Figure 5.4). Differences may be brought about by vehicle configuration and movement, resulting in sensor displacement and confused geographical location. To evaluate these effects on the position of measuring points, which in this study is important to ensure correct placement of sensor measurements inside the reference plots during vehicle passage, a separate experimental setup was used (see also supplemental material). Briefly, position accuracy was analysed by comparing measured and expected USH values of vehicle measurements in the close surrounding of wooden marks with known dimension and position. Erroneous measurements, classified with respect to target and sensor properties, were assigned to its spatial distance from the target edges. The position error is here expressed as the relative frequency of erroneous measurements within a distance class related to apparent target edges, where a USH change between low and high was expected (Figure 5.6).

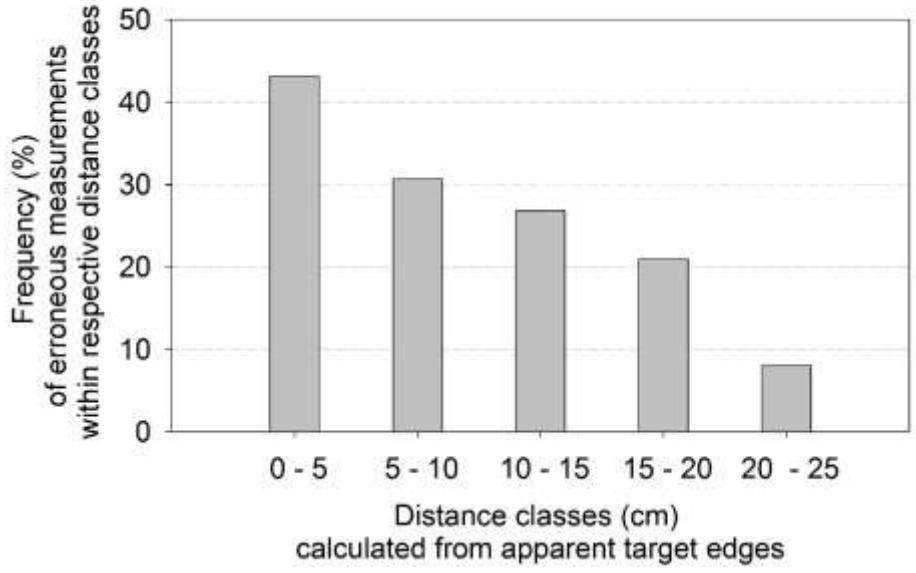

Figure 5.6 Frequency of erroneous USH measurements (% of all measurements within a distance class) at different distance from apparent target edges (considering target dimensions and sensor properties).

Error frequency declined with increasing distance from apparent target edges and the trend indicates a negligible risk of erroneous measurements, if the distance between two objects was more than 25 cm. Altogether the average position error was 8.5 ± 5.8 cm. Beside GPS errors of 1

- 2 cm, positioning inaccuracy observed in this study predominantly originated from undirected vehicle movements due to heaps and hollows of the ground surface. These errors could be compensated by a gyroscope, which can level out unbalanced sensor movements caused by the vehicle (Nagasaka et al., 2004). Further, measurement signal processing delays caused position offsets, which were in parts addressed in other studies, but are very specific to the respective vehicle construction. These position offsets could be compensated by appropriate mathematical models or coefficients in sensor position calculations (Zhao et al., 2010, Gottfried et al., 2012). Hence, although position errors were rather low, there are prospects for a further reduction. Regarding the precision of mobile measurements in the reference sampling plots, about 17 % of the measurements (mean position error of 8.5 cm divided by sampling plot width of 50 cm) can be expected to lie outside the sampling plot area, which may have contributed to the resulting discrepancy between static and mobile measurements (Figure 5.3 and Figure 5.4). However, the spatial accuracy, achieved with the current configuration of the mobile sensor system, can be considered adequate and may provide a solid basis for the creation of high-resolution maps.

5.4 Conclusions

The results from the present study suggest, that mobile multi-sensor systems, including ultrasonic and optical sensors, together with precise GPS can produce acceptable accuracies for biomass assessment in extremely heterogeneous grassland. Such systems may, for example, facilitate mapping of larger grassland areas at high spatial position accuracy, allowing the identification of nested structures within the vegetation. However, our findings also show the limits even advanced sensor systems have in the assessment of biomass of extremely heterogeneous grasslands, which is e.g. typical for very leniently stocked pastures. Thus, further research is necessary to be carried out to develop improved sensor systems for supporting practical grassland farming.

5.5 Supplement: Assessment of position accuracy – detailed information

To evaluate the position accuracy during mobile measurements within study plots (50 x 30 m), wooden planks were placed at the end of each vehicle lane at the outer edge of the plot border (Figure A5.1). With 120 x 40 x 11 cm (depth x width x height) targets had defined dimensions and allowed an unimpaired passage of the vehicle.

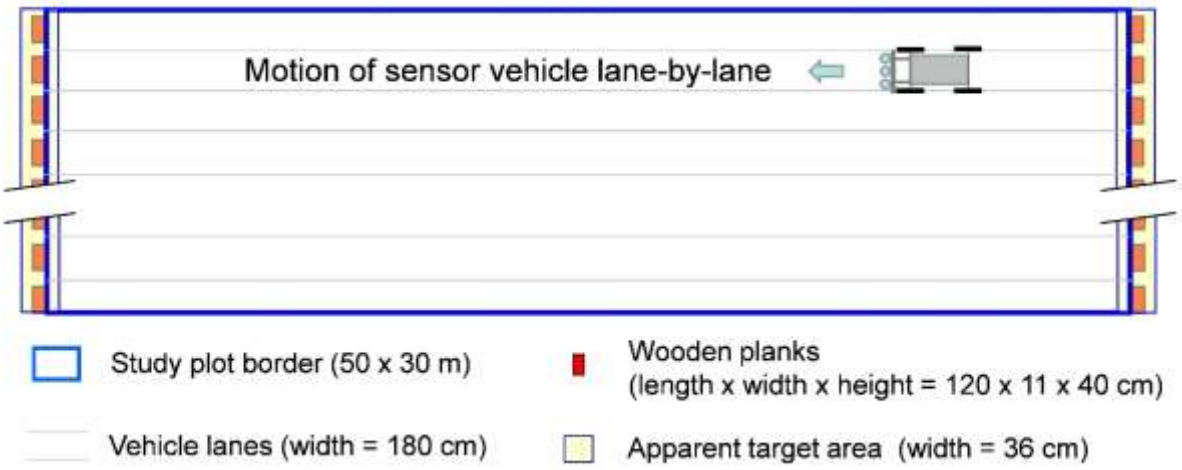

Figure A5.1 Display of reference targets (wooden planks) at the front ends of the study plot. Targets of defined dimensions and positions allowed the passage of the sensor vehicle moving lane-by-lane.

Position accuracy was assessed by identifying erroneous measurements with respect to apparent target edges. For this purpose, the mounted ultrasonic sensors were used as they provide both, high measurement densities along the lanes and sensitive reactions of the measurement signal at target detection. Depending on the field of view and the mount height of the sensor, targets were expected to be hit by the sound cone already at a distance of 12.5 cm on both sides of the target edges during passage, resulting in a total target detection range (apparent target area) of 36 cm width including the target depth of 11 cm (Figure A5.2).

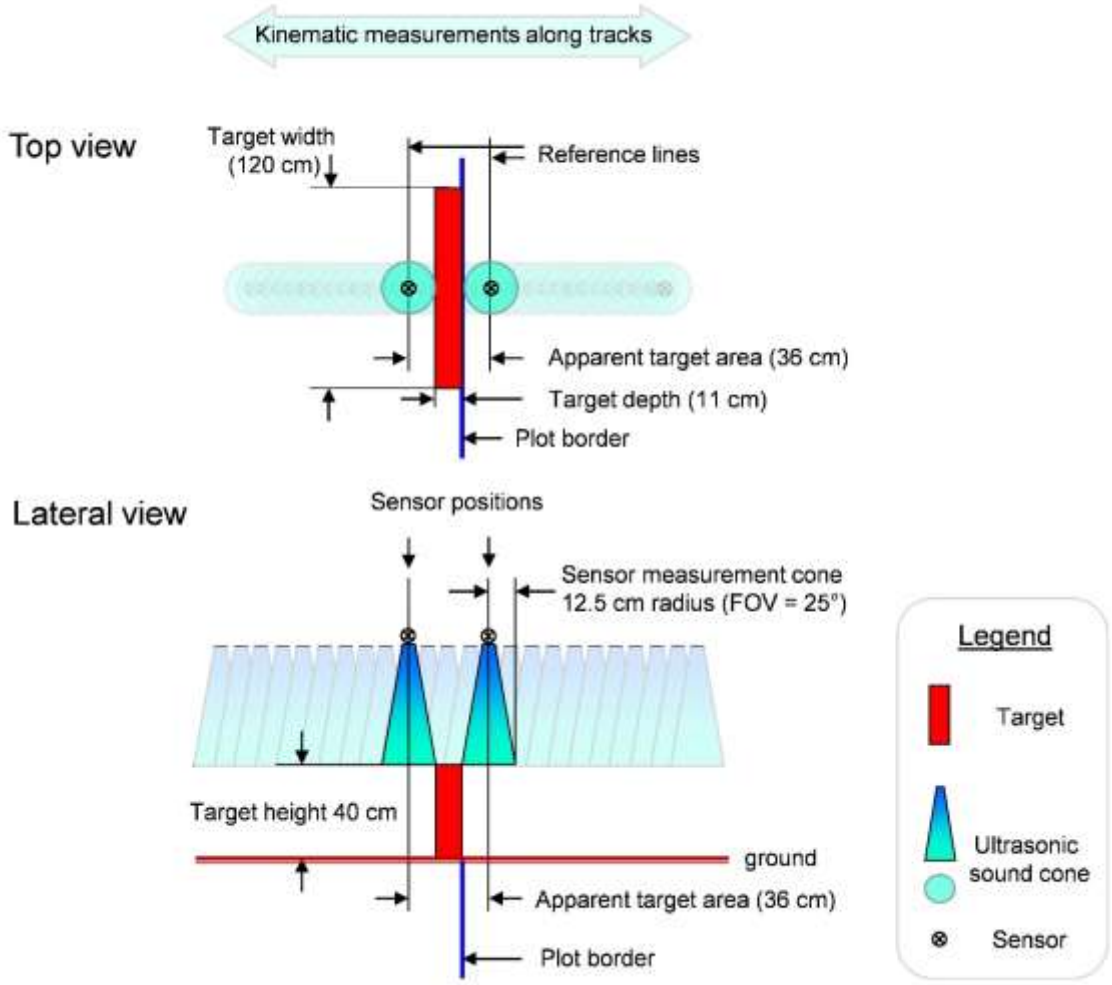

Figure A5.2 Display of a reference target, as used for assessing position accuracy and measured by ultrasonic sensors during passage of the vehicle. The two featured sensor positions show the distance range of expected target detection (apparent target area) independent of moving direction. These positions are used as reference lines for distinction and classification of correct and erroneous measurements.

A data set was generated using USH measurements within a 25 cm-distance around the apparent target edges (Figure A5.3). Recordings were performed in the moderately grazed study plot in April 2014 before vegetation started to grow. The low canopy height at this time of the year ensured a sufficient discrimination between grassland canopy and targets. USH measurements at locations within the investigated distance (n = 920) were attributed with their specific distance to the apparent edge of the targets. Though targets had a defined height of 40 cm, measured height values varied due to surface roughness and vehicle movements. This required the determination of the actual target height from the total dataset of USH values and to distinguish this from the sward heights. For this purpose, the data set was separated by using the inflection point of a height-sorted USH

histogram to group and classify readings into low grassland (mean = 8.7, SD = ± 5.6) and target (mean = 42.0, SD = ± 4.3) members. Figure A3 presents an example of the classified readings and their respective locations, illustrating point density and compliance with target values.

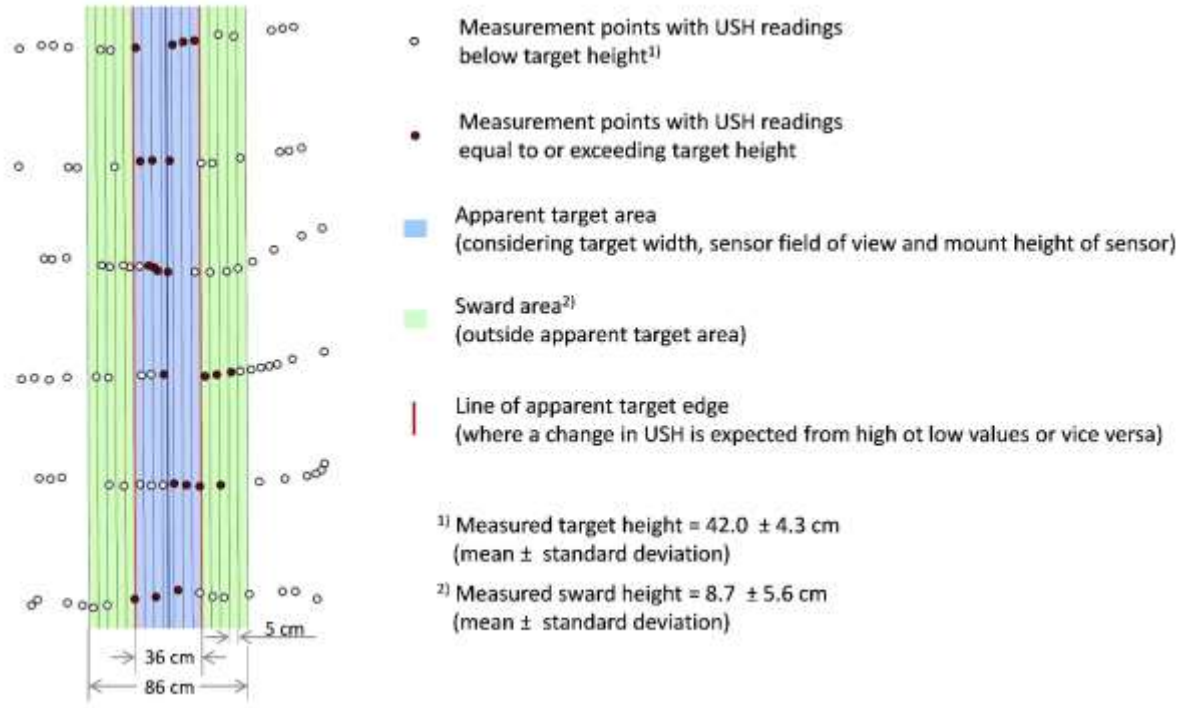

Figure A5.3 Locations of measurement points with ultrasonic sward height (USH) readings generated by vehicle-mounted sensors during the passage of targets for determining position accuracy. The diagram exemplarily shows a 3.4 x 1.7 m² map extract of the moderately stocked grassland paddock (see Fig 5.1).

6 General discussion and conclusions

This chapter reviews and discusses the findings of the conducted studies, which aimed to demonstrate the potential of using a combination of ultrasonic and canopy reflectance data to predict forage quantity and quality variables in extremely heterogeneous pastures. It also presents the final conclusions and recommendations for further research.

6.1 General summary and discussion

6.1.1 Exclusive sensors

Non-destructive techniques with high sampling density and spatial resolution are recommended to estimate biomass and quality parameters in grassland ecosystems (Pullanagari et al. 2012 and 2013). One of the most common methods currently used to assess sward canopy characteristics is spectral reflectance. Prediction of grassland biomass from height measurements is further method popular in grassland studies. Different methodologies were used in the various studies for estimation of biomass from height measurements. Estimating forage biomass with both physical height measurements using a commercial capacitance meter, rising plate meter and pasture rulers (meter sticks) (Sanderson et al. 2001; Fehmi et al. 2009; Dougherty et al. 2013) and sensor height measurements using laser (lidar) and ultrasonic sensors (Ehlert et al. 2009; Fricke et al. 2011; Pittman et al. 2015) has been developed in pasture management. Lidar (laser or 3D scanning) sensors measure distances by time-differential reflectance of a laser light while ultrasonic sensors are based on the measurements of reflected sound waves. The limitations associated with physical measurements of vegetation height and biomass estimation are labour and time intensiveness (Pittman et al. 2015). Additionally, those methods are not applicable to obtain spatial variability in large scale fields. Alternatively, sensor based methods may overcome the limitations associated with physical measurement methods. The prediction models developed in the present study by exclusive use of ultrasonic sward height (USH) or spectral data (Chapter 3 and 4) showed relatively lower accuracy compared to other researches. For example Biewer et al. (2009b), Fricke et al. (2011), Fricke and Wachendorf (2013) and Reddersen et al. (2014) received better calibration results for prediction of biomass yield and quality parameters using those sensors. It may reflect the fact that adaption of remote-sensing technologies in grazing systems is more difficult compared to cropping systems, due to the presence of complex heterogeneity. Grazing animals are selective in their foraging behaviour and influence grassland community, composition, structure and

productivity by patch or selective grazing. This behaviour creates spatially and temporally extremely dynamic environments (Correll et al., 2003; Schellberg et al., 2008). This can limit prediction of sward characteristics using ground-based sensors in complex pastoral environments and could lead to poor performance of those methods typically developed for more homogeneous grassland communities. In this study MPLSR used the information from all wavelengths to explain maximum variations in hyperspectral dataset and therefore accurate results were obtained (Chapter 3 and 4). A reduction in prediction accuracy was observed for each pasture parameters by limiting hyperspectral data into derived spectral variables. Although the results of MPLSR were satisfactory for both quantity and quality parameters, the hyperspectral sensors are expensive and significant data computation is needed (Starks et al., 2006). Therefore, such techniques are not straightforward and developing low cost instruments (such as multispectral sensors) are more desirable in order to quantify pasture characteristics. Among the tested spectral predictor variables derived from hyperspectral data, NDSI using 1 nm waveband selection was the best predictor of biomass and quality parameters. As in the present study, other studies have also shown better results by using narrow-waveband vegetation indices (VIs) compared to broad-waveband VIs in vegetation canopies (Thenkabail et al., 2000; Mutanga and Skidmore, 2004). Better understanding of the target parameters could be obtained by increasing the spatial resolution of the sensor as the sensor provides reasonable information with high precision (Schellberg et al., 2008). Moreover, most of the spectral variables could exceed the prediction accuracy of exclusive USH measurements for prediction of both biomass and quality parameters. Noticeably the performance of ultrasonic sensor for predicting quality parameters was very poor (Chapter 4). The results on exclusive approaches in Chapter 4 indicated that unlike ultrasonic sward height, hyperspectral data could be good predictor for quality in pastures with heterogeneous swards. This results were not consistent with those of Fricke and Wachendorf (2013) and Reddersen et al. (2014), where exclusive USH always achieved better prediction results than reflectance data in more homogenous swards. Therefore, exclusive ultrasonic sward height might not be a well suited predictor for biomass and quality variables in pastures with high levels of heterogeneity. Pasture canopies (as in our study site) are generally dominated by grass species which influence canopy structures by changes in their maturity levels. These kind of canopy structures with various layers of sward density could be a major limitation for ultrasonic sensor and limit its capability to detect true values of sward height in heterogeneous pastures. As it is demonstrated in chapter 3, the main limitation in diverse sward structure is that ultrasonic sensors provide a distance measurement based on signals reflecting from

top of the canopy regardless of sward density. Tall sparse species for instance, can influence the reflected echo (overlapping effect) and ultrasonic sward height does not reflect the actual canopy height. Another example could be dense canopy of some short paddocks in which canopy height does not represent sward density. Our findings showed, that both ultrasonic and spectral sensors faced limitations at more advanced developmental stages of swards when dead material accumulation and complexity of sward structures were maximum (Chapter 3 and 4). For biomass assessment high correlation between ultrasonic sward height and biomass was observed in the first sampling date while the analysis did not show a good agreement for the other dates (chapter 3). Some other researches also concluded that the use of ultrasonic measurements are more accurate at early stages, similarly to the situation found in our study (Fricke et al. 2011; Andújar et al. 2012). Fricke et al. 2011 stated the relationship between ultrasonic sward height and biomass can be influenced by species composition and phonological development. A saturation effect especially in pure grasses occurred by increasing in height detected by the sensor without continuous increase in leaf mass. Despite these limitations, some advantages derive from the use of ultrasonic sensors in pasture management. One of the main advantages could be the possibility of them for real time applications. Another advantage is the relatively low costs of these sensors that allow measuring the whole field with high spatial resolution using multiple sensors in parallel. Additionally, ultrasonic sensors are user-friendly and not affected by light conditions (Andújar et al. 2012). The possibility of ultrasonic sensors to be used in sensor fusion for obtaining more reliable estimations is also of a great importance (Adamchuk et al. 2011). Fricke and Wachendorf (2013) demonstrated that limitation of biomass assessment based on canopy height could partly be compensated by inclusion of spectral data. In overall, our finding emphasizes the fact that prediction of pasture characteristics only based on canopy height measurements or spectral variables derived from hyper spectral data could not be satisfactory. Therefore, combination of both sensors is very important in heterogeneous pastures.

6.1.2 Combined sensors

The combination of ultrasonic and spectral sensor data for the prediction of biomass and quality parameters produced in most cases significantly better results than their exclusive use. However sensor data fusion using ultrasonic and spectral variables gave more promising result for prediction of biomass compared to quality parameters and among quality parameters for acid detergent fiber predictions (Chapter 3 and 4). The amount of increase in R^2 for prediction of biomass by USH-NDSI combinations versus exclusive USH was higher in the present study in comparison with the investigations of Fricke and Wachendorf (2013) in legume-grass mixtures and Reddersen et al. (2014) in an extensively managed grassland. They reported maximum 20% increase in R^2 by USH-NDSI combinations whereas maximum 40% improvement in R^2 was observed in our study. This implies that the combination of both sensors is more important in heterogeneous pastures as stated before. From all the tested spectral variables, sensor data fusion by combining USH with narrow band NDSI or WorldView2 satellite broad bands increased the prediction accuracy for estimation of both quality and quantity variables while reducing the prediction error during the whole grazing season. Even though MPLSR resulted in much higher prediction accuracy compared to those spectral variable in exclusive use, such combinations (USH-NDSI or USH-WV2) can produce estimates comparable to (or even more accurate than) MPLSR method in terms of R^2 and standard error. The potential of developed models to predict temporal variations was further evaluated by including the datasets of different sampling dates. More accurate results were achieved when prediction models were developed separately for each sampling date. However, the prediction results differed with season and pasture parameters. This could be due to the seasonal variations of pasture characteristics, varying proportions of functional groups, species-specific traits and increased amounts of dead material. Cabrera-Bosquet et al. (2011) also found different prediction accuracies for estimation of aboveground biomass (R^2= 0.64-0.79) and nitrogen content in wheat (R^2 = 0.41-0.71) using NDVI measurements at different growth stages. This indicate the importance of multi-temporal data acquisition and subsequently date-specific calibrating models in order to increase model predictability for biomass and quality estimation using the suggested methods in heterogeneous pastures. Date-specific calibration results also suggested that the more precise sampling procedures which consider available range of attributes and their spatial and temporal variability could improve predictive capability of models. Best results for sensor combinations were achieved at the first half of the growing season when good performances of

either ultrasonic or reflectance sensor were observed. As both ultrasonic and spectral sensors have weaknesses at more advanced developmental stages of swards, the maximum accuracy was less comparing early to mid-growing season even though the improvement was achieved by sensor data fusion. Apart from complexity of sward structure which is a main limitation for ultrasonic sensor, the presence of a high proportion of dead materials in biomass can impact on the performance of the reflectance sensor either in exclusive use or combined with ultrasonic sensor (Chapter 3). The lower model accuracies for biomass and quality variables using combined sensors at the end of grazing season could mostly be due to the accumulation of senescent material. More investigations are needed to quantify such effects. Considering the limitations of ultrasonic sensor, the combined use of hyperspectral and lidar sensors which accurately measure three dimensional canopy structures and vertical heterogeneity might improve prediction accuracy of biomass and quality estimations. As a further matter, even though visible-near infrared spectral regions were identified as the most informative parts of the spectrum for the prediction models using NDSI band selection at different stages of grazing season, using a spectrometer with more spectral ranges (up to 2400nm) may improve the result. The second highest potential for biomass and quality prediction using sensor data fusion was shown for USH-WV2 combination which opens the doors towards the goal of being able to determine pasture characteristics from space in the way that can be used for decision making such as planning grazing time and intervals, forage removal and stocking rate adjustments. The relatively high prediction accuracy of WV2 bands points at the potential of the WordView-2 satellite system to provide large-scale images with an acceptable spatial resolution to assess larger pasture areas for practical field applications in farming practice. Radar satellites for example might be useful for this kind of sensor data fusion, as they can provide measures of vertical structure such as canopy height. The addition of this kind of new satellite platforms might provide the opportunity to monitor pasture biomass, growth rate and feed quality in more precise manner and over vast areas on which to base grazing management, feed budgeting and allocations in terms of planning, control and monitoring.

In Chapter 5 sensor combination was further investigated on a mobile platform integrated with global positioning system (GPS) to evaluate biomass prediction accuracies by site-specific measurements. Disparities between static and mobile measurements of NDSI compared to USH measurements was observed which could be the reason for lower accuracy of mobile biomass prediction by sensor vehicle in extensively managed pastures. In fact reflectance sensor relies on natural illumination source to capture spectra of vegetation canopies which could be inconsistent

and affect the spectral data capturing even in a very short time interval and have a distinct effect on vegetation indices (Qi et al., 1994). Moreover, unstable weather conditions (e.g. cloudy situation) influenced the resolution of data capturing by the sensor vehicle. The higher resolution (higher sampling points) is especially important in lenient and very lenient pastures where spatial variations are very high. High spatial resolution or sampling rate are recommended to estimate various grassland attributes through non-destructive methods to achieve suitable management practices (Dusseux et al., 2011). Sensor-vehicle position error ranges identified in the present research was rather low (8.5 ± 5.8 cm). However, attempts to reduce such impacts may improve accuracy of research results. In general, the findings in chapter 5 show such combined sensor technique can be utilized to produce high resolution maps with acceptable prediction accuracies at early to medium growth stages common for moderately and to some extent leniently grazed pastures. In the first application calibration models from the combination of USH and NDSI were used to generate 10 cm grid cell maps of fresh matter yield (FMY) through geostatistical interpolation method ordinary kriging with the spherical semivariogram model (figure 6.1). Such maps allow the information to be used in further analysis of spatio-temporal pasture dynamics e.g. to examine the effects of grazing intensities on spatial distribution patterns of sward characteristics in the target paddocks. Mapping and accurate quantifying grassland characteristics such as biomass, are needed over continuous periods to understand the effects of environmental and driving factors (grazing, droughts, etc.) on the spatial and temporal vegetation changes. The provided information could be very helpful for making effective grassland management decisions, for instance, improvement of short-grass patches by minimizing patch overgrazing, in order to sustain and restore forage resources and improve productivity and functioning. Fulkerson et al. (2005) reported that accurate and real-time measurements of pasture biomass can improve pasture productivity and utilization.

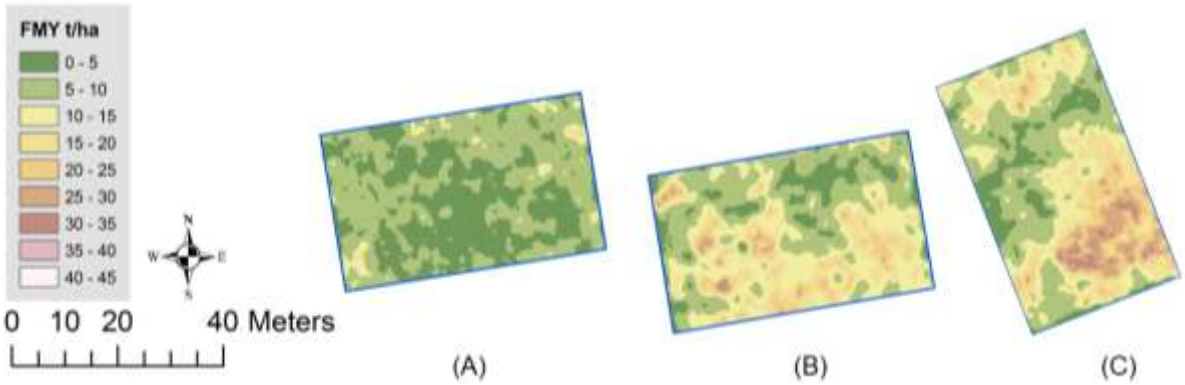

Figure 6.1 Spatial distribution maps of fresh matter yield in paddocks with different stocking rates: A) moderate B) lenient C) very lenient (3rd-5th June 2013).

To summarize, the developed technique of combining ultrasonic and hyperspectral sensors improved prediction accuracy of biomass and quality parameters compared with use of each individual sensor in pastures characterized by a high structural and phenological diversity. With data fusion sensor system performed on the field level, the applicability and performance might significantly improve in comparison with conventional measurement techniques which require considerable amount of time, cost and effort. The on-the-go measurements of sward characteristics using such combined sensors allow for non-destructive data collections over larger areas in much quicker and less time consuming manner. Although hyper-spectral radiometers are costly and not feasible for grassland managers and farmers, the combination of low-cost ultrasonic sward height with vegetation indices has the potential for developing cost-effective sensor methods for pastures in the future and may improve assessment of biomass and quality attributes for site-specific management. If applicable, data collected from such mobile platform can be implied in decision making process such as stocking rate adjustment or forage removal in grazing management. However, the complexity associated with pasture ecosystems due to interactions between selective grazing and vegetation phenology poses a huge challenge for sensor applications. Hence, extending the results of this study towards the practical reliability of these technologies and the development of new sensor fusion algorithms to overcome such limitations need further investigations.

6.2 Conclusions

(i) Exclusive ultrasonic sward height measurement might not be a well suited predictor for biomass and quality attributes in pastures with high levels of heterogeneity.

(ii) The results suggested that hyperspectral techniques such as MPLSR method can be used to determine pasture biomass and quality attributes with sufficient prediction accuracy. However, attempts to refine the methodology towards the goal of practical implementation at field scale by limiting the number of wavebands caused the loss of information and lower prediction accuracy for each pasture parameter.

(iii) Estimation of biomass and quality through sensor data fusion using field spectroscopy and ultrasonic sward height could be achieved with acceptable accuracy comparable with MPLSR method in pastures with diverse sward structure. However some factors such as high amount of senescent material, morphological development of pasture canopy and complexity of sward structure at more advance developmental stages of swards especially in extensively managed pastures might limit this possibility.

(iv) Prediction accuracy seems to be affected by species-specific traits obviously depending on phenological development according to the sampling dates. Better results were obtained for samples from spring and early summer.

(v) The performance of WV2-USH models based on WorldView2 satellite broad wavebands showed strong potential for prediction of biomass and to some extent for quality attributes suggesting that attempts to employ future satellite based sensors could be beneficial.

(vi) Even if future research is necessary to identify the limitations and improve sensor configurations, the present research of applying combined sensing technique on pasture canopies, could be seen as a step towards being able to measure and map pasture properties of interest in real time and at the field scale. Such techniques offer grazing managers accurate and timely methods for monitoring grasslands prior to and post-grazing in order to improve management practices.

6.3 Recommendations for future research

(i) Accuracy may be further increased by inclusion of more than two wavebands in hyperspectral vegetation indices derived by wavelength selection.

(ii) It has been shown that wavelengths related to visible and near infrared (e.g. water content bands) among other curve features were found to be most important. However expanding the wavelength up to the shortwave infrared regions (2400 nm) may further improve the results.

(iii) Due to spectral noise caused by shading and changeable natural illumination, a more robust and reliable selection of wavebands over a bandwidth of 50 nm or more might be preferred for NDSI band combinations over narrow band indices. This could minimize the effects of such noises in waveband selections and might lead to apply broadband multi-spectral sensors which are preferred by farmers due to cost and practicality.

(iv) Further work is important to examine other possible combination of spectral and height data to produce high resolution maps. In this respect fusion of hype-spectral and LIDAR (3D laser scanning) or RADAR data which obtain canopy structure with high resolution could be valuable.

(v) In this study a four-fold cross validation method was used to evaluate the performance of calibration models. However, testing the calibration equations on independent dataset would ensure their usefulness.

(vi) In order to improve the results, it could also be recommended to be aware of various factors affecting the accuracy of calibration models and try to minimize their impact as much as possible. It can be suggested to test such mobile sensor technique in homogenous grassland communities with one or few species type or different cutting systems. This would allow reduction of complexity existing in this research and enabling the full potential of the combined sensors to achieve more precise estimations of vegetation attributes of interest.

7 References

Adamchuk, V. I., Hummel, J. V., Morgan, M. T., Upadhyaya and S. K. (2004). On-the-go soil sensors for precision agriculture. *Comp. Elect. Agric*, 44(1): 71-91.

Adamchuck, V. I., Viscarra Rossel, R. A., Sudduth, K. A., & Lammers, P. S. (2011). Sensor fusion for precision agriculture. *Sensor fusion – foundation and applications*, edited by: Thomas, C., InTech, chap. 2, 27–40.

Aliah Baharom, S. N., Shibusawa, S., Kodaira, M., Kanda, R. (2015). Multiple-depth mapping of soil properties using a visible and near infrared real-time soil sensor for a paddy field. *Engineering in Agriculture, Environment and Food*, 8 (1), pp. 13–17. DOI: 10.1016/j.eaef.2015.01.002.

Anderson, M., Neale, C., LI, F., Norman, J., Kustas, W., Jayanthi, H., & Chavez, J. (2004). Upscaling ground observations of vegetation water content, canopy height, and leaf area index during SMEX02 using aircraft and Landsat imagery. *Remote Sensing of Environment*, 92 (4), 447–464. DOI: 10.1016/j.rse.2004.03.019.

Andújar, D., Weis, M., & Gerhards, R. (2012). An ultrasonic system for weed detection in cereal crops. Sensors, 12(12), 17343-17357.

Ayantunde, A. A., Hiernaux, P., Fernandez-Rivera, S., Van Keulen, H., & Udo, H. M. J. (1999). Selective grazing by cattle on spatially and seasonally heterogeneous rangeland in Sahel. *Journal of Arid Environments*, 42(4), 261-279.

Bakker, J. P., De Leeuw, J., Van Wieren, S. E. (1984). Micro-patterns in grassland vegetation created and sustained by sheep-grazing. *Vegetatio*, 55(3), 153-161.

Barnes, M. K., Norton, B. E., Maeno, M., Malechek, J. C. (2008). Paddock size and stocking density affect spatial heterogeneity of grazing. *Rangeland Ecology & Management*, 61(4), 380-388.

Biewer, S., Fricke, T., & Wachendorf, M. (2009a). Determination of Dry Matter Yield from Legume–Grass Swards by Field Spectroscopy. *Crop Science*, 49 (5), 1927–1936. DOI: 10.2135/cropsci2008.10.0608.

Biewer, S., Fricke, T., & Wachendorf, M. (2009b). Development of Canopy Reflectance Models to Predict Forage Quality of Legume–Grass Mixtures. *Crop Science*, 49 (5), 1917–1926. DOI: 10.2135/cropsci2008.11.0653.

Biewer, Sonja; Erasmi, Stefan; Fricke, Thomas; Wachendorf, Michael (2009c): Prediction of yield and the contribution of legumes in legume-grass mixtures using field spectrometry. *Precision Agric*, 10 (2), pp. 128–144. DOI: 10.1007/s11119-008-9078-9.

Blüthgen, N., Dormann, C. F., Prati, D., Klaus, V. H., Kleinebecker, T., Hölzel, N., ... & Müller, J. (2012). A quantitative index of land-use intensity in grasslands: integrating mowing, grazing and fertilization. *Basic and Applied Ecology*, 13(3), 207-220.

Boschetti, M., Bocchi, S., & Brivio, P. A. (2007). Assessment of pasture production in the Italian Alps using spectrometric and remote sensing information. *Agriculture, Ecosystems & Environment*, 118 (1-4), 267–272. DOI: 10.1016/j.agee.2006.05.024.

Cabrera-Bosquet, L., Molero, G., Stellacci, A., Bort, J., Nogués, S., & Araus, J. (2011). NDVI as a potential tool for predicting biomass, plant nitrogen content and growth in wheat genotypes subjected to different water and nitrogen conditions. *Cereal Research Communications*, 39(1), 147-159.

Cammarano, D., Fitzgerald, G., Casa, R., Basso, B. (2014). Assessing the Robustness of Vegetation Indices to Estimate Wheat N in Mediterranean Environments. *Remote Sensing*, 6 (4), pp. 2827–2844. DOI: 10.3390/rs6042827.

Castle, M. E. (1976). A simple disc instrument for estimating herbage yield, J Br *Grassl Soc*., 31, 37-40, DOI: 10.1111/j.1365-2494.1976.tb01113.x.

Chang, C.W., Laird, D. A., Mausbach, M. J., Hurburgh, C. R. (2001). Near-Infrared Reflectance Spectroscopy–Principal Components Regression Analyses of Soil Properties. *Soil Science Society of America Journal*, 65 (2), p. 480. DOI: 10.2136/sssaj2001.652480x.

Chen, P., Haboudane, D., Tremblay, N., Wang, J., Vigneault, P., & Baoguo, Li. (2010). New spectral indicator assessing the efficiency of crop nitrogen treatment in corn and wheat. *Remote Sensing of Environment*, 114 (9), 1987–1997. DOI: 10.1016/j.rse.2010.04.006.

Cho, M. A., Skidmore, A., Corsi, F., Wieren, S, E., & Sobhan, I. (2007). Estimation of green grass/herb biomass from airborne hyperspectral imagery using spectral indices and partial least squares regression. *International Journal of Applied Earth Observation and Geoinformation*, 9 (4), 414–424. DOI: 10.1016/j.jag.2007.02.001.

Cozzolino, D., Porker, K., Laws, M., (2015). An Overview on the Use of Infrared Sensors for in Field, Proximal and at Harvest Monitoring of Cereal Crops. *Agriculture*, 2015, 5, pp. 713-722. DOI:10.3390/agriculture5030713.

Clark, R. N., & Roush, T. L. (1984). Reflectance spectroscopy: Quantitative analysis techniques for remote sensing applications. *Journal of Geophysical Research*, 89 (B7), 6329. DOI: 10.1029/JB089iB07p06329.

Correll, O., Isselstein, J., Pavlu, V. (2003). Studying spatial and temporal dynamics of sward structure at low stocking densities: the use of an extended rising-plate-meter method. *Grass and Forage Science*, 58(4), 450-454.

Darvishzadeh, R., Skidmore, A., Schlerf, M., Atzberger, C., Corsi, F., & Cho, M. (2008). LAI and chlorophyll estimation for a heterogeneous grassland using hyperspectral measurements. *ISPRS Journal of Photogrammetry and Remote Sensing*, 63(4), 409-426.

Deaville, E. R., Flinn, P. C. (2000). Near-infrared (NIR) spectroscopy: an alternative approach for the estimation of forage quality and voluntary intake. In D. I. Givens, E. Owen, R. F. E. Axford, H. M. Omed (Eds.): *Forage evaluation in ruminant nutrition*. Wallingford: CABI, pp. 301–320.

Demetriades-Shah, T. H., Steven, M. D., & Clark, J. A., (1990). High resolution derivative spectra in remote sensing. *Remote Sensing of Environment*, 33 (1), pp. 55–64. DOI: 10.1016/0034-4257(90)90055-Q.

Diaconis, P., & Efron, B. (1983). Computer-intensive methods in statistics. Sci. Am. Volume 248, Issue 5, pp. 96–108.

Dougherty, M.; Burger, J.A.; Feldhake, C.M.; AbdelGadir, A.H. (2013). Calibration and use of plate meter regressions for pasture mass estimation in an Appalachian silvopasture. Arch. Agron. Soil Sci., 59, 305–315.

Duan, M. J., Gao, Q. Z., Wan, Y. F., Li, Y., Guo, Y. Q., Ganzhu, Z. B., Liu Y. T., & Qin, X. B. (2014). Biomass estimation of alpine grasslands under different grazing intensities using spectral vegetation indices. *Canadian Journal of Remote Sensing*, 37 (4), 413–421. DOI: 10.5589/m11-050.

Dumont, B., Rossignol, N., Loucougaray, G., Carrère, P., Chadoeuf, J., Fleurance, G., ... & Louault, F. (2012). When does grazing generate stable vegetation patterns in temperate pastures?. *Agriculture, ecosystems & environment*, 153, 50-56.

Dusseux, P.; Hubert-Moy, L.; Lecerf, R.; Gong, X.; Corpetti, Th. (2011). Identification of grazed and mown grasslands using a time series of high-spatial-resolution remote sensing images. In 6th International Workshop on the Analysis of Multi-temporal Remote Sensing Images (Multi-Temp). Trento, Italy, pp. 145–148.

Ehlert, D., Horn, H.-J., Adamek, R. (2008). Measuring crop biomass density by laser triangulation. *Computers and Electronics in Agriculture*, 61, 117–125.

FAO, (2010). Greenhouse Gas Emissions from the Dairy Sector: A life Cycle Assessment (A. P. a. Health, Trans.). Rome, Italy: Food and Agriculture Organization.

Farooque, A. A., Chang, Y. K., Zaman, Q. U., Groulx, D., Schumann, A. W., & Esau, T. J. (2013). Performance evaluation of multiple ground based sensors mounted on a commercial wild blueberry harvester to sense plant height, fruit yield and topographic features in real-time. *Computers and Electronics in Agriculture*, 91, 135–144. DOI: 10.1016/j.compag.2012.12.006.

Fava, F., Colombo, R., Bocchi, S., Meroni, M., Sitzia, M., Fois, N., Zucca, C. (2009). Identification of hyperspectral vegetation indices for Mediterranean pasture characterization. *International Journal of Applied Earth Observation and Geoinformation*, 11 (4), pp. 233–243. DOI: 10.1016/j.jag.2009.02.003.

Fehmi, J.S.; Stevens, J.M. (2009). A plate meter inadequately estimated herbage mass in a semi-arid grassland. Grass Forage Sci., 64, 322–327.

Flynn, E. S., Dougherty, C. T., Wendroth, O. (2008). Assessment of pasture biomass with the normalized difference vegetation index from active ground-based sensors. *Agronomy Journal*, 100(1), 114-121.

Fricke, T., Richter, F., & Wachendorf, M. (2011). Assessment of forage mass from grassland swards by height measurement using an ultrasonic sensor. *Computers and Electronics in Agriculture*, 79 (2), 142–152. DOI: 10.1016/j.compag.2011.09.005.

Fricke, T., & Wachendorf, M. (2013). Combining ultrasonic sward height and spectral signatures to assess the biomass of legume–grass swards. *Computers and Electronics in Agriculture*, 99, 236–247. DOI: 10.1016/j.compag.2013.10.004.

Fulkerson, W. J., McKean, K., Nandra, K. S., & Barchia, I. M. (2005). Benefits of accurately allocating feed on a daily basis to dairy cows grazing pasture. *Animal Production Science*, 45(4), 331-336.

Gherbin, P., De Franchi, A. S., Monteleone, M., & Rivelli, A. R. (2007). Adaptability and productivity of some warm-season pasture species in a Mediterranean environment. *Grass and Forage Science*, 62 (1), pp. 78–86. DOI: 10.1111/j.1365-2494.2007.00566.x.

Goel, N. S. (1988). Models of vegetation canopy reflectance and their use in estimation of biophysical parameters from reflectance data. *Remote Sensing Reviews*, 4 (1), pp. 1–212. DOI: 10.1080/02757258809532105.

Gottfried T., Auerswald K., Ostler U. (2012). Mobile correction for a spatial offset between sensor and position data in on-the-go sensor applications. *Computers and Electronics in Agriculture*, 84, 76-84.

Guo, X., Wilmshurst, J. F., Li, Z. (2010). Comparison of laboratory and field remote sensing methods to measure forage quality. *International journal of environmental research and public health*, 7 (9), pp. 3513–3530. DOI: 10.3390/ijerph7093513.

Hakl, J., Hrevušová, Z., Hejcman, M., Fuksa, P. (2012). The use of a rising plate meter to evaluate Lucerne (Medicago sativa L.) height as an important agronomic trait enabling yield estimation. *Grass and Forage Science*, 67, 589-596.

Hirata, M. (2000). Quantifying spatial heterogeneity in herbage mass and consumption in pastures. *Journal of Range Management*, 315-321.

Hobbs, N. T., Swift, D. M. (1988). Grazing in herds: when are nutritional benefits realized?. *American Naturalist*, pp. 760-764.

Hofmann, M., Kowarsch, N., Bonn, S., Isselstein, J. (2001). Management for biodiversity and consequences for grassland productivity. *Grassland Science*, Eur, (6), pp. 113–116.

Hutchings, N. J. (1992). Factors affecting sonic sward stick measurements: the effect of different leaf characteristics and the area of sward sampled. *Grass and Forage Science*, 47 (2), 153–160. DOI: 10.1111/j.1365-2494.1992.tb02258.x.

Hutchings, N. J., Phillips, A. H., & Dobson, R. (1990). An ultrasonic rangefinder for measuring the undisturbed surface height of continuously grazed grass swards. *Grass and Forage Science*, 45 (2), 119–127. DOI: 10.1111/j.1365-2494.1990.tb02192.x.

Inoue, Y., Penuelas, J., Miyata, A., & Mano, M. (2008). Normalized difference spectral indices for estimating photosynthetic efficiency and capacity at a canopy scale derived from hyperspectral and CO2 flux measurements in rice. *Remote Sensing of Environment*, 112 (1), 156–172. DOI: 10.1016/j.rse.2007.04.011.

Isselstein, J., Jeangros B, Pavlu V. (2005). Agronomic aspects of biodiversity targeted management of temperate grasslands in Europe – A review. *Agronomic research*, 3 (2), 139-151.

Jackson, R. D., & Huete, A. R. (1991). Interpreting vegetation indices. *Preventive Veterinary Medicine*, 11 (3-4), pp. 185–200. DOI: 10.1016/S0167-5877(05)80004-2.

Jacquemoud S., Baret F. (1990). a model of leaf optical properties spectra, *Remote Sensing of Environment*, 34(2), pp.75-91. DOI: 10.1016/0034-4257(90)90100-Z.

Jerrentrup, J. S., Wrage-Mönnig, N., Röver, K. U., & Isselstein, J. (2014). Grazing intensity affects insect diversity via sward structure and heterogeneity in a long-term experiment. *Journal of Applied Ecology*, 51(4), 968-977.

Jones, C. L., Maness, N. O., Stone, M. L., & Jayasekara, R. (2007). Chlorophyll Estimation Using Multispectral Reflectance and Height Sensing. *Transactions of the ASABE*, 50 (5), 1867–1872. DOI: 10.13031/2013.23938.

Kawamura, K., Betteridge, K., Sanches, I. D., Tuohy, Mike P., Costall, D., Inoue, Y. (2009). Field radiometer with canopy pasture probe as a potential tool to estimate and map pasture biomass and mineral components: A case study in the Lake Taupo catchment, New Zealand. *New Zealand Journal of Agricultural Research*, 52 (4), pp. 417–434. DOI: 10.1080/00288230909510524.

Klapp, E. L., & Stählin, A. (1936). Standorte, Pflanzengesellschaften und Leistung des Grünlandes. Stuttgart, Germany: Ulmer.

Kristensen, T., Søegaard, K., Kristensen I.S. (2005). Management of grasslands in intensive dairy livestock farming. *Livestock production science*, 96, (1), pp. 61-73. DOI:10.1016/j.livprodsci.2005.05.024

Kumar, L., Sinha, P., Taylor, S., & Alqurashi, A. F. (2015). Review of the use of remote sensing for biomass estimation to support renewable energy generation. *Journal of Applied Remote Sensing*, 9, DOI: 10.1117/1.JRS.9.097696.

Lan, Y., Zhang, H., Lacey, R., Hoffmann, W.C., Wu, W. (2009). Development of an Integrated Sensor and Instrumentation System for Measuring Crop Conditions. *Agricultural Engineering International*: the CIGR Ejournal. Manuscript IT 08 1115. Vol. XI. April.

Lee, H. J., Kawamura, K., Watanabe, N., Sakanoue, S., Sakuno, Y., Itano, S., Nakagoshi, N. (2011). Estimating the spatial distribution of green herbage biomass and quality by geostatistical analysis with field hyperspectral measurements. *Grassland Science*, 57 (3), pp. 142–149. DOI: 10.1111/j.1744-697X.2011.00221.x.

Li, F., Mistele, B., Hu, Y., Chen, X., Schmidhalter, U. (2014a). Reflectance estimation of canopy nitrogen content in winter wheat using optimised hyperspectral spectral indices and partial least squares regression. *European Journal of Agronomy*, 52, pp. 198–209. DOI: 10.1016/j.eja.2013.09.006.

Li, X., Zhang, Y., Bao, Y., Luo, J., Jin, X., Xu, X., et al. (2014b). Exploring the Best Hyperspectral Features for LAI Estimation Using Partial Least Squares Regression. *Remote Sensing*, 6 (7), pp. 6221–6241. DOI: 10.3390/rs6076221.

Marabel, M., & Alvarez-Taboada, F. (2013): Spectroscopic determination of aboveground biomass in grasslands using spectral transformations, Support Vector Machine and Partial Least Squares Regression. *Sensors*, 13 (8), pp. 10027–10051. DOI: 10.3390/s130810027.

Mazzetto, F., Calcante, A., Mena, A., & Vercesi, A. (2010). Integration of optical and analogue sensors for monitoring canopy health and vigour in precision viticulture. *Precision Agriculture*, 11 (6), 636–649. DOI: 10.1007/s11119-010-9186-1.

Milchunas, D. G., Varnamkhasti, A. S., Lauenroth, W. K., & Goetz, H. (1995). Forage quality in relation to long-term grazing history, current-year defoliation, and water resource. *Oecologia*, 101(3), pp. 366-374.

Muñoz-Huerta, R. F., Guevara-Gonzalez, R. G., Contreras-Medina, L. M., Torres-Pacheco, I., Prado-Olivarez, J., Ocampo-Velazquez, R. V. (2013). A Review of Methods for Sensing the Nitrogen Status in Plants: Advantages, Disadvantages and Recent Advances. *Sensors*, 13, 10823-10843. DOI:10.3390/s130810823.

Mutanga, O., & Skidmore, A. K. (2004). Narrow band vegetation indices overcome the saturation problem in biomass estimation. *International Journal of Remote Sensing*, 25 (19), 3999–4014. DOI: 10.1080/01431160310001654923.

Mutanga, O.; Skidmore, A. K.; Kumar, L.; Ferwerda, J. (2005). Estimating tropical pasture quality at canopy level using band depth analysis with continuum removal in the visible domain. *International Journal of Remote Sensing*, 26 (6), pp. 1093–1108. DOI: 10.1080/01431160512331326738.

Nagasaka Y., Umeda N., Kanetai Y., Taniwaki K., Sasaki Y. (2004). Autonomous guidance for rice transplanting using global positioning and gyroscopes. *Computers and Electronics in Agriculture*, 43, 223-234.

Nelder, J. A. (1994). The statistics of linear models: back to basics. *Statistics and Computing*, 4 (4), 221–234. DOI: 10.1007/BF00156745.

Nelder, J. A., Lane, P. W. (1995). The Computer Analysis of Factorial Experiments: In Memoriam—Frank Yates. *The American Statistician*, 49 (4), pp. 382–385. DOI: 10.1080/00031305.1995.10476189.

Numata, I., Roberts, D., Chadwick, O., Schimel, J., Galvao, L., & Soares, J. (2008). Evaluation of hyperspectral data for pasture estimate in the Brazilian Amazon using field and imaging spectrometers. *Remote Sensing of Environment*, 112 (4), 1569–1583. DOI: 10.1016/j.rse.2007.08.014.

Oudshoorn, F. W., Cornou, C., Hellwing, A. L. F., Hansen, H. H., Munksgaard, L., Lund, P., Kristensen, T. (2013). Estimation of grass intake on pasture for dairy cows using tightly and loosely mounted di- and tri-axial accelerometers combined with bite count. *Computers and Electronics in Agriculture*, 99, pp. 227-235. DOI: 10.1016/j.compag.2013.09.013.

Ouyang, W., Hao, F., Skidmore, A. K., Groen, T. A., Toxopeus, A. G., Wang, T. (2012). Integration of multi-sensor data to assess grassland dynamics in a Yellow River sub-watershed. *Ecological indicators*, 18, 163-170.

Park, R. S., Agnew, R. E., Gordon, F. J., Steen, R.W. J. (1998). The use of near infrared reflectance spectroscopy (NIRS) on undried samples of grass silage to predict chemical composition and digestibility parameters. *Animal Feed Science and Technology*, 72 (1-2), pp. 155–167. DOI: 10.1016/S0377-8401(97)00175-2.

Pavlů, V., Hejcman, M., Pavlů, L., Gaisler, J., Nežerková, P. (2006). Effect of continuous grazing on forage quality, quantity and animal performance. *Agriculture, Ecosystems & Environment*, 113 (1-4), pp. 349–355. DOI: 10.1016/j.agee.2005.10.010.

Pellissier, Paul A., Ollinger, S. V., Lepine, L. C., Palace, M. W., & McDowell, W. H. (2015). Remote sensing of foliar nitrogen in cultivated grasslands of human dominated landscapes. *Remote Sensing of Environment*, 167, pp. 88–97. DOI: 10.1016/j.rse.2015.06.009.

Peng Gong; R. P., Biging, G. S., & Larrieu, M. R. (2003). Estimation of forest leaf area index using vegetation indices derived from hyperion hyperspectral data. *Remote Sensing*, 41 (6), 1355–1362. DOI: 10.1109/TGRS.2003.812910.

Pepperl, & Fuchs, (2010). Sensors for the factory automation – Overview Standard Sensors. Available from: http://www.pepperl-fuchs.us/usa/downloads_USA/Sensing-your-needs-2010-01-EN.pdf

Pinter, P. J. (1993). Solar angle independence in the relationship between absorbed PAR and remotely sensed data for alfalfa. *Remote Sensing of Environment*, 46 (1), pp. 19–25. DOI: 10.1016/0034-4257(93)90029-W.

Pittman, J. J., Arnall, D. B., Interrante, S. M., Moffet, C. A., Butler, T. J. (2015). Estimation of biomass and canopy height in bermudagrass, alfalfa, and wheat using ultrasonic, laser, and spectral sensors. *Sensors* (Basel, Switzerland), 15 (2), pp. 2920–2943. DOI: 10.3390/s150202920.

Psomas, A., Kneubühler, M., Huber, S., Itten, K., & Zimmermann, N. E. (2011). Hyperspectral remote sensing for estimating aboveground biomass and for exploring species richness patterns of grassland habitats. *International Journal of Remote Sensing*, 32 (24), 9007–9031. DOI: 10.1080/01431161.2010.532172.

Pullanagari, R. R., Yule, I. J., Tuohy, M. P., Hedley, M. J., Dynes, R. A., & King, W. M. (2012a). In-field hyperspectral proximal sensing for estimating quality parameters of mixed pasture. *Precision Agriculture*, 13 (3), 351–369. DOI: 10.1007/s11119-011-9251-4.

Pullanagari, R. R., Yule, I. J., Hedley, M. J., Tuohy, M. P., Dynes, R. A., King, W. M. (2012b). Multi-spectral radiometry to estimate pasture quality components. *Precision Agric*, 13 (4), pp. 442–456. DOI: 10.1007/s11119-012-9260-y.

Pullanagari, R. R.; Yule, I. J.; Tuohy, M. P.; Hedley, M. J.; Dynes, R. A.; King, W. M. (2013). Proximal sensing of the seasonal variability of pasture nutritive value using multispectral radiometry. *Grass Forage Sci*, 68 (1), pp. 110–119. DOI: 10.1111/j.1365-2494.2012.00877.x.

Qi, J., Chehbouni, A., Huete, A. R., Kerr, Y. H., Sorooshian, S. (1994). A modified soil adjusted vegetation index. *Remote sensing of environment*, 48(2), 119-126.

Rahman, M. M., Lamb, D. W., Stanley, J. N., Trotter, M. G. (2014). Use of proximal sensors to evaluate at the sub-paddock scale a pasture growth-rate model based on light-use efficiency. *Crop Pasture Sci*. 65 (4), p. 400. DOI: 10.1071/CP14071.

Rattray, P.V., Brookes, I.M., Nicol, A.M. (2007). Pasture and supplements for grazing animals, New Zealand Society of Animal Production, no. 14, chapter 10.

Raymond, H. E. (1991). Airborne remote sensing of canopy water thickness scaled from leaf spectrometer data. *International Journal of Remote Sensing*, 12 (3), pp. 643–649. DOI: 10.1080/01431169108929679.

Reddersen, B., Fricke, & T., Wachendorf, M. (2014). A multi-sensor approach for predicting biomass of extensively managed grassland. *Computers and Electronics in Agriculture*, 109, 247–260. DOI: 10.1016/j.compag.2014.10.011.

Rhodes, B. D., Sharrow, S. H. (1990). Effect of Grazing by Sheep on the Quantity and Quality of Forage Available to Big Game in Oregon's Coast Range. *Journal of Range Management*, 43 (3), p. 235. DOI: 10.2307/3898680.

Rook, A., Tallowin. J. (2003). Grazing and pasture management for biodiversity bene t. *Animal Research*, 52 (2), 181-189. DOI: 10.1051/animres:2003014.

Safari, H., Fricke, T., Wachendorf, M., (2015). The potential of ultrasonic and hyperspectral sensor combination for the estimation and mapping of pasture biomass. Mitteilungen der Gesellschaft für Pflanzenbauwissenschaften, 27, 139-142.

Safari, H., Fricke, T., Wachendorf, M., (2016). Determination of fibre and protein content in heterogeneous pastures using field spectroscopy and ultrasonic sward height measurements. *Computers and Electronics in Agriculture*, 123, 256–263. DOI: 10.1016/j.compag.2016.03.002.

Sanderson, M.A.; Rotz, C.A.; Fultz, S.W.; Rayburn, E.B. (2001). Estimating forage mass with a commercial capacitance meter, rising plate meter, and pasture ruler. Agron. J., 93, 1281–1286.

Schellberg, J., Hill, M. J., Gerhards, R., Rothmund, M., & Braun, M. (2008). Precision agriculture on grassland: Applications, perspectives and constraints. *European Journal of Agronomy*, 29 (2-3), 59–71. DOI: 10.1016/j.eja.2008.05.005.

Shiratsuchi, L. S., Ferguson, R. B., Adamchuck, V. I., Shanahan, J. F., & Slater, G. P. (2009). Integration of ultrasonic and active canopy sensors to estimate the in-season nitrogen content for corn. In Proc. 2009 North Central Extension-Industry Soil Fertility Conf., Des Moines, IA (pp. 18-19).

Scimone, M., Rook, A.J., Garel, J.P., & Sahin, N. (2007): Effects of livestock breed and grazing intensity on grazing systems: 3. Effects on diversity of vegetation. Grass and Forage Science, 62 (2), 172-184. DOI: 10.1111/j.1365-2494.2007.00579.x

Scotford, I.M., & Miller, P.C.H. (2004). Combination of Spectral Reflectance and Ultrasonic Sensing to monitor the Growth of Winter Wheat. *Biosystems Engineering*, 87 (1), 27–38. DOI: 10.1016/j.biosystemseng.2003.09.009.

Silvia Cid, M., Miguel, A., Bizuela Cid, B. (1998). Heterogeneity in tall fescue pastures created and sustained by cattle grazing. *Range Manage*, no 6, 51:644-649.

Starks, P. J., Coleman, S. W., Phillips, W. A. (2004). Determination of Forage Chemical Composition Using Remote Sensing. *Rangeland Ecology & Management*, 57 (6), pp. 635–640. DOI: 10.2111/1551-5028(2004)057[0635:DOFCCU]2.0.CO;2.

Starks, P. J., Zhao, D., Phillips, W. A., & Coleman, S. W. (2006). Development of Canopy Reflectance Algorithms for Real-Time Prediction of Bermudagrass Pasture Biomass and Nutritive Values. *Crop Science*, 46 (2), p. 927. DOI: 10.2135/cropsci2005.0258.

Sui, R., & Thomasson, J. A. (2006). Ground-based sensing system for cotton nitrogen status determination. *Transactions of the ASABE*, 49(6), 1983-1991.

Summers, C. G., Putnam, D. H. (2008). Irrigated alfalfa management for Mediterranean and desert zones. Oakland, Calif.: University of California, *Agriculture and Natural Resources*, 3512, Chapter 16, Forage Quality and Testing.

Suttie, J. M., Reynolds, S. G., & Batello, C. (Eds.). (2005). Grasslands of the World (No. 34). Food & Agriculture Org.

Suzuki, Y., Okamoto, H., Takahashi, M., Kataoka, T., & Shibata, Y. (2012). Mapping the spatial distribution of botanical composition and herbage mass in pastures using hyperspectral imaging. *Grassland Science* 58 (1), 1–7. DOI: 10.1111/j.1744-697X.2011.00239.x.

Teague, W. R.; Dowhower, S. L. (2003). Patch dynamics under rotational and continuous grazing management in large, heterogeneous paddocks. *Journal of Arid Environments*, 53 (2), pp. 211–229. DOI: 10.1006/jare.2002.1036.

Teague, W. R.; Dowhower, S. L.; Waggoner, J. A. (2004). Drought and grazing patch dynamics under different grazing management. *Journal of Arid Environments*, 58 (1), pp. 97–117. DOI: 10.1016/S0140-1963(03)00122-8.

Thenkabail, P. S., Smith, R. B., & Pauw, E. (2000). Hyperspectral Vegetation Indices and Their Relationships with Agricultural Crop Characteristics. *Remote Sensing of Environment*, 71 (2), 158–182. DOI: 10.1016/S0034-4257(99)00067-X.

Thenkabail, P. S. (2012). Hyperspectral remote sensing of vegetation. Boca Raton: CRC Press.

Tobias, R. D. (1995). An introduction to partial least squares regression. Proc. Ann. SAS Users Group Int. Conf., 20th, Orlando, FL, pp. 2–5.

Thulin, S., Hill, M. J., Held, A., Jones, S., & Woodgate, P. (2012). Hyperspectral determination of feed quality constituents in temperate pastures: Effect of processing methods on predictive relationships from partial least squares regression. *International Journal of Applied Earth Observation and Geoinformation*, 19, pp. 322–334. DOI: 10.1016/j.jag.2012.06.006.

Van den Bos, J. & Bakker, J.P. (1990). The development of vegetation patterns by cattle grazing at low stock density in the Netherlands. *Biological Conservation*, 51, 263 – 272.

Vitali, M., Tamagnone, M., La Iacona, T., Lovisolo, C. (2013). Measurement of grapevine canopy leaf area by using an ultrasonic-based method. *J. Int. Sci. Vigne Vin*, 47(3), 183-189.

Wrage, N., Strodthoff, J., Cuchillo, H., Isselstein, J., Kayser, M. (2011). Phytodiversity of temperate permanent grasslands: ecosystem services for agriculture and livestock management for diversity conservation. *Biodiversity and Conservation*, 20, 3317-3339.

Wrage, N., Şahin Demirbağ, N., Hofmann, M., & Isselstein, J. (2012). Vegetation height of patch more important for phytodiversity than that of paddock. *Agriculture, Ecosystems & Environment*, 155, pp. 111–116. DOI: 10.1016/j.agee.2012.04.008.

Yang, X., & Guo, X. (2014). Quantifying Responses of Spectral Vegetation Indices to Dead Materials in Mixed Grasslands. *Remote Sensing*, 6 (5), 4289–4304. DOI: 10.3390/rs6054289.

Zhao, D., Starks, P. J., Brown, M. A., Phillips, W. A., Coleman, S. W. (2007). Assessment of forage biomass and quality parameters of bermudagrass using proximal sensing of pasture canopy reflectance. *Grassland Science*, 53 (1), pp. 39–49. DOI: 10.1111/j.1744-697X.2007.00072.x.

Zhao C., Huang W., Chen L., Meng Z., Wang Y., Xu F., (2010). A harvest area measurement system based on ultrasonic sensors and DGPS for yield map correction. *Precision Agriculture*, 11, 163-180.

Appendix

Table A.1 Selected prediction model equations of measured dry matter yield (DMY[a]) for single sensor approaches using sward height (USH[b]), principle component analysis derived components (PCA[c]), WorldView2 satellite broad bands (WV2[d]) and the best fit narrowband normalized difference spectral index (NDSI[e]) based on sensor specific wavelength selections of 1nm bandwidth.

Sensor variable	Equation
Common swards	
USH	DMY = 117.3400 + 6.320 USH
PCA	DMY = 276.375 - 0.929 P2 + 13.035 P4 + 17.091 P5
WV2	DMY = 194.89 + 37.38 B2 - 27.02 B6 + 14.60 B8
NDSI	DMY = -185 + 52137.6 NDSI
Date 1 [f]	
USH	DMY = 95.65 + 11.30 USH
PCA	DMY = 248.75 - 8.94 P3 + 17.10 P4
WV2	DMY = 157.7 + 272.3 B3 - 606.6 B4 + 382.5 B5
NDSI	DMY = 81.17 - 11520 NDSI + 8390 NDSI²
Date 2 [g]	
USH	DMY = 56.812 + 7.076 USH
PCA	DMY = 314.529 - 6.523 P2 + 17.324 P4
WV2	DMY = 262.29 - 62.04 B6 + 37.61 B7
NDSI	DMY = 70.89 + 93294.98 NDSI²
Date 3 [h]	
USH	DMY = 119.867 + 6.938 USH
PCA	n.s.
WV2	DMY = 287.66 - 992.11 B1 + 1106.70 B2 - 159.66 B5 - 35.32 B6 + 12.28 B8
NDSI	DMY = 334.33 + 20620.37 NDSI
Date 4 [i]	
USH	DMY = 74.596 + 6.803 USH
PCA	DMY = 237.60 + 1.65 P2 - 7.17 P3 + 19.56 P4 + 18.89 P5
WV2	DMY = 210.06 + 307.21 B2 - 209.12 B3 + 10.28 B8
NDSI	DMY = -672.2 + 200103.7 NDSI - 9604113.2 NDSI²

[a] DMY = Dry matter yield (g m^{-2}) as dependent variable.
[b] USH = Ultrasonic sward height as independent variable.
[c] PCA = Principle component analysis derived components as independent variables, P1-P5: the first to fifth components of PCA explaining 99% of variations.
[d] WV2 = WorldView2 satellite broad bands as independent variables; B1-B8: the first to eighth broad-bands of WV2. B1: coastal (400-450 nm), B2: blue (450-510 nm), B3: green (510-580 nm), B4: yellow (585-625 nm), B5: red (630-690 nm), B6: red edge (705-745 nm), B7: near infrared-1 (770-895 nm) and B8: near infrared-2 (869-900 nm).
[e] NDSI = Normalized difference spectral index.
[f] Date 1: 25th April-02nd May 2013; [g] Date 2: 3rd-5th June 2013; [h] Date 3: 21st-23rd August 2013; [i] Date 4: 30th September-2nd October 2013.

Table A.2 Selected prediction model equations of measured dry matter yield (DMY[a]) for combination of ultrasonic sward height (USH[b]) with principle component analysis derived components (PCA[c]), WorldView2 satellite broad bands (WV2[d]) and the best fit narrowband normalized difference spectral index (NDSI[e]). Narrowband NDSI is based on 1nm wavelengths.

Sensor variable	Equation
Common swards	
USH + PCA	DMY = 100.2 + 8.184 USH - 0.04066 USH² + 1.071 P1 + 0.3924 P2 - 2.2 P3 + 9.419 P4 + 2.175 P5 - 0.0007838 USH²*P2 + 0.006536 USH²*P5
USH + WV2	DMY = -56.9 + 11.4 USH - 0.945 USH² - 297 B1 + 122 B2 + 74.6 B5 - 37.3 B6 + 49.3 B7 - 24.3 B8 + 25.8 USH*B2 - 12.9 USH*B5 + 2.21 USH*B6 - 1.69 USH*B7 - 0.386 USH²*B2 + 0.19 USH²*B5 - 0.0469 USH²*B6 + 0.0327 USH²*B8
USH + NDSI	DMY = -258.84 + 6878.05 NDSI - 31676.93 NDSI² + 11.26 USH - 278.30 NDSI²*USH
Date 1 [f]	
USH + PCA	DMY = 173.39462 + 0.38331 USH² - 1.58788 P2 - 3.27930 P3 + 8.33715 P4 + 0.00728 USH²*P2 - 0.02982 USH²*P4
USH + WV2	DMY = -151.6281 - 35.4523 USH + 3.3842 USH² + 219.9241 B1 - 499.2112 B2 + 148.1979 B3 + 115.3572 B5 - 67.3600 B6 + 34.3782 B7 + 12.0774 USH*B2 + 0.8193 USH²*B1 - 0.5474 USH²*B3 - 0.4212 USH²*B5 + 0.2563 USH²*B6 - 0.1338 USH²*B7
USH + NDSI	DMY = 382.4 - 164800 NDSI + 21240000 NDSI² - 40.53 USH + 1.422 USH² + 27540 NDSI*USH - 796.9 NDSI*USH² - 3245000 NDSI²*USH + 98410 NDSI²*USH²
Date 2 [g]	
USH + PCA	DMY = 158.9235 + 3.7694 USH + 1.1908 P1 - 2.3815 P2 + 9.4247 P4 - 14.8022 P5 - 0.0866 USH*P2
USH + WV2	DMY = 1015.9200 - 44.8508 USH + 0.6454 USH² + 263.4808 B1 + 414.1362 B3 -1 92.3887 B4 - 151.0504 B5 - 135.7618 B6 + 27.6334 B8 + 1.7700 USH*B6 - 0.2910 USH²*B3 + 0.3364 USH²*B4 - 0.1538 USH²*B5
USH + NDSI	DMY = -108 + 8395000 NDSI² + 0.06292 USH²
Date 3 [h]	
USH + PCA	DMY = 23.08092 + 15.58384 USH - 0.15950 USH² + 4.38994 P4 - 0.01327 USH²*P4
USH + WV2	DMY = 258 + 0.0337 USH² - 695 B1 + 965 B2 - 186 B5 - 19.9 B6 - 0.294 USH²*B2 + 0.085 USH²*B5 + 0.0246 USH²*B6
USH + NDSI	DMY = 279.3 + 30060 NDSI - 21640000 NDSI² - 6.493 USH + 0.2146 USH² - 24.93 NDSI*USH² + 1466000 NDSI²*USH -21420 NDSI²*USH²
Date 4 [i]	
USH + PCA	DMY = -14.57418 + 19.02536 USH - 0.33208 USH² + 4.83465 P1 - 5.09728 P2 - 58.87350 P3 + 9.87182 P4 + 15.59774 P5 - 0.53616 USH*P1 + 0.74975 USH*P2 + 6.30272 USH*P3 + 0.01272 USH²*P1 - 0.01779 USH²*P2 - 0.14825 USH²*P3
USH + WV2	DMY = 358 - 0.316 USH - 0.067 USH² - 1490 B1 + 855 B2 + 167 B3 - 1050 B4 + 865 B5 + 29.1 B8 + 44.6 USH*B1 + 75.1 USH*B4 - 75.9 USH*B5 - 3.41 USH*B8 - 1.11 USH²*B3 + 0.632 USH²*B5 + 0.0878 USH²*B8
USH + NDSI	DMY = 1518 - 258000 NDSI + 10130000 NDSI² - 184.3 USH + 4.935 USH² + 32820 NDSI*USH - 800.2 NDSI*USH² - 1271000 NDSI²*USH + 30040 NDSI²*USH²

[a] DMY = Dry matter yield (g m^{-2}) as dependent variable.
[b] USH = Ultrasonic sward height as independent variable.
[c] PCA = Principle component analysis derived components as independent variables, P1-P5: the first to fifth components of PCA explaining 99% of variations.
[d] WV2 = WorldView2 satellite broad bands as independent variables; B1-B8: the first to eighth broad-bands of WV2. B1: coastal (400-450 nm), B2: blue (450-510 nm), B3: green (510-580 nm), B4: yellow (585-625 nm), B5: red (630-690 nm), B6: red edge (705-745 nm), B7: near infrared-1 (770-895 nm) and B8: near infrared-2 (869-900 nm).
[e] NDSI = Normalized difference spectral index.
[f] Date 1: 25th April-02nd May 2013; [g] Date 2: 3rd-5th June 2013; [h] Date 3: 21st-23rd August 2013; [i] Date 4: 30th September-2nd October 2013.

Table A.3 Selected prediction model equations of measured fresh matter yield (FMY[a]) for single sensor approaches using sward height (USH[b]), principle component analysis derived components (PCA[c]), WorldView2 satellite broad bands (WV2[d]) and the best fit narrowband normalized difference spectral index (NDSI[e]) based on sensor specific wavelength selections of 1nm bandwidth.

Sensor variable	Equation
Common swards	
USH	FMY = 213.851 + 24.243 USH
PCA	FMY = 823.89 - 12.56 P2 + 8.87 P3 + 48.45 P4 + 43.31 P5
WV2	FMY = 587.415 - 139.496 B3 + 26.719 B7
NDSI	FMY = 520.7 + 1541000 NDSI²
Date 1 [f]	
USH	FMY = 224.67 + 38.01 USH
PCA	FMY = 739.56 - 6.15 P2 - 17.18 P3 + 66.64 P4
WV2	FMY = 522 + 929 B3 – 1984 B4 + 1175 B5
NDSI	FMY = -306.2 + 7914188.3 NDSI²
Date 2 [g]	
USH	FMY = 531.1739 + 0.4369 USH²
PCA	FMY = 1240.18 + 8.14 P1 - 29.39 P2 + 76.94 P4
WV2	FMY = 247.0 - 233.6 B6 + 159.7 B7
NDSI	FMY = 381.96 - 164981.65 NDSI
Date 3 [h]	
USH	FMY = 398.37 + 12.96 USH
PCA	n.s.
WV2	FMY = -242.5 - 887.4 B1 + 813.1 B3 - 269.5 B6 + 98.7 B8
NDSI	FMY = 814.45 - 49756.21 NDSI
Date 4 [i]	
USH	FMY = -73.053 + 38.104 USH - 0.397 USH²
PCA	FMY = 567.54 - 15.51 P3 + 57.91 P4
WV2	FMY = 322.72 + 880.95 B1 - 470.35 B3 + 29.19 B8
NDSI	FMY = -116.4 + 415039.2 NDSI²

[a] FMY = Fresh matter yield (g m^{-2}) as dependent variable.
[b] USH = Ultrasonic sward height as independent variable.
[c] PCA = Principle component analysis derived components as independent variables, P1-P5: the first to fifth components of PCA explaining 99% of variations.
[d] WV2 = WorldView2 satellite broad bands as independent variables; B1-B8: the first to eighth broad-bands of WV2. B1: coastal (400-450 nm), B2: blue (450-510 nm), B3: green (510-580 nm), B4: yellow (585-625 nm), B5: red (630-690 nm), B6: red edge (705-745 nm), B7: near infrared-1 (770-895 nm) and B8: near infrared-2 (869-900 nm).
[e] NDSI = Normalized difference spectral index.
[f] Date 1: 25th April-02nd May 2013; [g] Date 2: 3rd-5th June 2013; [h] Date 3: 21st-23rd August 2013; [i] Date 4: 30th September-2nd October 2013.

Table A.4 Selected prediction model equations of measured fresh matter yield (FMY[a]) for combination of ultrasonic sward height (USH[b]) with principle component analysis derived components (PCA[c]), WorldView2 satellite broad bands (WV2d) and the best fit narrowband normalized difference spectral index (NDSI[e]). Narrowband NDSI is based on 1nm wavelengths.

Sensor variable	Equation
Common swards	
USH + PCA	FMY = 273 + 21.3 USH + 0.00854 USH² + 2.67 P1 - 5.12 P2 + 10.1 P3 + 13.3 P4 + 24.5 P5 + 0.00234 USH²*P1 - 0.00491 USH²*P2 - 0.0078 USH²*P3 + 0.0217 USH²*P4
USH + WV2	FMY = -64.1 + 28 USH - 0.32 USH² + 0.02 B6 + 133 B7 - 123 B8 -0.0537 USH²*B6 + 0.0371 USH²*B7
USH + NDSI	FMY = 284.3 - 89850 NDSI + 3075000 NDSI² + 33.51 USH - 0.2058 USH² - 148.5 NDSI*USH² + 24840 NDSI²*USH²
Date 1 [f]	
USH + PCA	FMY = 251.50739 + 34.36009 USH + 0.05971 USH² + 2.67943 P1 - 5.65457 P2 + 26.07072 P5 - 0.00718 USH²*P1 + 0.00879 USH²*P2
USH + WV2	FMY = -682.8045 + 23.2794 USH + 2.3413 USH² - 279.9660 B2 + 254.4490 B5 - 74.1385 B6 + 312.9831 B7 - 249.4671 B8 - 0.0416 USH²*B7
USH + NDSI	FMY = -728 + 151600 NDSI + 17.35 USH + 1.486 USH² - 137.6 NDSI*USH²
Date 2 [g]	
USH + PCA	FMY = 801.393 + 9.983 USH + 8.101 P1 - 15.396 P2 + 51.360 P4 - 0.355 USH*P2
USH + WV2	FMY = 2773.8962 - 113.3589 USH + 1.5103 USH² + 978.6096 B3 - 558.6443 B5 - 432.9397 B6 + 117.4014 B7 + 4.7236 USH*B6 - 0.2408 USH²*B3
USH + NDSI	FMY = 1664.26 - 22748.47 NDSI + 56.82 USH - 991.32 NDSI*USH
Date 3 [h]	
USH + PCA	FMY = 232.243 + 20.898 USH - 7.031 P1 + 11.167 P3 + 0.482 USH*P1
USH + WV2	FMY = -1693.534 + 174.799 USH - 2.587 USH² - 1580.496 B1 + 1702.654 B2 - 27.101 B5 - 21.480 USH*B5 + 0.328 USH²*B5
USH + NDSI	FMY = 223.4 - 28970 NDSI - 5481000 NDSI² + 11.86 USH + 0.04179 USH² + 389600 NDSI²*USH - 6274 NDSI²*USH²
Date 4 [i]	
USH + PCA	FMY = 287.79 + 11.68 USH + 34.93 P4
USH + WV2	FMY = 21.634 - 20.601 USH + 1.461 USH² + 993.944 B2 - 5257.223 B3 + 3913.686 B4 - 986.951 B5 + 528.143 B6 + 418.253 USH*B3 - 251.372 USH*B4 - 47.379 USH*B6 - 9.673USH²*B3 + 5.756 USH²*B4 + 1.079 USH²*B6
USH + NDSI	FMY = -2342 + 224900 NDSI – 4112000 NDSI² + 123.8 USH + 3.999 USH² - 837.2 NDSI*USH² - 448400 NDSI²*USH + 37060 NDSI²*USH²

[a] FMY = Fresh matter yield (g m^{-2}) as dependent variable.
[b] USH = Ultrasonic sward height as independent variable .
[c] PCA = Principle component analysis derived components as independent variables, P1-P5: the first to fifth components of PCA explaining 99% of variations.
[d] WV2 = WorldView2 satellite broad bands as independent variables; B1-B8: the first to eighth broad-bands of WV2. B1: coastal (400-450 nm), B2: blue (450-510 nm), B3: green (510-580 nm), B4: yellow (585-625 nm), B5: red (630-690 nm), B6: red edge (705-745 nm), B7: near infrared-1 (770-895 nm) and B8: near infrared-2 (869-900 nm).
[e] NDSI = Normalized difference spectral index.
[f] Date 1: 25th April-02nd May 2013; [g] Date 2: 3rd-5th June 2013; [h] Date 3: 21st-23rd August 2013; [i] Date 4: 30th September-2nd October 2013.

Table A.5 Selected prediction model equations of measured dead material proportion (DMP[a]) for spectral sensor approaches using principle component analysis derived components (PCA[b]), WorldView2 satellite broad bands (WV2[c]) and the best fit narrowband normalized difference spectral index (NDSI[d]) based on sensor specific wavelength selections of 1nm bandwidth.

Sensor variable	Equation
Common swards	
PCA	DMP = 31.6079 - 0.1185 P1 + 0.6640 P2 - 0.9934 P3 + 0.9441 P4
WV2	DMP = 39.04 + 13.00 B2 + 46.22 B3 - 76.71 B4 + 34.76 B5 - 6.74 B7 + 4.98 B8
NDSI	DMP = 39.3876 + 1353.2198 NDSI
Date 1 [e]	
PCA	DMP = 31.9167 + 0.2360 P2 - 1.1425 P3
WV2	DMP = 11.401 + 37.853 B3 - 59.617 B4 + 29.213 B5 - 22.551 B7 +21.438 B8
NDSI	DMP = 1.641 + 1452 NDSI + 144100 $NDSI^2$
Date 2 [f]	
PCA	DMP = 9.1870 + 0.1351 P2 - 0.3018 P3
WV2	DMP = 22.482 - 0.302 B7
NDSI	DMP = 6.622 + 2330 NDSI + 1220000 $NDSI^2$
Date 3 [g]	
PCA	DMP = 39.9904 - 0.5356 P1 + 0.5244 P3
WV2	DMP = 68.236 + 57.048 B3 - 78.439 B4 + 33.448 B5 - 2.591 B7
NDSI	DMP = -15.49 + 3375.02 NDSI
Date 4 [h]	
PCA	DMP = 237.60 + 1.65 P2 - 7.17 P3 + 19.56 P4 + 18.89 P5
WV2	DMP = 39.593 + 39.119 B3 - 52.682 B4 + 26.897 B5 - 1.804 B7
NDSI	DMP = 27.919 + 7341.182 NDSI

[a] DMP = Dead material proportion (% of dry matter yield) as dependent variable.
[b] PCA = Principle component analysis derived components as independent variables, P1-P5: the first to fifth components of PCA explaining 99% of variations.
[c] WV2 = WorldView2 satellite broad bands as independent variables; B1-B8: the first to eighth broad-bands of WV2. B1: coastal (400-450 nm), B2: blue (450-510 nm), B3: green (510-580 nm), B4: yellow (585-625 nm), B5: red (630-690 nm), B6: red edge (705-745 nm), B7: near infrared-1 (770-895 nm) and B8: near infrared-2 (869-900 nm).
[d] NDSI = Normalized difference spectral index.
[f] Date 1: 25th April-02nd May 2013; [g] Date 2: 3rd-5th June 2013; [h] Date 3: 21st-23rd August 2013; [i] Date 4: 30th September-2nd October 2013.

Table A.6 Prediction model equations of acid detergent fibre (ADF) and crude protein (CP) in the biomass of heterogeneous pastures from ultrasonic sward height (USH) for common (N=323) and date-specific dataset (N=108).

Variable		Equation
ADF (% of DM)	C[a]	ADF = 23.129551 + 0.541768 USH - 0.005717 USH²
	Sp[b]	ADF = 24.0954 + 0.1936 USH
	Sm[c]	ADF = 22.00577 + 0.67592 USH - 0.00695 USH²
	Au[d]	ADF = 21.99615 + 0.75354 USH - 0.00926 USH²
CP (% of DM)	C	CP = 12.50761 - 0.04055 USH
	Sp	CP = 12.509158 - 0.132532 USH + 0.001871 USH²
	Sm	CP = 11.728851 - 0.000976 USH²
	Au	n.s.[e]

[a] C: common dataset; [b] Sp: spring dataset; [C] Sm: summer dataset; [d] Au: autumn dataset; [e] n.s. not significant

Table A.7 Prediction model equations of acid detergent fibre (ADF) and crude protein (CP) in the biomass of heterogeneous pastures from best-fit normalized difference spectral index (NDSI) exclusively and as a combination with ultrasonic sward height (USH) for common (N=323) and date-specific dataset (N=108).

Variable			Equation
ADF (% of DM)	C[a]	ex[e]	ADF = 14.46 + 877.02 NDSI
		co[f]	ADF = 17.8 + 46500 NDSI² + 0.411 USH - 0.00244 USH² - 538 NDSI²*USH
	Sp[b]	ex	ADF = 33.201 - 1010.311 NDSI
		co	ADF = 33.17 - 10580 NDSI + 2272000 NDSI² - 0.009842 USH + 280.7 NDSI*USH - 73280 NDSI²*USH
	Sm[c]	ex	ADF = -56.51 + 4610.84 NDSI - 53901.40 NDSI²
		co	ADF = -10.8 + 2010 NDSI – 18000 NDSI² + 0.462 USH - 11.1 NDSI*USH
	Au[d]	ex	ADF = 13.027 + 1983.273 NDSI
		co	ADF = 22.66 + 1083 NDSI + 80530 NDSI² + 0.8106 USH - 0.01276 USH²
CP (% of DM)	C	ex	CP = 70.48 - 236.17 NDSI + 227.12 NDSI²
		co	CP = 42.2070 - 121.7472 NDSI + 109.3326 NDSI² - 0.2239 USH + 0.4501 NDSI*USH
	Sp	ex	CP = 32.5 - 1885.5 NDSI + 38254.5 NDSI²
		co	CP = 280.3372 - 788.7756 NDSI - 11.0845 USH + 0.1263 USH² + 33.6308 NDSI*USH - 0.3923 NDSI*USH² - 25.7730 NDSI²*USH + 0.3069 NDSI²*USH²
	Sm	ex	CP = 29.0 - 112.3 NDSI + 139.2 NDSI²
		co	n.s.[g]
	Au	ex	CP = 23.157 - 44.127 NDSI
		co	n.s.

a C: common dataset; b Sp: spring dataset; C Sm: summer dataset; d Au: autumn dataset. e ex: exclusive NDSI; f co: combination of USH and NDSI. g n.s: not significant.

Table A.8 Prediction model equations of acid detergent fibre (ADF) and crude protein (CP) in the biomass of heterogeneous pastures from WorldView2 satellite bands exclusively and as a combination with ultrasonic sward height (USH) for common (N=323) and date-specific swards (N=108).

Variable			Equation
ADF (% of DM)	C[a]	ex[e]	ADF = 36.4312 - 16.5894 B1 + 21.4739 B2 + 10.2287 B3 - 18.7016 B4 + 5.5000 B5 - 2.7202 B7 + 2.2975 B8
		co[f]	28.07 + 0.1661 USH + 0.001961 USH² - 60.16 B1 + 61.44 B2 + 14.23 B3 -22.1 B4 + 2.189 B5 - 2.016 B6 - 7.420 B7 + 7.735 B8 + 3.287 USH*B1-2.777 USH*B2 + 0.1981 USH*B5 + 0.1652 USH*B6 + 0.1524 USH*B7 -0.2373 USH*B8 - 0.04473 USH²*B1+ 0.03182 USH²*B2 - 0.00256 USH²*B6 + 0.001454 USH²*B8
	Sp[b]	ex	n.s.
		co	ADF = 29.752933 - 0.222049 USH + 0.008552 USH² - 73.934980 B1 + 57.622116 B2 - 2.698515 B5 - 0.153467 B7 + 3.170420 USH*B1 -2.092045 USH*B2 - 0.037068 USH²*B1 + 0.023058 USH²*B2
	Sm[c]	ex	ADF = 50.145 - 31.234 B1 + 35.328 B2 + 15.115 B3 - 16.357 B4 - 2.268 B6
		co	ADF = 40.6 + 0.0982 USH + 0.000731 USH² - 117 B1 + 124 B2 + 25.5 B3 -37.6 B4 - 4.31 B5 - 15.4 B7 + 13.6 B8 + 5.54 USH*B1 - 5.61 USH*B2 + 0.814 USH*B5 + 0.41 USH*B7 - 0.379 USH*B8 - 0.0612 USH²*B1 + 0.0616 USH²*B2 -0.0129 USH²*B3 + 0.02 USH²*B4 - 0.0169 USH²*B5
	Au[d]	ex	ADF = 31.301 + 28.621 B3 - 38.608 B4 + 18.146 B5 - 2.754 B6 - 4.757 B7 + 4.974 B8
		co	ADF = 29 + 0.183 USH - 0.000141 USH²- 53.8 B1+ 72.3 B2 + 21.8 B3 - 30 B4 - 0.228 B5 - 7.14 B6 - 0.168 B7 + 2.89 B8 + 1.94 USH*B1 - 2.76 USH*B2 + 0.594 USH*B5 + 0.367 USH*B6 - 0.194 USH*B7 - 0.00524 USH²*B6 + 0.00298 USH²*B7
CP (% of DM)	C	ex	CP = 8.6371 + 10.9692 B1- 6.3544 B2 - 2.2856 B3 + 0.5074 B6
		co	CP = 10.028589 - 0.026711 USH - 0.000901 USH² + 7.488305 B1 - 3.164376 B2 - 3.891008 B3 + 5.303302 B4 - 4.018177 B5 + 0.227481 B7 + 0.232754 USH*B2 - 0.114974 USH*B4 - 0.005556 USH²*B2 + 0.001040 USH²*B3 + 0.002017 USH²*B5
	Sp	ex	CP = 4.7205 + 4.1397 B1 - 1.2364 B4 + 0.2199 B6
		co	CP = -15.3 + 0.97 USH - 0.00946 USH² - 18.8 B1 + 22 B2 - 10.7 B3 + 3.70 B4 - 1.21 B5 + 2.63 B6 + 1.45 B7 - 1.55 B8 + 1.55 USH*B1 - 1.40 USH*B2 + 0.299 USH*B3 - 0.0883 USH*B6 - 0.0186 USH²*B1 + 0.0153 USH²*B2 - 0.00561 USH²*B4 + 0.00337 USH²*B5 + 0.000854 USH²*B6
	Sm	ex	CP = 13.419 + 2.212 B2 - 3.711 B3 + 0.383 B7
		co	CP = 12.347291 + 0.103984 USH - 0.002744 USH² + 6.905206 B1 -3.696828 B2 - 3.002849 B3 + 0.334154 B7 - 0.003516 USH²*B1 + 0.002763 USH²*B2
	Au	ex	CP = 10.943 + 9.002 B2 - 7.320 B3 + 5.639 B4 - 6.061 B5 + 0.810 B6
		co	CP = 14.123517 - 0.003319 USH² + 8.417694 B2 - 4.790308 B3 + 4.445703 B4 - 6.194896 B5 + 0.228072 B7 + 0.000518 USH²*B4

[a] C: common dataset; [b] Sp: spring dataset; [C] Sm: summer dataset; [d] Au: autumn dataset. [e] ex: exclusive satellite bands; [f] co: combination of USH and satellite bands. [g] n.s: not significant.

WorldView2 satellite broad bands as independent variables; B1-B8: the first to eighth broad-bands of WV2. B1: coastal (400-450 nm), B2: blue (450-510 nm), B3: green (510-580 nm), B4: yellow (585-625 nm), B5: red (630-690 nm), B6: red edge (705-745 nm), B7: near infrared-1 (770-895 nm) and B8: near infrared-2 (869-900 nm)